Master Thesis 2020

Tailor-made Synthesis of Multisubstituted Pyridines and Their Application as Dinucleating Ligands

Professor Nagatoshi Nishiwaki

Department of Chemistry Kochi University of Technology

1225089 Mao Arita

Preface

The studies on this thesis were carried out under direction of Prof. Dr. Nagatoshi Nishiwaki and Dr. Akitaka Ito at Department of School of Environmental Science and Engineering, Graduate School of Engineering, Kochi University of Technology, for four years since 2016.

First of all, the author hearty appreciation goes Prof. Dr. Nagatoshi Nishiwaki for the individual guidance, suggestion and encouragement through the present studies were priceless value for my studies. The author also would like to express his great gratitude to Dr. Akitaka Ito for the kind instruction and support for the present studies. The author is hearty thanks to Dr. Soichi Yokoyama for a lot of discussions and guidance on the organic, computational and photochemistry.

The author is thankful to Prof. Dr. Kazuya Kobiro, Prof. Dr. Ryuchi Sugimoto, Assoc. Prof. Dr. Masataka Ohtani and Dr. Kai Kan at School of Engineering, Kochi University of Technology, for their fruitful discussions during the course of the present studies.

The author warmly thanks past and present members of Nishiwaki laboratory and KUT Chemistry course because they have provided a lot of priceless experiences and memory to the author. Especially, Mr. Kento Iwai, Ms. Saki Naitou and Ms. Yurie Horikawa and afforded fruitful discussions and taught me a lot of experimental operation. Mr. Yushi Matsui and Ms. Mayuka Taomoto have offered warm friendship for 4 years. The author is grateful to Mr. Yasuyuki Kuroda for leading juniors together for two years.

Finally, I would like to express my deepest attention to my parents, Mr. Hironari Arita and Ms. Kazumi Arita for their constant assistant and encouragements. Mao Arita

CONTENTS

PART I TAILOR-MADE SYNTHESIS OF MULTISUBSTITUTED PYRIDINES AND THEIR APPLICATIONS

Chapter 1 Introduction

Polyarylpyridines are widely used in various applications, such as synthetic intermediates for medicines,[1] ligands for organometals,[2] and fluorophorescent chemosensors.[3] In recent years, they have also been found to play an important role in materials science because of their specific electronic properties.[4] While the utility of polyarylpyridines has increased, introduction of the desired aryl/alkyl group at the desired position remains difficult, and considerable efforts have been undertaken in this regard.[5–10] Although Suzuki–Miyaura coupling is usually employed for arylation of the pyridine framework,[6] different leaving groups should be introduced in advance for site-selective arylation *via* multistep reactions, which increases the difficulty of synthesis and decreases the total yields. Indeed, there are only three papers reporting fully and differently arylated pyridines.[7–10] In 2014, Schmitt *et al*. synthesized pyridines possessing five different aryl groups for the first time *via* 13 steps, which included regiocontrolled modification of the pyridine ring and subsequent Suzuki–Miyaura coupling reactions (Scheme 1, method a).[7] Later, Yamaguchi *et al*. succeeded in reducing the number of reaction steps by adopting Diels-Alder-type ring transformation as the key step (methods b and c).[8,9] Despite the successful synthesis of fully and differently arylated pyridines, the substituents could not be readily altered to other aryl or alkyl groups readily because of the tedious experimental manipulations, poor availability of the corresponding substrates, and need for separation of spontaneously formed regioisomers. Hence, there is great demand for a simple method to synthesize diverse arylated pyridines. In our previous work,[11] we demonstrated an efficient synthetic method for polysubstituted nicotinates

via the condensation of an enamino ester with an α,β-unsaturated carbonyl compound in the presence of $FeCl_3$ (method d). This protocol facilitates the introduction of different alkyl/aryl groups at the desired positions of the pyridine framework by simply altering the starting materials. This advantage prompted me to employ β-pyridylenamine **1** as a push-pull alkene instead of the enamino ester, which afforded fully arylated pyridines *via* only three steps including the synthesis of substrates **1** and **2** (method e).

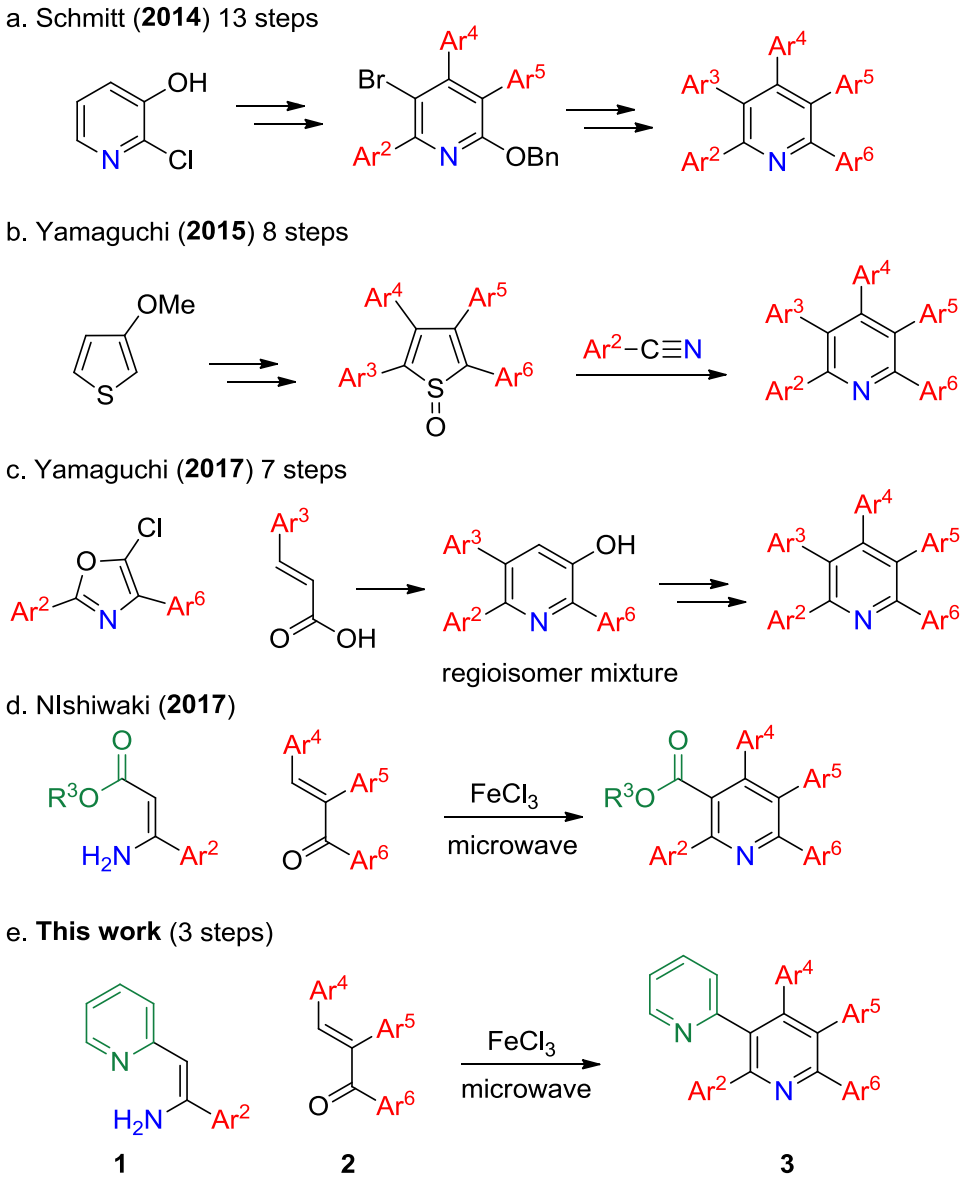

Scheme 1. Synthesis of fully and differently arylated pyridines.

Chapter 2 Results and Discussion

2.1 Synthesis of β-(2-pyridyl)enamine and enones

β-(2-Pyridyl)enamines **1A–D** were efficiently prepared as a single isomer by the condensation of benzonitriles with 2-methylpyridine[12] (Table 1, Entries 1–4). On the other hand, condensation using 4-methylpyridine afforded only the hydrolysis product of **1E** (Entry 5). In the case of *p*-nitrotoluene, a complex mixture was obtained without any detectable formation of **1F** (Entry 6). Hence, the 2-pyridyl group is considered to stabilize enamine **1** by intramolecular hydrogen bonding. Indeed, the ^{1}H NMR spectrum showed a signal due to one of the NH hydrogens at δ *circa* 6 ppm, but a signal due to the other hydrogen was not observed because of exchange with water present in the solvent. Enones **2a–l** were easily prepared by simply mixing the corresponding aldehydes and ketones under alkaline conditions, respectively. For the preparation of α,β-disubstituted enones **2m–t**, it was more effective to heat a solution of an aldehyde and a ketone in toluene using Dean-Stark apparatus in the presence of piperidinium acetate.

Table 1. Preparation of enamines **1**.

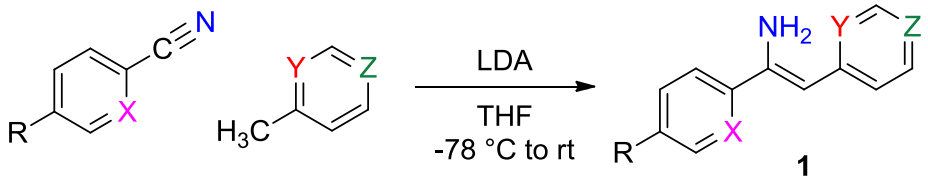

Entry	R	X	Y	Z	Enamine **1**	Yield /%
1	H	CH	N	CH	**1A**	98
2	Me	CH	N	CH	**1B**	91
3	Cl	CH	N	CH	**1C**	94
4	CF_3	CH	N	CH	**1D**	86
5	Me	CH	CH	N	**1E**	0[a]
6	Me	CH	CH	C-NO_2	**1F**	0
7	H	N	N	CH	**1G**	78

[*a*]1-(4-Methylphenyl)-2-(4-pyridyl)ethanone was obtained in 75% yield.

2.2 Synthesis of multisubstituted pyridines

When benzylideneacetone **2a** was reacted with β-(2-pyridyl)enamine **1A** in the presence of $FeCl_3$ in a sealed tube at 180 °C under microwave irradiation, 6-methyl-2,4-diphenyl-3-(2-pyridyl)pyridine (**3Aa**) was isolated in 84% yield (Table 2, Entry 1). This reaction was not suppressed by the presence of the bulky naphthyl group at the reaction site (Entry 2). While an electron-donating methyl group on the α-phenyl group (R^2) of **1** facilitated the condensation, electron-withdrawing groups slightly decreased the yields of pyridines **3**, presumably due to the decreased nucleophilicity of enamines **1C** and **1D** (Entries 3–5). Chalcone derivatives **2c–l** were more easily treatable than methyl ketones **2a** and **2b**, and underwent the condensation to afford 2,3,4,6-tetraarylpyridines, which facilitated the modification of the substituents at the 4-, 5- and 6-positions of the pyridine framework (Entries 6–20). The reaction using enones **2c–f** readily proceeded without any notable effect of the electronic nature of R^4 to give the corresponding products **3Bc–f** and **3Ce** respectively (Entries 6–10). On the contrary, this reaction was considerably affected by the substituent on the phenyl group (R^6) (Entries 11–13). Since both electron-donating and electron-withdrawing groups decreased the yields of products **3Bh** and **3Bi**, the low reactivity was considered to be due to the poor solubility of enones **2h** and **2i**. Indeed, 2-methoxyphenyl ketone **2j** showed higher reactivity than **2i** because of its increased solubility (Entries 13 and 14). Furthermore, 2,3,5,6-tetraarylpyridines **3Bm** and **3Bn** could be prepared by using α-arylated enones **2m** and **2n** were used (Entries 17 and 18). Next, we attempted the synthesis of fully substituted pyridines using α,β-disubstituted enones **2o–r**. In the case of α-methylated enone **2o**, pyridine **3Bo** was obtained in a similar yield as **3Bg** (Entries 11 and 19). When α-arylated enone **2p** was used, fully and differently substituted pentaarylpyridine **3Bp** was obtained, although the yield was

considerably decreased (Entry 20). The low reaction efficiency of **2p** was considered to be due to the instability caused by the disturbed conjugation. Structural optimization by DFT calculations [B3LYP/6-31g(d,p)] indicated that both chlorophenyl and benzoyl groups were distorted by around 40° angles as a result of steric repulsion with the α-aryl group, and the α-aryl group itself was distorted by around 85° angle from the enone plane (Figures 1). Indeed, when enone **2p** was subjected to the reaction conditions in the absence of **1B**, 82% of **2p** was decomposed to afford a complex mixture. This problem was overcome by increasing the molar ratio (**2p**:**1B**) from 1:5 to 1:2 (Entries 20 and 21). Consequently, pentaarylpyridines **3Bp–r** were synthesized in only three steps, among which the structure of **3Br** was confirmed by X-ray crystallography (Entries 20–23 and Figure 2). With this method, the aryl groups could be easily modified by altering benzonitriles, benzaldehyde, and benzyl phenyl ketones.

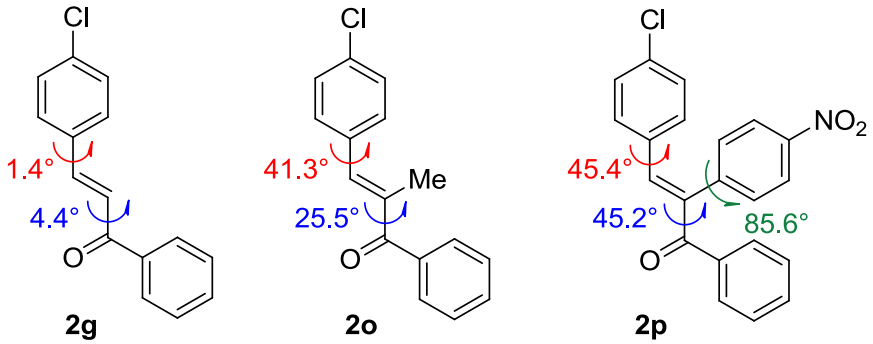

Figure 1. Optimized structures of **2g**, **2o** and **2p**.

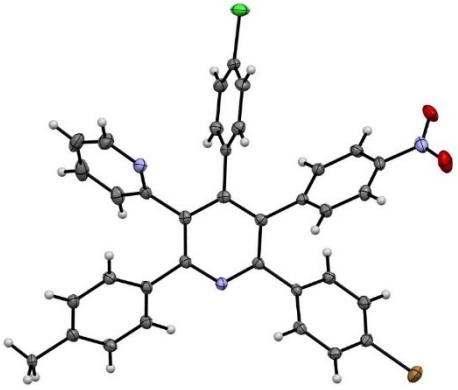

Figure 2. ORTEP diagram (50% thermal ellipsoids) of **3Br**.

Table 2. Synthesis of polyarylated pyridines **3**.

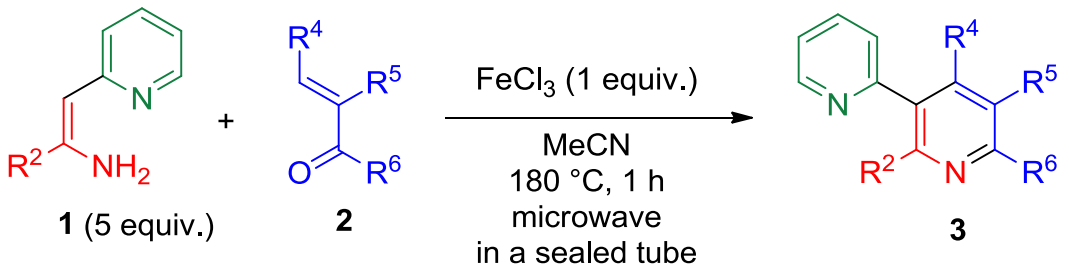

Entry	Enamine **1**		Enone **2**				Poduct	
	R^2		R^4	R^5	R^6			/%
1	Ph	**1A**	Ph	H	Me	**2a**	**3Aa**	84
2	4-MeC_6H_4	**1B**	2-Naphthyl	H	Me	**2b**	**3Bb**	66
3	4-MeC_6H_4	**1B**	Ph	H	Me	**2a**	**3Ba**	86
4	4-ClC_6H_4	**1C**	Ph	H	Me	**2a**	**3Ca**	71
5	4-$F_3CC_6H_4$	**1D**	Ph	H	Me	**2a**	**3Da**	69
6	4-MeC_6H_4	**1B**	4-$MeOC_6H_4$	H	4-MeC_6H_4	**2c**	**3Bc**	56
7	4-MeC_6H_4	**1B**	Ph	H	4-MeC_6H_4	**2d**	**3Bd**	67
8	4-MeC_6H_4	**1B**	4-FC_6H_4	H	4-MeC_6H_4	**2e**	**3Be**	64
9	4-ClC_6H_4	**1C**	4-FC_6H_4	H	4-MeC_6H_4	**2e**	**3Ce**	76
10	4-MeC_6H_4	**1B**	4-NCC_6H_4	H	4-MeC_6H_4	**2f**	**3Bf**	76
11	4-MeC_6H_4	**1B**	4-ClC_6H_4	H	Ph	**2g**	**3Bg**	72
12	4-MeC_6H_4	**1B**	4-ClC_6H_4	H	4-$O_2NC_6H_4$	**2h**	**3Bh**	35
13	4-MeC_6H_4	**1B**	4-ClC_6H_4	H	4-$MeOC_6H_4$	**2i**	**3Bi**	39
14	4-MeC_6H_4	**1B**	4-ClC_6H_4	H	2-$MeOC_6H_4$	**2j**	**3Bj**	61
15	4-MeC_6H_4	**1B**	4-*tert*-BuC_6H_4	H	4-ClC_6H_4	**2k**	**3Bk**	57
16	4-MeC_6H_4	**1B**	4-$MeOC_6H_4$	H	4-$O_2NC_6H_4$	**2l**	**3Bl**	29
17	4-MeC_6H_4	**1B**	H	4-$O_2NC_6H_4$	Ph	**2m**	**3Bm**	51
18	4-MeC_6H_4	**1B**	H	4-$O_2NC_6H_4$	4-$MeOC_6H_4$	**2n**	**3Bn**	38
19	4-MeC_6H_4	**1B**	4-ClC_6H_4	Me	Ph	**2o**	**3Bo**	62
20	4-MeC_6H_4	**1B**	4-ClC_6H_4	4-$O_2NC_6H_4$	Ph	**2p**	**3Bp**	13
21[a]	4-MeC_6H_4	**1B**	4-ClC_6H_4	4-$O_2NC_6H_4$	Ph	**2p**	**3Bp**	26
22[a]	4-MeC_6H_4	**1B**	Ph	4-$O_2NC_6H_4$	Ph	**2q**	**3Bq**	21
23[a]	4-MeC_6H_4	**1B**	4-ClC_6H_4	4-$O_2NC_6H_4$	4-BrC_6H_4	**2r**	**3Br**	10

[*a*] 2 Equiv. of enamine **1B** were used.

2.3 Study on reaction mechanism

When the reaction atmosphere was changed from air to argon, the yield of **3Ba** decreased to 64%, which indicated that oxygen is necessary for the efficient reaction (Table 3, Entries 1 and 2). However, a complicated mixture of compounds was obtained when the reaction was conducted under oxygen (Entry 3), and decomposition of the substrates was observed. When a catalytic amount of $FeCl_3$ was used under argon atmosphere, the reaction was considerably suppressed; however, the same reaction under air afforded **3Ba** in 72% yield (Entries 4 and 5).

Table 3. Study on reaction atmosphere and catalyst loading in the reaction of **1B** and **2a**.

Entry	$FeCl_3$ /equiv.	Atmosphere	Yield of **3Ba** /%
1	1	Air	86
2	1	Argon	64
3	1	Oxygen	69
4	0.2	Argon	39
5	0.2	Air	72
6	0.2[a]	Air	69
7	0.2[b]	Air	78

[*a*] Molecular sieves 3A (100 mg) was added. [*b*] *p*-Benzoquinone (1 equiv.) was added.

A plausible mechanism for the reaction is shown in Scheme 2. The reaction is initiated by the attack of **1B** onto enone **2a'** activated by $FeCl_3$. After cyclization and dehydration, the resulting dihydropyridine **4** was oxidized by $FeCl_3$ to afford **3Ba**, and oxygen in the air reoxidized the reduced iron species, and the reaction proceeded with a catalytic amount of $FeCl_3$. Another reaction mechanism initiated by imine formation is also acceptable (Scheme 3). We consider the former mechanism is more plausible based on our insights obtained from the study using push-pull alkenes, β-nitroenamines.[13] In both reaction mechanisms, a water is eliminated during the condensation between an amino

and a carbonyl group, which might cause the competitive hydrolysis of the substrates. However, no effect was observed even when the reaction was conducted in the presence of molecular sieves (Table 3, Entry 6). This is presumably due to the reversible releasing of water under the employed conditions. Furthermore, *p*-benzoquinone was added to facilitate the oxidation of intermediately formed dihydropyridine **4** or **4'**, which increased the yield of **3Ba** to 78% (Entry 7), which indicates a possibility to establish an efficient catalytic system for synthesis of polysubstituted pyridines.

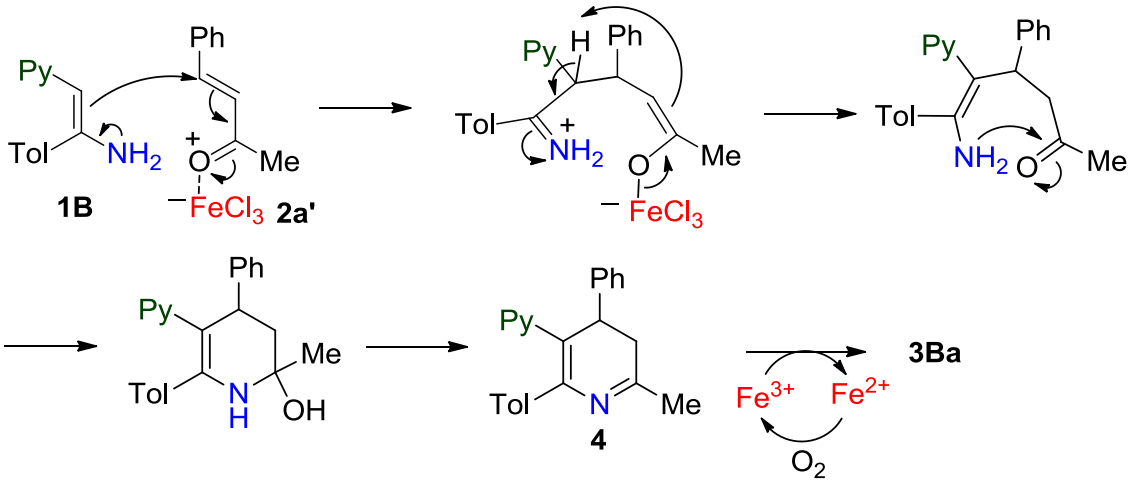

Scheme 2. A plausible mechanism.

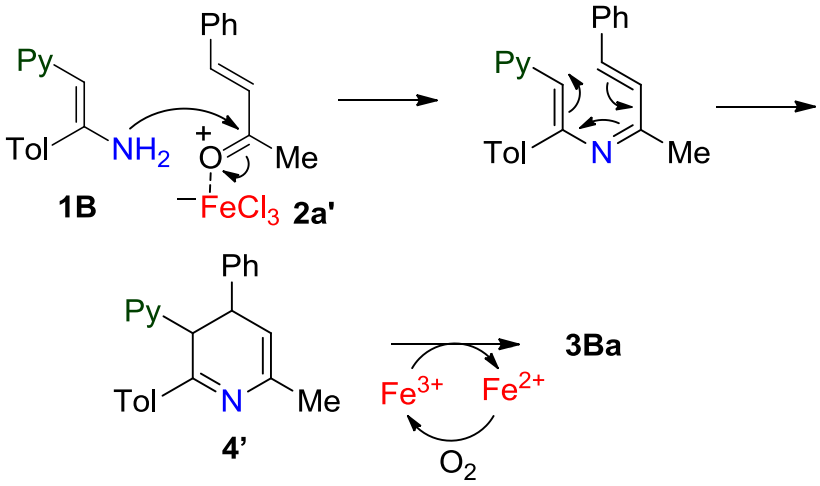

Scheme 3. Another acceptable reaction mechanism.

2.4 Synthesis of bipyridine and terpyridine scaffolds

My protocol facilitated the synthesis and molecular design of multiply substituted pyridines **3** by simple alteration of substrates **1** and **2**. This advantage prompted us to synthesize substituted bipyridine **3Bs** and terpyridine **3Gs** (Scheme 4). Enamine **1B** reacted with enone **2s** to furnish bipyridine **3Bs**. However, α-(2-pyridyl)enamine **1G** did not undergo the reaction at all; this is thought to be due to the formation of a complex of **1G** with $FeCl_3$ because the reaction mixture became purple immediately after the addition of $FeCl_3$. This abovementioned problem was overcome by replacing the Lewis acid from $FeCl_3$ to the non-coordinating $InCl_3$, and terpyridine **3Gs** was successfully produced although 1 equiv. $InCl_3$ was necessary for the efficient reaction. Furthermore, fully arylated bipyridine **3Ct** could be synthesized in 17% yield by the condensation of enamine **1C** with (α,β-diaryl)ethenyl pyridyl ketone **2t** in the presence of $FeCl_3$ (Figure 3).

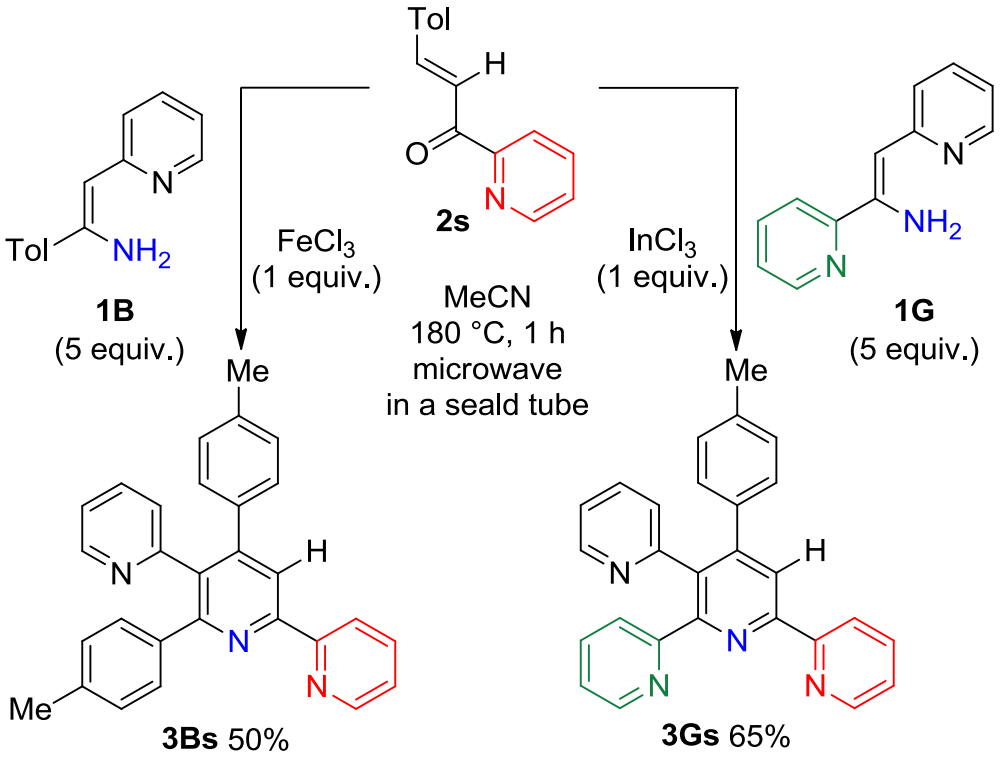

Scheme 4. Synthesis of oligopyridines **3Bs** and **3Gs**.

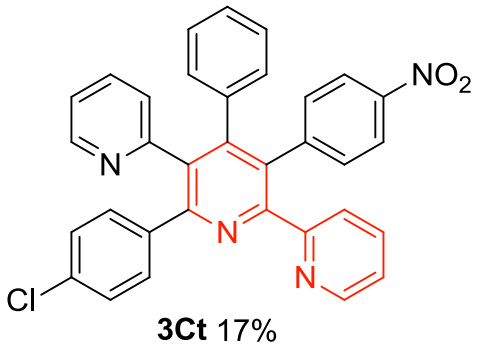

3Ct 17%

Figure 3. Fully arylated bipyridine **3Ct**.

2.5 Design and synthesis of ligand for transition metal complex

In last sections, a synthetic method for polysubstituted 3-(2-pyridyl)pyridines was established. This method facilitates modification of the pyridine ring on demand by altering substrates. This feature can be applied to molecular design of new ligands. The 2-phenylpyridine framework is well known to serve as a bidentate ligand. My synthesized pyridines possess two 2-phenylpyridine partial structures, which is considered to serve as a dinucleating ligand (**3L**) as illustrated in Figure 4. The presence of the 2-pyridyl group at the 3-position and central pyridine ring are considered to coordinate to different metals, respectively. In order to recognize two different metals and inhibit the formation of coordination polymer, different coordination ability should be added. Hence, the carboxy group is introduced into the 6-position.

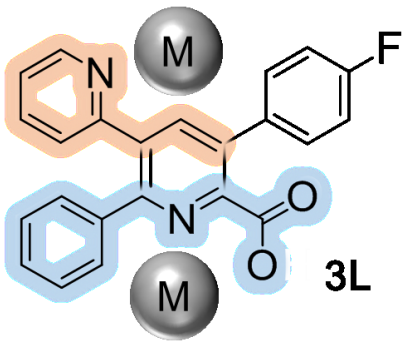

Figure 4. Conceptual illustration of a novel compound serve as a dinucleating ligand.

Compound **3L** was synthesized *via* two steps as shown in Scheme 5. β-(2-Pyridyl)enamine was condensed with 3-(4-fluorophenyl)-3-buten-2-one in the presence of $FeCl_3$ to afford triarylated pyridine (**3Au**) in 69% yield. The methyl group was then converted to a carboxy group upon oxidation using $KMnO_4$, which afforded ligand **3L** in 46% yield. The structure was confirmed by NMR, IR and high-resolution mass spectroscopies (HR-MS).

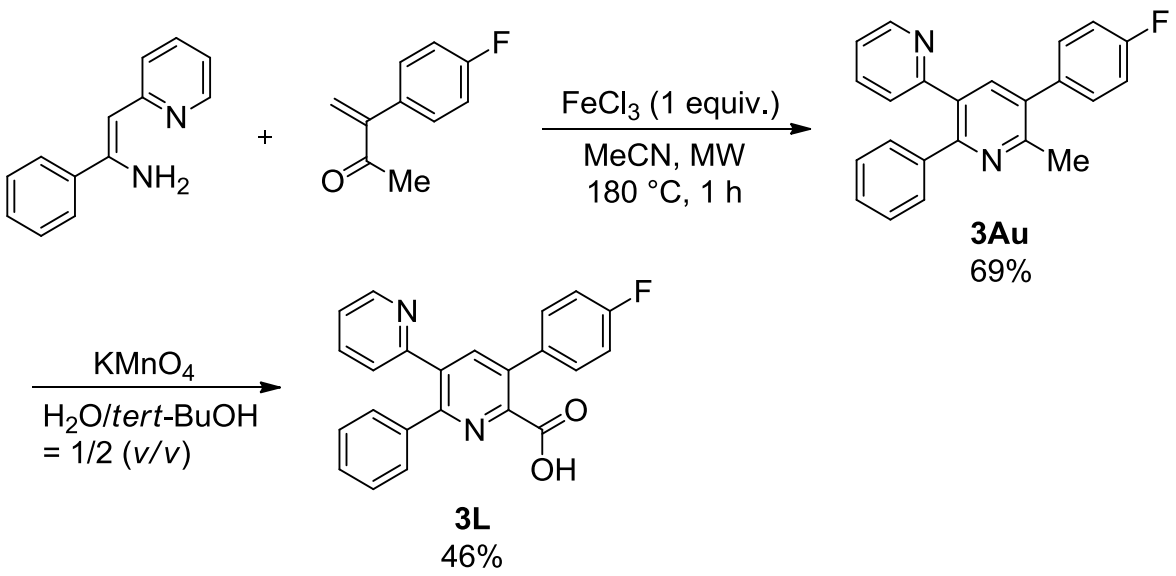

Scheme 5. Synthetic procedure of **3L**.

2.6 Synthesis of platinum mononuclear complex

Compound **3L** was allowed to react with *cis*-dichloridobis(dimethyl sulfoxide)platinum(II) in the presence of sodium acetate in a sealed tube at 110 °C. The HR-MS spectrum indicated the formation of chlorido[3-(4-fluorophenyl)-6-phenyl-5-(2-pyridyl)-2-pyridinecarboxylato]platinum(II) sodium salt (**4L**$_{Na}$) in the reaction mixture; however, it could not be isolated because of low solubility in common organic solvents such as ethanol, methanol, *N*,*N*-dimethylformamide (DMF) and dimethyl sulfoxide (DMSO). In order to increase the solubility and to facilitate the purification, cation exchange from sodium ion to tetra-*n*-butylammonium (TBA) ion was attempted. When a suspension of **4L**$_{Na}$ in acetone was treated with excess amount of tetrabutylammonium chloride (TBACl), **4L**$_{TBA}$ was obtained in 76% crude yield (Scheme 6). Although the formation of **4L**$_{TBA}$ was confirmed by ^{1}H NMR and HR-MS, it was still a mixture with TBACl. Several attempts such as washing with water, gel permeation chromatography, and alumina column chromatography, was employed to remove the TBACl, however, only decomposition of **4L**$_{TBA}$ was observed.

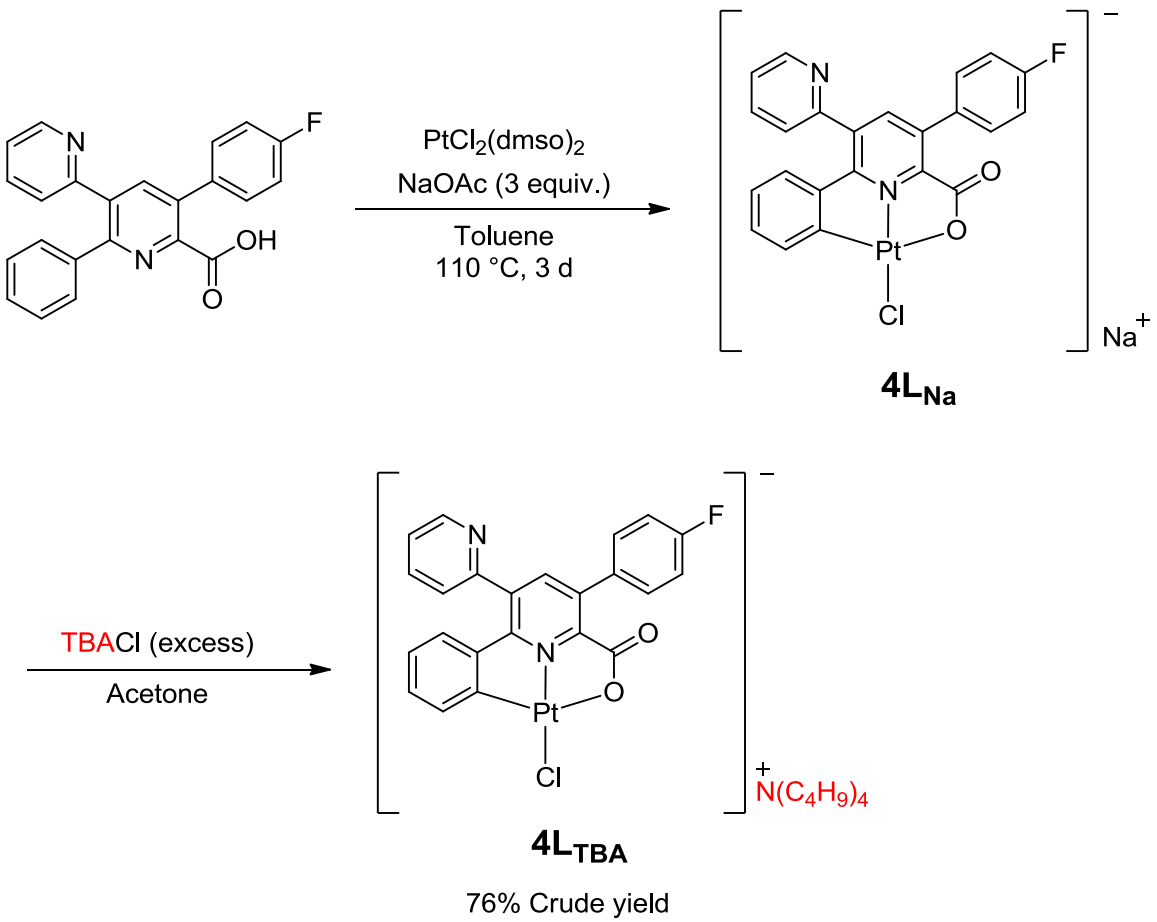

Scheme 6. Synthesis of platinum complexes.

2.7 Recrystallization of $4L_{TBA}$ and X-ray crystallographic analysis

Although several attempts for purification were failed, recrystallization from methanol/chloroform was possible, which afforded a single crystal. As a result of X-ray crystallographic analysis, the structure of the crystalline product was determined to be trinuclear platinum complex (**$4L_{Pt3}$**) (Figure 5), which was also supported by HR-MS. However, further analysis could not be performed because **$4L_{Pt3}$** was not dissolved in the common organic solvents. The structural difference of the complex is considered to depend the concentration. In the concentrated solution, platinum is easily coordinated by chloride ion to form mononuclear complex because excess amounts of chlorides present around platinum. On the other hand, the complex aggregates during the recrystallization because the concentration of chloride is low resulted from dilution by the solvent. In this case, 2-pyridyl group at the 3-position coordinates platinum of another molecule closed together to form a trinuclear platinum complex.

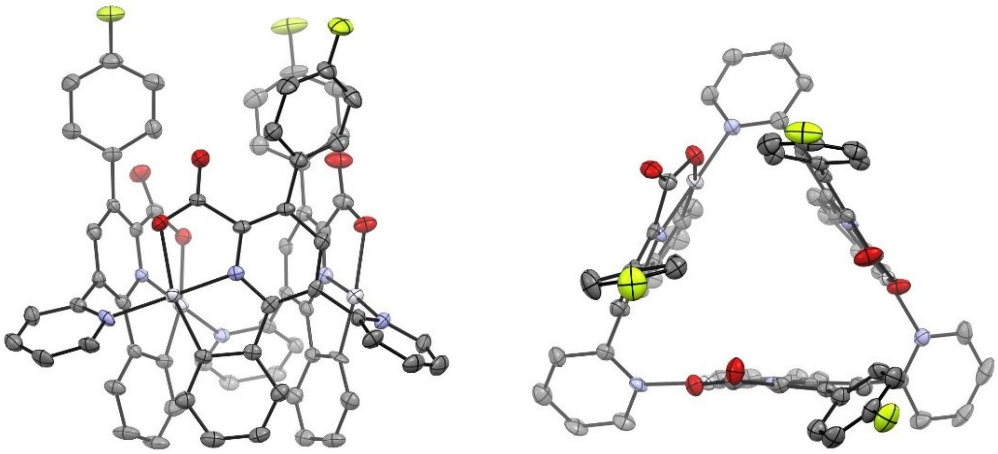

Figure 5. ORTEP of the single crystal structure of **$4L_{Pt3}$**. Ellipsoids are shown at the 50% probability level. Hydrogen atoms are omitted for clarity.

2.8 Measurement of absorption spectra of $4L_{Pt3}$, $4L_{TBA}$ and 3L in $CHCl_3$

Figure 6 shows absorption spectra of the compounds **$4L_{Pt3}$**, **$4L_{TBA}$** and **3L** in chloroform. The absorption bands of **$4L_{Pt3}$** and **$4L_{TBA}$** observed at around 272 and 299 nm could be assigned to the ππ* transition of the ligand (ligand-centered (LC) transition), which is closely similar to the vibrionic structure to that of **3L**. In addition, the metal-to-ligand charge transfer (MLCT) absorption bands of **$4L_{Pt3}$** and **$4L_{TBA}$** were also observed at 361 and 389 nm, respectively. The MLCT absorption band of **$4L_{Pt3}$** was shifted to shorter wavelength than that of **$4L_{TBA}$**.

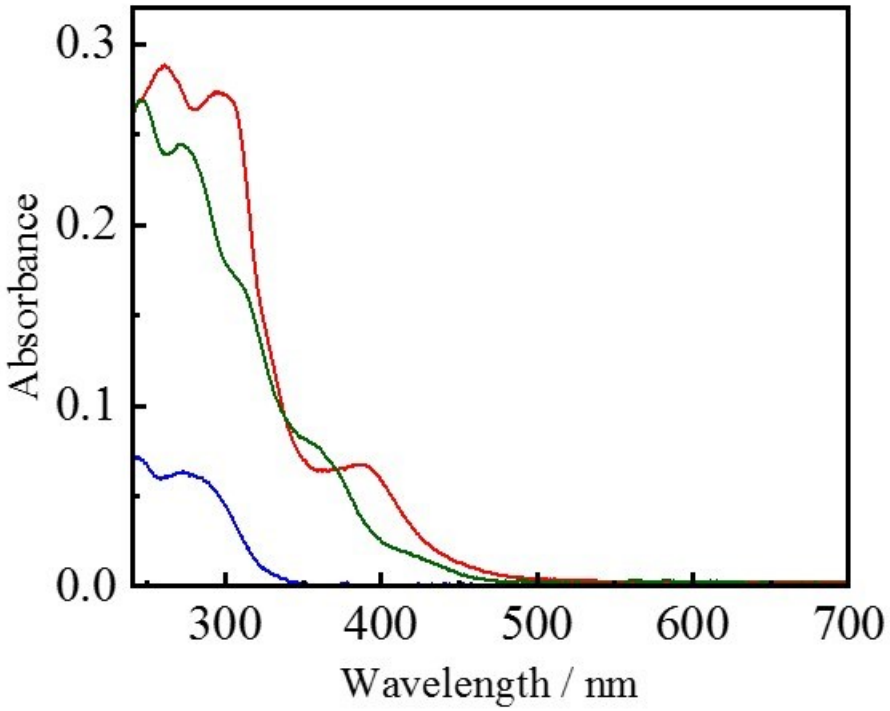

Figure 6. Absorption spectra of **$4L_{Pt3}$** (green), **$4L_{TBA}$** (red) and **3L** (blue) in $CHCl_3$.

This result is considered to be due to the energy gap change of the two molecular orbitals (e_g and t_{2g}) caused by the ligand-field splitting of the d orbital. A planar four-coordinating platinum complex can be regarded as a lack of ligand in the z-axis from the octahedral structure, thus the molecular orbital will split as shown in Figure 7. The value of the ligand-field splitting energy (Δ_o) of pyridine is larger than that of chloride in the spectrochemical series, in **4L$_{Pt3}$**, the d_{xy} orbitals were more stabilized than that in the chlorine-substituted product, which results in the shift to shorter wavelength of the MLCT absorption band.

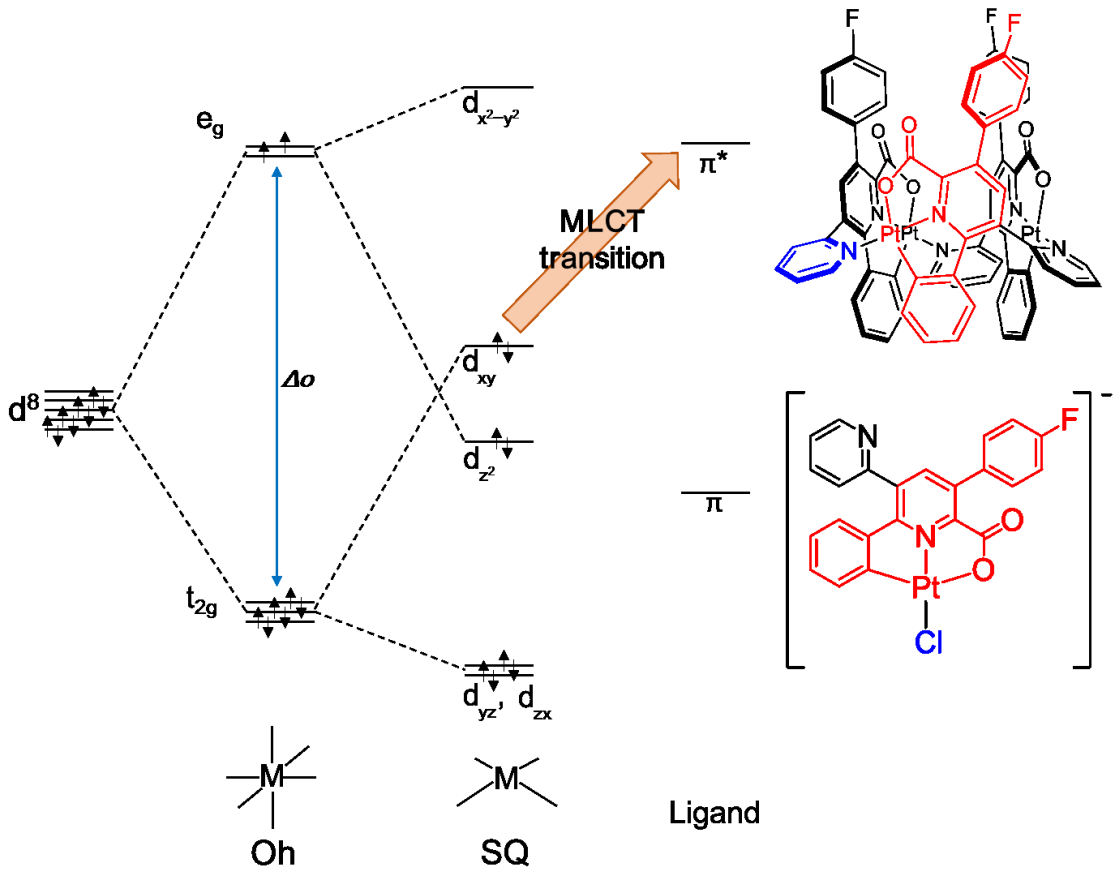

Figure 7. Energy level diagram of a four-coordinate planar structure.

Chapter 3 Conclusions

Synthesis of polyarylpyridines was presented, which was achieved upon condensation of β-(2-pyridyl)enamine **1** and α,β-unsaturated ketone **2** in the presence of $FeCl_3$ under air. In this reaction, $FeCl_3$ plays the role of not only an acid catalyst but also an oxidant for the intermediate dihydropyridine. The substituents can be easily modified by altering the substrates to obtain tri-, tetra- and pentaarylpyridines **3** from commercially available reagents *via* only three steps.

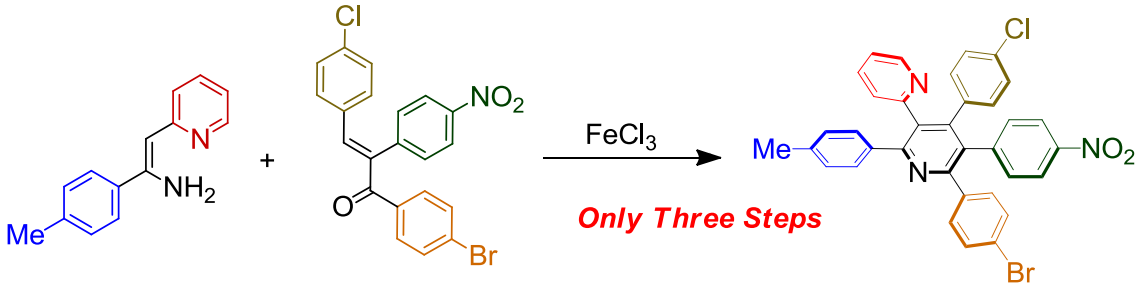

The prepared polysubstituted pyridines possess two coordination sites, which was expected to afford multinuclear complexes. In this study, ligand **3L** was designed and synthesized *via* two steps. The ligand **3L** formed a mononuclear complex with platinum, which was found to aggregate to form a cage-type trinuclear complex during the recrystallization.

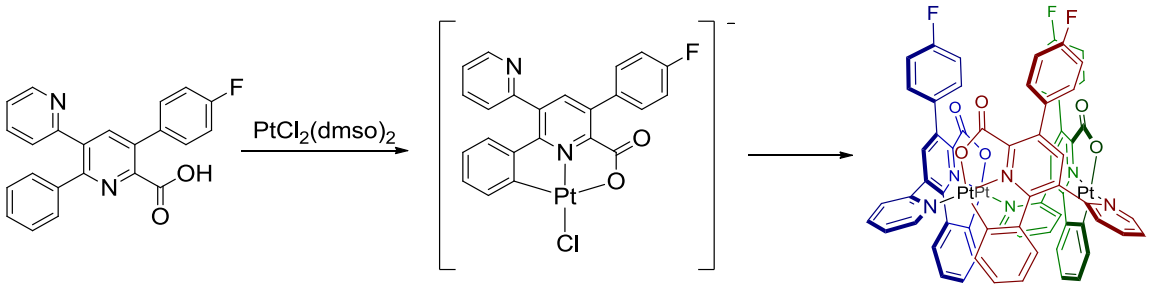

The results obtained here will provide useful insights for synthetic chemistry of heterocyclic compounds and for coordination chemistry.

Chapter 4 Experimental section

4.1 Synthesis and Identifications. All reagents were purchased from commercial sources and used without further purification. Dry acetonitrile was also purchased from commercial source and used as received.

^{1}H and ^{13}C NMR spectra were recorded on Bruker DPX-400 spectrometer (400 MHz and 100 MHz, respectively) in $CDCl_3$ using tetramethylsilane as an internal standard (0.00 ppm). When stereoisomers were obtained as a mixture, integral value for the *E* isomer was indicated as H*E*, and that for the *Z* isomer was indicated as H*Z* in the ^{1}H NMR. The assignments of the ^{13}C NMR were performed by DEPT experiments. IR spectra were recorded on a JASCO FT/IR-4200 spectrometer equipped with an ATR detector. High-resolution mass spectra were obtained on an AB SCEIX Triplet TOF 4600 mass spectrometer. Melting points were recorded on an SRS-Optimelt automated melting point system and were uncorrected. Microwave heating was performed by Anton-Paar Microwave 300 (850 W, 2455 MHz) using 10 mL glass vessel. Data collection for X-ray crystal analysis was performed on Rigaku/R-AXIS RAPID (CuKα λ = 1.54187 Å), Rigaku/XtaLAB Synergy-S/Cu (CuKα λ = 1.54187 Å) diffractometers and Rigaku XtaLAB Synergy-S/Mo system (λ = 0.71073 Å (Mo-Kα)). The single crystal of **3Br** and **4L$_{Pt3}$** were obtained by recrystallization from $CHCl_3$–Hexane and $CHCl_3$–Methanol, respectively. The structures were solved by direct methods (ShelXL) and refined through full-matrix least-squares techniques on *F*2 using ShelXL and Olex2 crystallographic software packages.[14−16]

***1-amino-1-phenyl-2-(2-pyridyl)ethene* (1A);[12] Typical Procedure.** Enamines **1** were prepared according to the method described in literature.[12] To a solution of

diisopropylamine (1.0 g, 10 mmol) in tetrahydrofuran (10 mL), a solution of *n*-butyllithium (1.6 mol/dm^3 (M) in *n*-hexane, 6.9 mL, 11 mmol) was added at −70 °C. After stirring for 0.5 h at the same temperature, 2-methylpyridine (0.73 g, 10 mmol) was added dropwise, and the resultant mixture was stirred for further 1 h. Benzonitrile (1.0 g, 10 mmol) was gradually added to the solution, and stirred at −70 °C for 1 h. After elevating the reaction temperature, the solution was stirred at room temperature for further 1 h. After quenching the reaction with water, the mixture was extracted with ethyl acetate (30 mL × 3). The organic layer was dried over magnesium sulfate, and was concentrated under reduced pressure. The residue was washed with hexane (30 mL) to afford **1A** as a yellow solid (1.92 g, 9.8 mmol, 98%). ^{1}H NMR (400 MHz, $CDCl_3$) δ 8.44 (1H, ddd, *J* = 4.8, 2.0, 1.2 Hz), 7.63–7.61 (2H, m), 7.48 (1H, ddd, *J* = 8.0, 8.0, 2.0 Hz), 7.39–7.36 (3H, m), 7.00 (1H, ddd, *J* = 8.0, 1.2, 1.2 Hz), 6.84 (1H, ddd, *J* = 8.0, 4.8, 2.0 Hz), 6.90–6.63 (1H, br), 5.48 (1H, s). Other enamines **1B–D** and **1G** were prepared by condensation of the corresponding benzonitrile derivatives and methylarenes in the same way.

1-Amino-1-(4-methylphenyl)-2-(2-pyridyl)ethene **(1B).**[17] Yellow solid (1.91 g, 9.1 mmol, 91%). ^{1}H NMR (400 MHz, $CDCl_3$) δ 8.44 (1H, ddd, *J* = 4.8, 1.2, 0.8 Hz), 7.52 (2H, d, *J* = 8.0 Hz), 7.49 (1H, ddd, *J* = 8.4, 8.4, 1.6 Hz), 7.21 (2H, d, *J* = 8.0 Hz), 7.00 (1H, ddd, *J* = 8.4, 0.8, 0.8 Hz), 6.84 (1H, ddd, *J* = 8.4, 4.8, 1.2 Hz), 6.93–6.67 (1H, br), 5.47 (1H, s), 2.38 (3H, s).

1-Amino-1-(4-chlorophenyl)-2-(2-pyridyl)ethene **(1C).**[17] Yellow solid (2.17 g, 9.4 mmol, 94%). ^{1}H NMR (400 MHz, $CDCl_3$) δ 8.45 (1H, ddd, *J* = 6.0, 1.6, 1.2 Hz), 7.55 (2H, d, *J* = 8.4 Hz), 7.49 (1H, ddd, *J* = 8.0, 1.6, 1.6 Hz), 7.36 (2H, d, *J* = 8.4 Hz), 7.00 (1H, ddd, *J* = 8.0, 1.2, 1.2 Hz), 6.84 (1H, ddd, *J* = 8.0, 6.0, 1.6 Hz), 6.83–6.65 (1H, br),

5.45 (1H, s).

1-Amino-2-(2-pyridyl)-1-[4-(trifluoromethyl)phenyl]ethane **(1D).** Yellow solid (2.28 g, 8.6 mmol, 86%). Mp 120.3–120.7 °C. ^{1}H NMR (400 MHz, $CDCl_3$) δ 8.48 (1H, ddd, *J* = 4.8, 1.2, 0.8 Hz), 7.75 (2H, d, *J* = 8.0 Hz), 7.65 (2H, d, *J* = 8.0 Hz), 7.53 (1H, ddd, *J* = 8.0, 8.0, 1.6 Hz), 7.05 (1H, ddd, *J* = 8.0, 0.8, 0.8 Hz), 6.91 (1H ddd, *J* = 8.0, 4.8, 1.2 Hz), 6.99–6.67 (1H, br), 5.52 (1H, s), 2.38 (3H, s); ^{13}C NMR (100 MHz, $CDCl_3$) δ 159.3 (C), 148.6 (C), 147.6 (CH), 143.5 (C), 135.8 (CH), 130.5 (C, q, *J* = 136.0Hz), 126.4 (CH), 125.6 (CH, q, *J* = 3.8 Hz), 125.5 (C, q, *J* =271.0 Hz), 122.6 (CH), 118.0 (CH), 97.19 (CH); IR (KBr/cm^{-1}) 3466, 1733, 1618, 1473, 1335, 1168, 1112, 1077, 845, 800, 749; HRMS (ESI/TOF) calcd. for $[M+H]^+$ $C_{14}H_{12}F_3N_2$: 265.0947, found: 265.0945.

1-Amino-1,2-bis(2-pyridyl)ethene **(1G).**[18] Yellow solid (1.53 g, 7.8 mmol, 78%). ^{1}H NMR (400 MHz, CD_3CN) δ 8.59 (1H, ddd, *J* = 4.8, 2.0, 1.2 Hz), 8.46 (1H, ddd, *J* = 4.8, 2.0, 0.8 Hz), 7.88 (1H, ddd, *J* =8.4, 0.8, 0.8), 7.76 (1H, ddd, *J* = 8.4, 8.4, 2.0 Hz), 7.56 (1H, ddd, *J* = 8.0, 8.0, 2.0 Hz), 7.30 (1H, ddd, *J* = 8.4, 4.8, 0.8 Hz), 7.13 (1H, ddd, *J* = 8.0, 0.8, 0.8 Hz), 6.91 (1H, ddd *J* = 8.0, 4.8, 2.0 Hz), 6.83–6.65 (1H, br), 5.99 (1H, s).

Synthesis of enones 2. Enones **2** were prepared by aldol condensation by **Method a** or **Method b** except for commercially available **2a**.

Method a: To a methanol solution (30 mL) of 2-napthaldehyde (1.56 g, 10 mmol) and acetone (0.74 mL, 10 mmol), 0.5 M aqueous solution of potassium hydroxide (20 mL, 10 mmol) was added. The resultant mixture was stirred at room temperature for 0.5 h. Precipitated solid was collected by filtration to afford 4-(2-naphthyl)-3-buten-2-one (**2b**)[19] as a colorless solid (1.96 g, 10 mmol, quant.). The product was used for the

subsequent condensation with enamine **1** without further purification. ^{1}H NMR (400 MHz, $CDCl_3$) δ 7.94 (1H, s), 7.86–7.81 (3H, m), 7.68–7.64 (1H, m), 7.65 (1H, d, *J* = 16.4 Hz), 7.52–7.50 (2H, m), 2.41 (3H, s). Other enones **2c–l** were prepared in the same way. When product was formed as an oil, the mixture was extracted with dichloromethane (30 mL × 3), and the organic layer was dried over magnesium sulfate, and concentrated. The residual oil was used for the subsequent condensation with enamine **1** without further purification. For the preparation of α,β-disubstituted enones, **Method b** was effective rather than **Method a**.

3-(4-Methoxyphenyl)-1-(4-methylphenyl)-2-propen-1-one **(2c).**[20] Colorless solid (1.01 g, 4.0 mmol, 40%). ^{1}H NMR (400 MHz, $CDCl_3$) δ 7.93 (2H, d, *J* = 8.4 Hz), 7.77 (1H, d, *J* = 15.6 Hz), 7.60 (2H, d, *J* = 8.8 Hz), 7.34 (1H, d, *J* = 15.6 Hz), 7.29 (2H, d, *J* = 8.4 Hz), 6.93 (2H, *J* = 8.8 Hz), 3.85 (3H, s), 2.43 (3H, s).

1-(4-Methylphenyl)-3-phenyl-2-propen-1-one **(2d).**[20] Yellow oil (2.00 g, 9.0 mmol, 90%). ^{1}H NMR (400 MHz, $CDCl_3$) δ 7.93 (2H, d, *J*= 8.4 Hz), 7.79 (1H, d, *J* = 15.6 Hz), 7.64–7.62 (2H, m), 7.52 (1H, d, *J* = 15.6 Hz), 7.41–7.39 (3H, m), 7.29 (2H, d, *J* = 8.4 Hz), 2.42 (3H, s).

3-(4-Fluorophenyl)-1-(4-methylphenyl)-2-propen-1-one **(2e).**[21] Colorless solid (2.11 g, 8.8 mmol, 88%). ^{1}H NMR (400 MHz, $CDCl_3$) δ 7.93 (2H, d, *J* = 8.0 Hz), 7.76 (1H, d, *J* = 16.0 Hz), 7.65–7.61 (2H, m), 7.45 (1H, d, *J* = 16.0 Hz), 7.30 (2H, d, *J* = 8.0 Hz), 7.13–7.08 (2H, m), 2.44 (3H, s).

3-(4-Cyanophenyl)-1-(4-methylphenyl)-2-propen-1-one **(2f).**[22] Colorless solid (1.21 g, 4.9 mmol, 49%). ^{1}H NMR (400 MHz, $CDCl_3$) δ 7.93 (2H, d, *J* = 8.0 Hz), 7.76 (1H, d, *J*

= 18.0 Hz), 7.41–7.69 (4H, m), 7.60 (1H, d, *J* = 18.0 Hz), 7.32 (2H, d, *J* = 8.0 Hz), 2.45 (3H, s).

3-(4-Chlorophenyl)-1-phenyl-2-propen-1-one **(2g).**[23] Yellow solid (1.65 g, 6.8 mmol, 68%). ^{1}H NMR (400 MHz, $CDCl_3$) δ 8.03–8.00 (2H, m), 7.75 (1H, d, *J* = 16.0 Hz), 7.56–7.57 (3H, m), 7.52–7.48 (2H, m), 7.39 (2H, d, *J* = 8.4 Hz).

3-(4-Chlorophenyl)-1-(4-nitrophenyl)-2-propen-1-one **(2h).**[24] Yellow solid (2.88 g, 10 mmol, quant.) ^{1}H NMR (400 MHz, $CDCl_3$) δ 8.35 (2H, d, *J* = 8.8 Hz), 8.12 (2H, d, *J* = 8.8 Hz), 7.80 (1H, d, *J* =16.4 Hz), 7.59 (2H, d, *J* = 8.4 Hz), 7.45 (1H, d, *J* = 16.4 Hz), 7.42 (2H, d, *J* = 8.4 Hz).

3-(4-Chlorophenyl)-1-(4-methoxyphenyl)-2-propen-1-one **(2i).**[24] Yellow solid (1.80 g, 6.6 mmol, 66%). ^{1}H NMR (400 MHz, $CDCl_3$) δ 8.03 (2H, d, *J* = 8.8 Hz), 7.74 (1H, d, *J* = 16.0 Hz), 7.56 (2H, d, *J* = 8.4 Hz), 7.50 (1H, d, *J* = 16.0 Hz), 7.38 (2H, *J* = 8.4 Hz), 6.98 (2H, d, *J* = 8.6 Hz), 3.89 (3H, s).

3-(4-Chlorophenyl)-1-(2-methoxyphenyl)-2-propen-1-one **(2j).**[25] Yellow oil (2.62 g, 9.6 mmol. 96%). ^{1}H NMR (400 MHz, $CDCl_3$) δ 7.62 (1H, dd, *J* = 7.6, 1.6 Hz), 7.57 (1H, d, *J* = 16.0 Hz), 7.50–7.46 (3H, m), 7.38–7.35 (2H, m), 7.35 (1H, d, *J* = 16.0 Hz), 7.05 (1H, ddd, *J* = 7.6, 7.6, 1.2 Hz), 7.00 (1H, d, *J* = 8.4 Hz), 3.91 (3H, s).

1-(4-Chlorophenyl)-3-[4-(1,1-dimethylethyl)phenyl]-2-propen-1-one **(2k).**[26] Colorless solid (1.97 g, 6.6 mmol, 66%). ^{1}H NMR (400 MHz, $CDCl_3$) δ 7.96 (2H, d, *J* = 8.8 Hz), 7.80 (1H, d, *J* = 15.6 Hz), 7.58 (2H, d, *J* = 8.4 Hz), 7.48 (2H, d, *J* = 8.4 Hz), 7.45 (1H, d, *J* = 15.6 Hz), 7.44 (2H, d, *J* = 8.8 Hz), 1.35 (9H, s).

3-(4-Methoxyphenyl)-1-(4-nitrophenyl)-2-propen-1-one **(2l).**[27] Yellow solid (2.07 g, 7.3 mmol, 73%). ^{1}H NMR (400 MHz, $CDCl_3$) δ 8.34 (2H, d, *J* = 9.2 Hz), 8.13 (2H, d, *J* = 9.2 Hz), 7.82 (1H, d, *J* = 15.6 Hz), 7.62 (2H, d, *J* = 8.4 Hz), 7.35 (1H, d, *J* = 15.6 Hz), 6.96 (2H, d, *J* = 8.4 Hz), 3.87 (3H, s).

Method b: To a toluene solution (50 mL) of 4-chlorobenzaldehyde (1.40 g, 10 mmol) and propanoylbenzene (1.34 g, 10 mmol), piperidine (0.20 mL, 2.0 mmol) and acetic acid (0.11 mL, 2.0 mmol) were added. The resultant mixture was heated under reflux using Dean-Stark apparatus for 1 d. After concentration, the residue was treated with column chromatography on silica gel to afford 3-(4-chlorophenyl)-2-methyl-1-phenyl-2-propen-1-one (**2o**)[28] as colorless needles (1.05 g, 4.1 mmol, 41%). ^{1}H NMR (400 MHz, $CDCl_3$) δ 7.74–7.72 (2H, m), 7.55 (1H, ddd, *J* = 7.6, 0.6, 0.6 Hz), 7.47–7.44 (2H, m), 7.38–7.32 (4H, m), 7.10 (1H, d, *J* = 1.2 Hz), 2.23 (3H, d, *J* = 1.2 Hz). Other enones **2m–t** were prepared in the same way.

2-(4-Nitrophenyl)-1-phenyl-2-propen-1-one **(2m).**[29] Yellow oil (1.24 g, 4.9 mmol, 49%). 1H NMR (400 MHz, $CDCl_3$) δ 8.22 (2H, d, *J* = 8.8 Hz), 7.90–7.87 (2H, m), 7.62 (2H, d, *J* = 8.8 Hz), 7.49–7.45 (3H, m), 6.26 (1H,s), 5.88 (1H, s).

1-(4-Methoxyphenyl)-2-(4-nitrophenyl)-2-propen-1-one **(2n).** Yellow oil (2.21 g, 7.8 mmol, 78%). ^{1}H NMR (400 MHz, $CDCl_3$) δ 8.20 (2H, d, *J* = 9.2 Hz), 7.90 (2H, d, *J* = 9.2 Hz), 7.61 (2H, d, *J* = 8.8 Hz), 6.94 (2H, d, *J* = 8.8 Hz), 6.18 (1H, s), 5.79 (1H, s), 3.88 (3H, s); ^{13}C NMR (100 MHz, $CDCl_3$) δ 194.8 (C), 164.1 (C), 147.6 (C), 146.5 (C), 143.5 (C), 132.4 (CH), 129.3 (C), 127.9 (CH), 123.9 (CH), 123.0 (CH_2), 113.9 (CH), 55.6 (CH_3); IR (ATR/cm^{-1}) 1654, 1593, 1512, 1342, 1257, 1165, 848, 705; HRMS (ESI/TOF)

calcd. for $[M+H]^+$ $C_{16}H_{14}NO_4$: 284.0917, found: 284.0909.

3-(4-Chlorophenyl)-2-(4-nitrophenyl)-1-phenyl-2-propen-1-one **(2p).** Colorless needles (1.49 g, 4.1 mmol, 41%). Mp 133.9–134.2 °C. ^{1}H NMR (400 MHz, $CDCl_3$) δ 8.22 (2H, d, *J* = 8.8 Hz), 7.85–7.83 (2H, m), 7.61–7.57 (1H, m), 7.51–7.45 (4H, m), 7.32 (1H, s), 7.19 (2H, d, *J* = 8.4 Hz), 6.98 (2H, d, *J* = 8.4 Hz); ^{13}C NMR (100 MHz, $CDCl_3$) δ 196.2 (C), 147.6 (C), 143.2 (C), 140.9 (CH), 139.1 (C), 137.4 (C), 135.7 (C), 132.7 (CH), 132.3 (C), 131.4 (CH), 130.9 (CH), 129.7, (CH), 128.9 (CH), 128.6 (CH), 124.1 (CH); IR (KBr/cm^{-1}) 1725, 1650, 159, 1518, 1254, 1091, 854, 752, 700; HRMS (ESI/TOF) calcd. for $[M+H]^+$ $C_{21}H_{15}ClNO_3$: 364.0735, found: 364.0723.

2-(4-Nitrophenyl)-1,3-diphenyl-2-propen-1-one **(2q).** White powder (2.37 g, 7.2 mmol, 72%, *E*/*Z* = 61/39). Mp 157.2–158.0 °C. ^{1}H NMR (400 MHz, $CDCl_3$) δ 8.22–8.19 (2H*E*, m), 8.22–8.19 (2H*Z*, m), 7.96–7.94 (2H*Z*, m), 7.86–7.84 (2H*E*, m), 7.62 (2H*Z*, d, *J* = 6.8 Hz), 7.61–7.57 (1H*E*, m), 7.51–7.46 (2H*E*, m), 7.51–7.46 (2H*Z*, m), 7.39–7.19 (6H*E*, m), 7.39–7.19 (7H*Z*, m), 7.04 (2H*E*, d, *J* = 8.0 Hz); ^{13}C NMR (100 MHz, $CDCl_3$) δ 198.3 (C), 196.6 (C), 147.4 (C), 147.3 (C), 144.3 (C), 143.7 (C), 142.7 (CH), 138.64 (C), 138.62 (C), 137.7 (C), 135.8 (C), 134.5 (C), 134.2 (CH), 133.8 (C), 133.6 (CH), 132.6 (CH), 131.0 (CH), 130.3 (CH), 129.8 (CH), 129.7 (CH), 129.6 (CH), 129.2 (CH), 128.9 (CH), 128.6 (CH), 128.5 (CH), 127.1 (CH), 124.2 (CH), 123.9 (CH) Signals for these isomers could not be distinguished, and a CH signal is lacked presumably due to overlapping; IR (KBr/cm^{-1}) 1594, 1647, 1517, 1344, 1253, 848, 695; HRMS (ESI/TOF) calcd. for $[M+H]^+$ $C_{21}H_{16}NO_3$: 330.1124, found: 330.1113.

1-(Bromophenyl)-3-(4-chlorophenyl)-2-(4-nitrophenyl)-2-propen-1-one **(2r).** Yellow powder (2.86 g, 6.5 mmol, 65%, *E*/*Z* = 70/30). Mp 168.7–169.3 °C. ^{1}H NMR (400 MHz,

$CDCl_3$) δ 8.24–8.20 (2H*E*, m), 8.24–8.20 (2H*Z*, m), 7.79 (2H*Z*, d, *J* = 8.8 Hz), 7.69 (2H*E*, d, *J* = 8.8 Hz), 7.62 (2H*E*, d, *J* = 8.8 Hz), 7.59 (2H*Z*, d, *J* = 9.2 Hz), 7.53 (2H*Z*, d, *J* = 9.2 Hz), 7.44 (2H*E*, d, *J* = 8.8 Hz), 7.31 (1H*E*, s), 7.29 (1H*Z*, s), 7.22–7.19 (2H*E*, m), 7.22–7.19 (2H*E*+2H*Z*, m), 6.97 (2H*Z*, d, *J* = 8.4 Hz); ^{13}C NMR (100 MHz, $CDCl_3$) δ 197.0 (C), 195.1 (C), 147.6 (C), 143.6 (C), 142.9 (C), 141.2 (CH), 138.8 (C), 138.7 (C) 136.2 (C), 136.0 (C), 134.4 (C), 132.8 (C), 132.5 (CH), 132.3 (CH), 132.0 (C), 131.9 (CH), 131.5 (CH), 131.2 (CH), 130.9 (CH), 130.8 (CH), 130.3 (CH), 129.1 (CH), 129.0 (CH), 127.9 (C), 127.1 (CH), 124.3 (CH), 124.1 (CH) three quaternary carbon signals could not be observed; IR (KBr/cm^{-1})1657, 1585, 1515, 1346, 1251, 1017, 1010, 852, 819; HRMS (ESI/TOF) calcd. for $[M+H]^+$ $C_{21}H_{14}BrClNO_3$: 441.9840, found: 441.9834.

3-(4-Methylphenyl)-1-(2-pyridyl)-2-propen-1-one **(2s).**[30] Dark brown solid (0.71 g, 3.2 mmol, 32%). ^{1}H NMR (400 MHz, $CDCl_3$) δ 8.73 (1H, ddd, *J* = 4.8, 1.2, 0.8 Hz), 8.25 (1H, d, *J* = 16.0 Hz), 8.18 (1H, ddd, *J* = 8.0, 1.2, 1.2 Hz), 7.93 (1H, d, *J* = 16.0 Hz), 7.88 (1H, ddd, *J* = 8.0, 8.0, 1.2 Hz), 7.64 (2H, d, *J* = 8.0 Hz), 7.48 (1H, ddd, *J* = 8.0, 4.8, 1.2 Hz), 7.22 (2H, d, *J* = 8.0 Hz), 2.39 (3H, s).

2-(4-Nitrophenyl)-3-phenyl-1-(2-pyridyl)-2-propen-1-one **(2t).** Brown oil (1.55 g, 4.7 mmol, 47%). ^{1}H NMR (400 MHz, $CDCl_3$) δ 8.25 (1H, ddd, *J* = 4.8, 1.6, 0.8 Hz), 8.20 (2H, d, *J* = 8.8 Hz), 7.96–7.94 (2H, m), 7.71 (2H, d, *J* = 8.8 Hz), 7.62 (1H, ddd, *J* = 8.0, 8.0, 1.2 Hz), 7.48 (1H, tt, *J* = 7.2, 1.2 Hz), 7.39–7.33 (3H, m), 7.27 (1H, s), 7.04 (1H, ddd, *J* = 8.0, 4.8, 1.2 Hz); ^{13}C NMR (100 MHz, $CDCl_3$) δ 197.1 (C), 152.4 (C), 148.9 (CH), 147.6 (C), 143.3 (C), 141.9 (C), 137.1 (C), 136.6 (CH) 133.0 (CH), 130.7 (CH), 128.7 (CH), 128.6 (C), 127.3 (CH), 124.5 (CH), 124.2 (CH), 122.7 (CH); IR (KBr/cm^{-1}) 1668, 1595, 1516, 1343, 1222, 1109, 854, 719; HRMS (ESI/TOF) calcd. for $[M+H]^+$

$C_{20}H_{15}N_2O_3$: 331.077, found: 331.1075.

General method of synthesis of polysubstitued pyridines 3. To a solution of 1-amino-1-phenyl-2-(2-pyridinyl)ethene (**1A**) (98.1 mg, 0.5 mmol) in dry acetonitrile (15 mL), were added 4-phenyl-3-buten-2-one (**2a**) (15.0 mg, 0.1 mmol) and iron(III) chloride (12.7 mg, 0.1 mmol), and the resultant solution was heated at 180 °C for 1 h under microwave irradiation. After evaporation of the solvent, the residue was dissolved in ethyl acetate (10 mL). The solution was filtered through silica gel short column, and was further eluted with ethyl acetate (30 mL). The eluted solution was dried over magnesium sulfate, filtered and concentrated under reduced pressure. The residue was purified by flash column chromatography on silica gel (eluent: hexane/ethyl acetate = 8/2) to afford polysubstituted pyridine **3Aa** (27.1 mg, 0.084 mmol, 84%) as a yellow oil. When other enamines **1B–D** and enones **2b–t** were used, reactions were performed in the same way.

6-Methyl-2,4-diphenyl-3-(2-pyridyl)pyridine **(3Aa)**. Yellow oil (27.1 mg, 0.084 mmol, 84%). ^{1}H NMR (400 MHz, $CDCl_3$) δ 8.36 (1H, ddd, *J* = 4.9, 1.6, 0.9 Hz), 7.34 (1H, ddd, *J* = 7.7, 7.7, 1.8 Hz), 7.27–7.26 (2H, m), 7.23 (1H, s), 7.20–7.16 (6H, m), 7.10–7.07 (2H, m), 6.96 (1H, ddd, *J* = 7.7, 4.9, 0.9 Hz), 6.89 (1H, ddd, *J* = 7.7, 0.9, 0.9 Hz), 2.70 (3H, s); ^{13}C NMR (100 MHz, $CDCl_3$) δ 157.8 (C), 157.7 (C), 157.6 (C), 151.2 (C), 150.0 (C), 148.9 (CH), 140.7 (C), 139.3 (CH), 135.2 (CH), 131.2 (C), 129.6 (CH), 129.0 (CH), 127.9 (CH), 127.7 (CH), 127.3 (CH), 126.7 (CH), 123.0 (CH), 121.2 (CH), 24.5 (CH_3); IR (ATR/cm^{-1}) 1589, 1539, 1280, 1029, 748, 698; HRMS (ESI/TOF) calcd. for $[M+H]^+$ $C_{23}H_{19}N_2$: 323.1542, found: 323.1540.

6-Methyl-2-(4-methylphenyl)-4-phenyl-3-(2-pyridyl)pyridine **(3Ba).** Yellow solid (29.0

mg, 0.086 mmol, 86%). Mp 58.2–58.8 °C. ^{1}H NMR (400 MHz, $CDCl_3$) δ 8.37 (1H, ddd, *J* = 4.8, 1.6, 0.8 Hz), 7.35 (1H, ddd, *J* = 7.6, 7.6, 1.2 Hz), 7.20–7.15 (6H, m), 7.09–7.07 (2H, m), 6.99–6.96 (3H, m) 6.89 (1H, ddd, *J* = 8.0, 1.2, 1.2 Hz), 2.69 (3H, s), 2.26 (3H, s); ^{13}C NMR (100 MHz, $CDCl_3$) δ 157.9 (C), 157.9 (C), 157.8 (C), 150.0 (C), 148.9 (CH), 139.5 (C), 137.8 (C), 137.1 (C), 135.3 (CH), 131.0 (C), 129.5 (CH), 129.0(CH), 128.4 (CH), 127.9 (CH), 127.3 (CH), 126.8 (CH), 122.8 (CH), 121.2 (CH), 24.6 (CH_3), 21.1 (CH_3); IR (ATR/cm^{-1}) 1587, 1565, 1539, 1444, 1019, 700; HRMS (ESI/TOF) calcd. for $[M+H]^+$ $C_{24}H_{21}N_2$: 337.1699, found: 337.1708.

2-(4-Methylphenyl)-6-methyl-4-(2-naphthyl)-3-(2-pyridyl)pyridine **(3Bb).** Yellow solid (25.5 mg, 0.066 mmol, 66%). Mp 107.3–107.8 °C. ^{1}H NMR (400 MHz, $CDCl_3$) δ 8.35 (1H, dd, *J* = 5.2, 2.0 Hz), 7.75–7.69 (3H, m), 7.60 (1H, d, *J* = 8.4 Hz), 7.45–7.43 (2H, m), 7.34–7.29 (1H, ddd, *J* = 7.6, 7.6, 1.2 Hz), 7.32 (1H, s), 7.20 (2H, d, *J* = 8.0 Hz), 7.10 (1H, dd, *J* = 8.4, 1.6 Hz), 6.98 (2H, d, *J* = 8.4 Hz), 6.95 (1H, d, *J* = 7.6 Hz), 6.93 (1H, d, *J* = 7.6 Hz), 2.72 (3H, s), 2.26 (3H, s); ^{13}C NMR (100 MHz, $CDCl_3$) δ 157.9 (C), 157.8 (C), 149.9 (C), 148.9 (CH), 137.8 (C), 137.1 (C), 137.3 (CH), 135.4 (CH), 133.0 (C), 133.3 (C), 132.3 (C), 131.2 (C), 129.6 (CH), 128.5 (CH), 128.4 (CH), 127.5 (CH), 127.3 (CH), 126.9 (CH), 126.8 (CH), 126.2 (CH), 126.1 (CH), 123.1 (CH), 121.3 (CH), 24.5 (CH_3), 21.2 (CH_3) One signal (C) was not observed presumably due to overlapping; IR (ATR/cm^{-1}) 1586, 1539, 1508, 1470, 1435, 822, 802, 748; HRMS (ESI/TOF) calcd. for $[M+H]^+$ $C_{28}H_{23}N_2$: 387.1855, found: 387.1841.

4-(4-Methoxylphenyl)-2,6-bis(4-methylphenyl)-3-(2-pyridyl)pyridine **(3Bc).** Yellow solid (24.8 mg, 0.056 mmol, 56%). Mp 72.3–72.8 °C. ^{1}H NMR (400 MHz, $CDCl_3$) δ 8.43 (1H, ddd, *J* = 4.8, 1.6, 0.8 Hz), 8.07 (2H, d, *J* = 8.4 Hz), 7.72 (1H, s), 7.41 (1H, ddd, *J* =

7.6, 7.6, 1.6 Hz), 7.27 (2H, d, *J* = 8.4 Hz), 7.26 (2H, d, *J* = 8.8 Hz), 7.07 (2H, d, *J* = 6.4 Hz), 7.04 (1H, ddd, *J* = 7.6, 4.8, 1.6 Hz), 6.99 (2H, d, *J* = 8.0 Hz), 6.97 (1H, ddd, *J* = 8.6, 4.8, 4.8 Hz), 6.72 (2H, d, *J* = 8.8 Hz), 3.76 (3H, s), 2.41 (3H, s), 2.28 (3H, s); ^{13}C NMR (100 MHz, $CDCl_3$) δ 158.9 (C), 158.1 (C), 157.8 (C), 156.2 (C), 150.2 (C), 149.0 (CH), 139.0 (C), 138.1 (C), 137.2 (C), 136.4 (C), 135.5 (CH), 131.9 (C), 131.8 (C), 130.3 (CH), 129.8 (CH), 129.4 (CH), 128.4 (CH), 127.0 (CH), 126.8 (CH), 121.4 (CH), 119.6 (CH), 113.4 (CH), 55.2 (CH_3), 21.3 (CH_3), 21.2 (CH_3); IR (KBr/cm^{-1}) 1510, 1462, 1442, 1370, 1112, 1021, 736, 622; HRMS (ESI/TOF) calcd. for $[M+H]^+$ $C_{31}H_{27}N_2O$: 443.2117, found: 443.2106.

2,6-Bis(4-methylphenyl)-4-phenyl-3-(2-pyridyl)pyridine **(3Bd).** Yellow solid (27.7 mg, 0.067 mmol, 67%). Mp 69.1–70.1 °C. ^{1}H NMR (400 MHz, $CDCl_3$) δ 8.41 (1H, ddd, *J* = 4.8, 1.6, 0.8 Hz), 8.07 (2H, d, *J* = 8.4 Hz), 7.74 (1H, s), 7.40 (1H, ddd, *J* = 7.6, 7.6, 1.6 Hz), 7.29–7.26 (4H, m), 7.23–7.21 (3H, m), 7.15–7.14 (2H, m), 7.03–7.00 (3H, m), 6.96 (1H, ddd, *J* = 7.6, 0.8, 0.8 Hz), 2.41 (3H, s), 2.28 (3H, s); ^{13}C NMR (100 MHz, $CDCl_3$) δ 157.9 (C), 157.8 (C), 156.3 (C), 150.6 (C), 148.9 (CH), 142.0 (C), 139.7 (C), 139.1 (C), 137.9 (C), 137.3 (C), 136.3 (C), 135.4 (CH), 129.8 (CH), 129.4 (CH), 129.1 (CH), 128.4 (CH), 127.9 (CH), 127.3 (CH), 127.0 (CH), 126.8 (CH), 121.4 (CH), 119.6 (CH), 21.3 (CH_3), 21.2 (CH_3); IR (KBr/cm^{-1}) 1587, 1531, 1508, 1292, 1248, 1180, 826, 803; HRMS (ESI/TOF) calcd. for $[M+H]^+$ $C_{30}H_{25}N_2$: 413.2012, found: 413.2012.

4-(4-Fluorophenyl)-2,6-bis(4-methylphenyl)-3-(2-pyridyl)pyridine **(3Be).** Yellow plates (30.6 mg, 0.071 mmol, 71%). Mp 163.6–164.3 °C. ^{1}H NMR (400 MHz, $CDCl_3$) δ 8.43 (1H, ddd, *J* = 4.8, 1.6, 0.8 Hz), 8.07 (2H, d, *J* = 8.0 Hz), 7.71 (1H, s), 7.41 (1H, ddd, *J* = 7.6, 7.6, 2.0 Hz), 7.27–7.26 (4H, m), 7.13 (2H, m), 7.05–6.99 (3H, m), 6.94 (1H, ddd, *J*

= 7.6, 2.0, 2.0 Hz), 6.92–6.88 (2H, m), 2.41 (3H, s), 2.29 (3H, s); ^{13}C NMR (100 MHz, $CDCl_3$) δ 162.1 (C, d, *J* = 245.0 Hz), 157.9 (C), 157.8 (C), 156.4 (C), 149.6 (C), 149.1 (CH), 139.2 (C), 137.9 (C), 137.4 (C), 136.2 (C), 135.7 (C, d, *J* = 3.1 Hz), 135.5 (CH), 131.8 (C), 130.8 (CH, d, *J* = 8.1 Hz), 129.8 (CH), 129.4 (CH), 128.4 (CH), 127.0 (CH), 126.7 (CH), 121.5 (CH), 119.5 (CH), 115.1 (CH, d, *J* = 21.2 Hz), 21.3 (CH_3), 21.2 (CH_3); ^{19}F NMR (376 MHz, $CDCl_3$) δ −114.58 (tt, *J* = 5.6, 2.6 Hz); IR (ATR/cm^{-1}) 1724, 1585, 1504, 1275, 1118, 1018, 821, 802, 756; HRMS (ESI/TOF) calcd. for $[M+H]^+$ $C_{30}H_{24}FN_2$: 431.1918, found: 431.1928.

4-(4-Cyanophenyl)-2,6-bis(4-methylphenyl)-3-(2-pyridyl)pyridine **(3Bf).** Yellow solid (33.3 mg, 0.076 mmol, 76%). Mp 118.3–119.1 °C. ^{1}H NMR (400 MHz, $CDCl_3$) δ 8.40 (1H, ddd, *J* = 4.0, 1.8, 0.8 Hz), 8.07 (2H, d, *J* = 8.0 Hz), 7.69 (1H, s), 7.51 (2H, d, *J* = 8.4 Hz), 7.42 (1H, ddd, *J* = 7.6, 7.6, 1.8 Hz), 7.29 (2H, d, *J* = 8.0 Hz), 7.28–7.24 (4H, m), 7.05 (1H, ddd, *J* = 7.6, 4.8, 1.2 Hz), 7.02 (2H, d, *J* = 7.9 Hz), 6.95 (1H, ddd, *J* = 7.6, 0.8, 0.8 Hz), 2.42 (3H, s), 2.29 (3H, s); ^{13}C NMR (100 MHz, $CDCl_3$) δ 158.0 (C), 157.1 (C), 156.6 (C), 149.2 (CH), 148.9 (C), 144.7 (C), 139.5 (C), 137.7 (C), 137.4 (C), 135.8 (C), 135.7 (CH), 131.7 (CH), 131.5 (C), 129.8 (CH), 129.8 (CH), 129.5 (CH), 128.5 (CH), 127.0 (CH), 126.7 (CH), 121.7 (CH), 118.8 (CH), 118.6 (C), 111.3 (C), 21.3 (CH_3), 21.2 (CH_3); IR (ATR/cm^{-1}) 2228, 1724, 1586, 1503, 1421, 1370, 1184, 1115, 1021, 826, 803, 624; HRMS (ESI/TOF) calcd. for $[M+H]^+$ $C_{31}H_{24}N_3$: 438.1964, found: 438.1944.

4-(4-Chlorophenyl)-2-(4-methylphenyl)-6-phenyl-3-(2-pyridyl)pyridine **(3Bg).** Yellow solid (31.2 mg, 0.072 mmol, 72%). Mp 154.8–155.4 °C. ^{1}H NMR (400 MHz, $CDCl_3$) δ 8.43 (1H, ddd, *J* = 4.8, 1.6, 0.8 Hz), 8.18 (2H, d, *J* = 8.4 Hz), 7.72 (1H, s), 7.50–7.41 (4H, m), 7.26 (2H, d, *J* = 8.0 Hz), 7.20 (2H, d, *J* = 8.4 Hz), 7.09 (2H, d, *J* = 8.4 Hz), 7.04 (1H,

ddd, J = 4.8, 1.2, 1.2 Hz), 7.01 (2H, d, J = 8.0 Hz), 6.94 (1H, ddd, J = 7.6, 4.8, 0.8 Hz), 2.28 (3H, s); ^{13}C NMR (100 MHz, $CDCl_3$) δ 158.0 (C), 157.5 (C), 156.4 (C), 149.5 (C), 149.2 (CH), 138.9 (C), 138.1 (C), 137.7 (C), 137.5 (C), 135.6 (CH), 133.6 (C), 132.0 (C), 130.4 (CH), 129.8 (CH), 129.2 (CH), 128.7 (CH), 128.5 (CH), 128.2 (CH), 127.2 (CH), 126.7 (CH), 121.6 (CH), 119.7 (CH), 21.2 (CH_3); IR (ATR/cm^{-1}) 1586, 1531, 1491, 1419, 1371, 1018, 826, 749; HRMS (ESI/TOF) calcd. for $[M+H]^+$ $C_{29}H_{22}ClN_2$: 433.1466, found: 433.1466.

4-(4-Chlorophenyl)-2-(4-methylphenyl)-6-(4-nitrophenyl)-3-(2-pyridyl)pyridine **(3Bh).** Yellow solid (16.7 mg, 0.035 mmol, 35%). Mp 100.9–101.3 °C. ^{1}H NMR (400 MHz, $CDCl_3$) δ 8.38 (1H, ddd, J = 4.9, 2.0, 0.8 Hz), 8.27 (4H, br s), 7.73 (1H, s), 7.37 (1H, ddd, J = 7.7, 7.7, 1.8 Hz), 7.25 (2H, d, J = 7.8 Hz), 7.22 (2H, d, J = 8.6 Hz), 7.09 (2H, d, J = 8.6 Hz), 7.07–7.06 (1H, m), 7.03 (2H, d, J = 7.8 Hz), 6.96 (1H, ddd, J = 7.7, 0.8, 0.8 Hz), 2.30 (3H, s); ^{13}C NMR (100 MHz, $CDCl_3$) δ 157.6 (C), 155.9 (C), 152.7 (C), 149.0 (C), 148.2 (CH), 147.3 (C), 143.7 (C), 136.9 (C), 136.5 (C), 136.1 (C), 134.7 (CH), 132.9 (C), 132.4 (C), 129.2 (CH), 128.6 (CH), 127.5 (CH), 127.3 (CH), 126.8 (CH), 125.5 (CH), 122.9 (CH), 120.8 (CH), 119.3 (CH), 20.1 (CH_3); IR (ATR/cm^{-1}) 1585, 1516, 1342, 1261, 1091, 1018, 802, 729, 698; HRMS (ESI/TOF) calcd. for $[M+H]^+$ $C_{29}H_{21}CN_3O_2$: 478.1316, found: 478.1301.

4-(4-Chlorophenyl)-6-(4-methoxyphenyl)-2-(4-methylphenyl)-3-(2-pyridyl)pyridine **(3Bi).** White solid (13.9 mg, 0.039 mmol, 39%). Mp 79.7–80.4 °C. ^{1}H NMR (400 MHz, $CDCl_3$) δ 8.43 (1H, ddd, J = 4.0, 1.6, 0.8 Hz), 8.13 (2H, d, J = 9.2 Hz), 7.68 (1H, s), 7.41 (1H, ddd, J = 7.6, 7.6, 1.6 Hz), 7.25 (2H, d, J = 8.0 Hz), 7.19 (2H, d, J = 8.8 Hz), 7.09 (2H, d, J = 8.0 Hz), 7.07–6.99 (5H, m), 6.94 (1H, ddd, J = 7.6, 0.8, 0.8 Hz), 3.87 (3H, s),

2.29 (3H, s); ^{13}C (100 MHz, $CDCl_3$) δ 160.7 (C), 157.8 (C), 157.6 (C), 156.0 (C), 149.4 (C), 149.1 (CH), 138.2 (C), 137.8 (C), 137.4 (C), 135.5 (CH), 133.5 (C), 131.5 (C), 131.3 (C), 130.3 (CH), 129.8 (CH), 128.44 (CH), 128.41 (CH), 128.2 (CH), 126.7 (CH), 121.5 (CH), 118.8 (CH), 114.0 (CH), 55.3 (CH_3), 21.1(CH_3); IR (KBr/cm^{-1}) 1500, 1370, 1112, 1021, 736, 622; HRMS (ESI/TOF) calcd. for $[M+H]^+$ $C_{23}H_{17}ClN_2$: 357.1153, found: 357.1147.

***4-(4-Chlorophenyl)-6-(2-methoxyphenyl)-2-(4-methylphenyl)-3-(2-pyridyl)pyridine* (3Bj).** Yellow solid (28.2 mg, 0.061 mmol, 61%). Mp 141.3–141.8 °C. ^{1}H NMR (400 MHz, $CDCl_3$) δ 8.43 (1H, ddd, *J* = 4.8, 1.6, 0.8 Hz), 8.00 (1H, dd, *J* = 7.6, 2.0 Hz), 7.87 (1H, s), 7.43–7.36 (2H, m), 7.23 (2H, d, *J* = 8.0 Hz), 7.17 (2H, d, *J* = 8.8 Hz), 7.08 (2H, d, *J* = 8.8 Hz), 7.11–6.95 (6H, m), 3.88 (3H, s), 2.27 (3H, s); ^{13}C (100 MHz, $CDCl_3$) δ 157.8 (C), 157.7 (C), 157.3 (C), 155.2 (C), 149.1 (CH), 148.2 (C), 138.3 (C), 137.8 (C), 137.2 (C), 135.6 (CH), 133.4 (C), 131.6 (CH), 130.5 (CH), 130.1 (CH), 129.8 (CH), 128.8 (C), 128.6 (C), 128.4 (CH), 128.1 (CH), 126.7 (CH), 124.4 (CH), 121.5 (CH), 121.2 (CH), 111.5 (CH), 55.7 (CH_3), 21.2 (CH_3); IR (KBr/cm^{-1}) 1500, 1370, 1112, 1021, 736, 622; HRMS (ESI/TOF) calcd. for $[M+H]^+$ $C_{30}H_{23}ClN_2O$: 463.1571, found:463.1571.

***2-(4-chlororphenyl)-4-[(1,1-dimethylethyl)-phenyl]-6-(4-methylphenyl)-5-(2-pyridyl)pyridine* (3Bk).** White solid (27.9 mg, 0.057 mmol, 57%). Mp 118.9–119.7 °C. ^{1}H NMR (400 MHz, $CDCl_3$) δ 8.41 (1H, ddd, *J* = 4.9, 1.8, 0.9 Hz), 8.11 (2H, d, *J* = 8.6 Hz), 7.74 (1H, s), 7.43 (2H, d, *J* = 8.6 Hz), 7.39 (1H, ddd, *J* = 7.7, 7.7, 1.8 Hz), 7.26-7.21 (4H, m), 7.06 (2H, d, *J* = 8.5 Hz), 7.04–7.00 (3H, m), 6.96 (1H, ddd, *J* = 7.7, 0.9, 0.9 Hz), 2.28 (3H, s), 1.27 (9H, s); ^{13}C NMR (100 MHz, $CDCl_3$) δ 158.1 (C), 157.7 (C), 154.8 (C), 150.7 (C), 150.5 (C), 149.0 (CH), 137.8 (C), 137.6 (C), 137.3 (C), 136.3 (C), 135.4 (CH),

135.1 (C), 132.4 (C), 129.7 (CH), 128.8 (CH), 128.7 (CH), 128.41 (CH), 128.40 (CH), 126.7 (CH), 124.9 (CH), 121.4 (CH), 119.8 (CH), 34.5 (CH_3), 31.2 (C), 21.1 (CH_3); IR (ATR/cm^{-1}) 1585, 1531, 1492, 1365, 1091, 1014, 829, 802; HRMS (ESI/TOF) calcd. for $[M+H]^+$ $C_{33}H_{30}ClN_2$: 489.2092, found: 489.2073.

6-(4-Methoxyphenyl)-2-(4-methylphenyl)-4-(4-nitrophenyl)-3-(2-pyridyl)pyridine **(3Bl).** Yellow needles (13.7 mg, 0.029 mmol, 29%). Mp 115.8–116.8 °C. ^{1}H NMR (400 MHz, $CDCl_3$) δ 8.45 (1H, ddd, *J* = 4.8, 1.6, 0.8 Hz), 8.36–8.31 (4H, m), 7.82 (1H, s) 7.44 (1H, ddd, *J* = 7.6, 7.6, 2.0 Hz), 7.25 (2H, d, *J* = 8.4 Hz), 7.09–7.04 (5H, m), 6.98 (1H, ddd, *J* = 7.6, 0.8, 0.8 Hz) 6.77 (2H, ddd, *J* = 8.8, 2.8, 2.8 Hz), 3.77 (3H, s), 2.30 (3H, s); ^{13}C NMR (100 MHz, $CDCl_3$) δ 159.3 (C), 158.6 (C), 157.5 (C), 153.6(C), 150.8 (C), 149.2 (CH), 148.2 (C), 145.1 (C), 137.7 (C), 137.5 (C), 135.6 (CH), 133.5 (C), 131.3 (C), 130.3 (CH), 129.7 (CH), 128.5(CH), 127.9 (CH), 126.6 (CH), 123.9 (CH), 121.7 (CH), 120.7 (CH), 113.7 (CH), 55.2 (CH_3), 21.2 (CH_3); IR (ATR/cm^{-1}) 1512, 1341, 1249, 1179, 1022, 700; HRMS (ESI/TOF) calcd. for $[M+H]^+$ $C_{30}H_{24}N_3O_3$: 474.1812, found: 474.1813.

2-(4-Methylphenyl)-5-(4-nitrophenyl)-6-phenyl-3-(2-pyridyl)pyridine **(3Bm).** White solid (24.4 mg, 0.051 mmol, 51%). Mp 255.5–256.2 °C ^{1}H NMR (400 MHz, $CDCl_3$) δ 8.71 (1H, ddd, *J* = 4.4, 1.6, 0.8 Hz), 8.14 (2H, d, *J* = 8.8 Hz), 8.09 (1H, s), 7.50 (1H, ddd, *J* = 8.0, 8.0, 2.0 Hz), 7.46 (2H, d, *J* = 8.8 Hz), 7.45 (2H, *J* = 8.0 Hz), 7.40 (2H, d, *J* = 8.0 Hz), 7.30–7.29 (3H, m), 7.22 (1H, ddd, *J* = 7.6, 4.8, 1.2 Hz), 7.11–7.08 (3H, m), 2.34 (3H, s); ^{13}C (100 MHz, $CDCl_3$) δ 157.3 (C), 156.7 (C), 156.2 (C), 150.0 (CH), 146.9 (C), 146.7 (C), 140.9 (CH), 139.1 (C), 138.5 (C), 136.5 (C), 135.8 (CH), 133.3 (C), 131.9 (C), 130.4 (CH), 130.1 (CH), 129.9 (CH), 128.9 (CH), 128.5 (CH), 128.2 (CH), 125.3 (CH), 123.6 (CH), 122.2 (CH), 21.3 (CH_3); IR (ATR/cm^{-1}) 1595, 1518, 1427, 750, 701; HRMS

(ESI/TOF) calcd. for $[M+H]^+$ $C_{29}H_{21}ClN_3O_2$: 478.1316, found: 478.1301.

6-(4-Methoxyphenyl)-2-(4-methylphenyl)-5-(4-nitrophenyl)-3-(2-pyridyl)pyridine **(3Bn).** White solid (18.0 mg, 0.038 mmol, 38%). Mp 234.4–235.1 °C. ^{1}H NMR (400 MHz, $CDCl_3$) δ 8.71 (1H, ddd, *J* = 4.8, 1.8, 0.9 Hz), 8.16 (2H, d, *J* = 8.9 Hz), 8.06 (1H, s), 7.50 (1H, ddd, *J* = 7.7, 7.7, 1.8 Hz), 7.47 (2H, d, *J* = 8.9 Hz), 7.40 (2H, d, *J* = 8.9 Hz), 7.39 (2H, d, *J* = 8.0 Hz), 7.20 (1H, ddd, *J* = 7.7, 4.8, 0.9 Hz), 7.10 (2H, d, *J* = 8.0 Hz), 7.07 (1H, ddd, *J* = 7.7, 0.9, 0.9 Hz), 6.80 (2H, d, *J* = 8.9 Hz), 3.80 (3H, s), 2.34 (3H, s); ^{13}C NMR (100 MHz, $CDCl_3$) δ 159.9 (C), 157.4 (C), 156.5 (C), 155.7 (C), 151.6 (C), 149.9 (CH), 147.1 (C), 146.8 (C), 141.0 (CH), 138.4 (C), 136.6 (C), 135.7 (CH), 132.8 (C), 131.6 (CH), 131.5 (C), 130.4 (CH), 129.9 (CH), 128.8 (CH), 125.2 (CH), 123.6 (CH), 122.1 (CH), 113.6 (CH), 55.2 (CH_3), 21.2 (CH_3); IR (ATR/cm^{-1}) 1516, 1504, 1427, 1342, 1249, 1172, 1029, 852, 794, 698; HRMS (ESI/TOF) calcd. for $[M+H]^+$ $C_{30}H_{24}N_3O_3$: 474.1812, found: 474.1797.

4-(4-Chlorophenyl)-5-methyl-2-(methylphenyl)-6-phenyl-3-(2-pyridyl)pyridine **(3Bo).** Yellow solid (27.7 mg, 0.062 mmol, 62%). Mp 86.4–87.3 °C. ^{1}H NMR (400 MHz, $CDCl_3$) δ 8.37 (1H, ddd, *J* = 4.8, 1.6, 0.8 Hz), 7.65 (2H, ddd, *J* = 6.8, 1.6, 1.6 Hz), 7.45 (2H, ddd, *J* = 7.2, 1.2, 1.2 Hz), 7.41–7.32 (2H, m), 7.22–7.17 (4H, m), 7.02–7.01 (2H, brd, *J* = 7.6 Hz), 6.96–6.93 (3H, m), 6.89 (1H, ddd, *J* = 7.6, 1.2, 1.2 Hz), 2.24 (3H, s), 2.11 (3H, s); ^{13}C NMR (100 MHz, $CDCl_3$) δ 154.5 (C), 149.7 (C), 148.8 (CH), 141.1 (C), 137.5 (C), 137.1 (C), 137.0 (C), 135.3 (CH), 132.9 (C), 132.8 (C), 130.65 (CH), 130.62 (C), 129.6 (CH), 129.4 (C), 129.2 (C), 128.4 (CH), 128.1 (CH), 128.0 (CH), 127.9 (CH), 127.2 (CH), 126.3 (CH), 121.2 (CH), 21.1 (CH_3), 18.2 (CH_3); IR (ATR/cm^{-1}) 1585.4, 1566.2, 1539.2, 1492.9, 1392.6, 1087.8, 1018.4, 8293, 771.5, 744.5, 702.1; HRMS

(ESI/TOF) calcd. for $[M+H]^+$ $C_{30}H_{24}ClN_2$: 447.1622, found: 447.1639.

4-(4-Chlorophenyl)-2-(4-methylphenyl)-5-(4-nitrophenyl)-6-phenyl-3-(2-pyridyl)pyridine **(3Bp).** Yellow solid (7.2 mg, 0.013 mmol, 13%). Mp 165.3–166.1 °C. ^{1}H NMR (400 MHz, $CDCl_3$) δ 8.40 (1H, ddd, *J* = 4.8, 1.6, 0.8 Hz), 7.90 (2H, d, *J* = 8.8 Hz), 7.38 (1H, ddd, *J* = 7.6, 7.6, 1.6 Hz), 7.33–7.28 (4H, m), 7.23–7.20 (3H, m), 7.07 (2H, d, *J* = 8.8 Hz), 7.02–6.98 (3H, m), 6.95–6.91 (3H, m), 6.77–6.73 (2H, br), 2.28 (3H, s); ^{13}C NMR (100 MHz, $CDCl_3$) δ 157.3 (C), 157.2 (C), 157.1 (C), 149.0 (CH), 148.8 (C), 146.3 (C), 145.5 (C), 139.8 (C), 137.9 (C), 137.0 (C), 135.6 (CH), 133.0 (C), 132.1 (CH), 131.2 (C), 130.1 (CH), 129.8 (CH), 128.5 (CH), 128.0 (CH), 127.9 (CH), 127.7 (CH), 126.3 (CH), 122.8 (CH), 121.6 (CH), 21.2 (CH_3), Three signals (CH×1, C×2) were not observed presumably due to overlapping.; IR (ATR/cm^{-1}) 1585, 1519, 1489, 1388, 1346, 1018, 852, 763, 736, 702; HRMS (ESI/TOF) calcd. for $[M+H]^+$ $C_{35}H_{25}ClN_3O_2$: 554.1629, found: 554.1611.

2-(4-Methylphenyl)-5-(4-nitrophenyl)-4,6-diphenyl-3-(2-pyridyl)pyridine **(3Bq).** White solid (10.9 mg, 0.021 mmol, 21%). Mp 263.1–263.6 °C. ^{1}H NMR (400 MHz, $CDCl_3$) δ 8.38 (1H, ddd, *J* = 4.8, 1.6, 0.8 Hz), 7.86 (2H, d, *J* = 8.8 Hz), 7.35–7.31 (5H, m), 7.22–7.19 (3H, m), 7.06 (2H, d, *J* = 9.2 Hz), 7.00 (2H, d, *J* = 8.0 Hz), 6.97–6.92 (5H, m), 6.86–6.74 (2H, br), 2.28 (3H, s); ^{13}C (100 MHz, $CDCl_3$) δ 157.5 (C), 157.2 (C), 156.9 (C), 150.0 (C), 148.8 (CH), 146.1 (C), 145.9 (C), 140.1 (C), 137.7 (C), 137.3 (C), 137.1 (C), 135.4 (CH), 133.1 (C), 132.2 (CH), 131.4 (C), 130.1 (CH), 129.8 (CH), 128.5 (CH), 128.4 (CH), 127.9 (CH), 127.8 (CH), 127.4 (CH), 126.8 (CH), 126.3 (CH), 122.6 (CH), 121.4 (CH), 21.2 (CH_3); IR (KBr/cm^{-1}) 1586, 1518, 1396, 1345, 1275, 851, 749, 701; HRMS (ESI/TOF) calcd. for $[M+H]^+$ $C_{35}H_{26}N_3O_2$: 520.2019, found: 520.2018.

6-(4-Bromophenyl)-4-(4-chlorophenyl)-2-(4-methylphenyl)-5-(4-nitrophenyl)-3-(2-pyridyl)pyridine **(3Br).** Colorless needles (6.3 mg, 0.010 mmol, 10%). Mp 264.6–265.1 °C. ^{1}H NMR (400 MHz, $CDCl_3$) δ 8.39 (1H, ddd, *J* = 4.8, 1.6, 0.8 Hz), 7.94 (2H, d, *J* = 8.8 Hz), 7.40 (1H, ddd, *J* = 7.6, 7.6, 1.6 Hz), 7.34 (2H, d, *J* = 8.8 Hz), 7.27 (2H, d, *J* = 7.6 Hz), 7.21 (2H, d, *J* = 8.4 Hz), 7.06 (2H, d, *J* = 8.8 Hz), 7.02–7.00 (3H, m), 6.94 (2H, d, *J* = 8.8 Hz), 6.93 (1H, d, *J* = 7.6 Hz), 6.77–6.73 (2H, br), 2.28 (3H, s); ^{13}C NMR (100 MHz, $CDCl_3$) δ 157.5 (C), 157.0 (C), 155.7 (C), 149.0 (CH), 146.4 (C), 145.1 (C), 138.7 (C), 138.0 (C), 136.8 (C), 135.6 (CH), 135.4 (C), 133.3 (C), 133.1 (C), 132.1 (CH), 131.7 (CH), 131.1 (CH), 129.7 (CH), 128.6 (CH), 127.7 (CH), 126.2 (CH), 123.1 (CH), 122.7 (C), 121.7 (CH), 21.2 (CH_3), Three signals (CH×1, C×2) were not observed presumably due to overlapping.; IR (ATR/cm^{-1}) 1520, 1485, 1346, 1087, 1010, 748; HRMS (ESI/TOF) calcd. for $[M+H]^+$ $C_{35}H_{24}BrClN_3O_2$: 632.0734, found: 632.0708. CCDC number: 1951931.

2,4-Bis(4-methylphenyl)-3,6-di(2-pyridyl)pyridine **(3Bs).** White solid (20.7 mg, 0.050 mmol, 50%). Mp 89.9–90.7 °C. ^{1}H NMR (400 MHz, $CDCl_3$) δ 8.68 (1H, ddd, *J* = 4.8, 1.6, 0.8 Hz), 8.63 (1H, ddd, *J* = 7.2, 0.8, 0.8 Hz), 8.61 (1H, s), 8.44 (1H, ddd, *J* = 4.8, 1.6, 0.8 Hz), 7.81 (1H, ddd, *J* = 7.6, 7.6, 1.6 Hz), 7.40 (1H, ddd, *J* = 7.6, 7.6, 1.6 Hz), 7.31 (1H, ddd, *J* = 7.6, 4.8, 1.2 Hz), 7.27 (2H, d, *J* = 6.8 Hz), 7.08–6.97 (8H, m), 2.29 (3H, s), 2.28 (3H, s); ^{13}C NMR (100 MHz, $CDCl_3$) δ 157.9 (C), 157.6 (C), 156.1 (C), 154.9 (C), 150.9 (C), 149.1 (CH), 149.0 (CH), 137.9 (C), 137.3 (C), 137.1 (C), 136.8 (CH), 136.4 (C), 135.4 (CH), 133.6 (C), 129.8 (CH), 129.1 (CH), 128.6 (CH), 128.4 (CH), 126.8 (CH), 123.7 (CH), 121.6 (CH), 121.4 (CH), 120.6 (CH), 21.2 (CH_3), 21.1 (CH_3); IR (ATR/cm^{-1})1585, 1511, 1260, 793, 749; HRMS (ESI/TOF) calcd. for $[M+H]^+$ $C_{29}H_{23}N_3$: 414.1964, found: 414.1964.

***2-(4-Chlorolphenyl)-6-methyl-4-phenyl-3-(2-pyridyl)pyridine* (3Ca).** Yellow solid (25.3 mg, 0.071 mmol, 71%). Mp 108.9–109.4 °C. ^{1}H NMR (400 MHz, $CDCl_3$) δ 8.38 (1H, ddd, *J* = 4.8, 1.6, 0.8 Hz), 7.37 (1H, ddd, *J* = 7.6, 7.6, 2.0 Hz), 7.23 (1H, s), 7.22–7.17 (5H, m), 7.14 (2H, d, *J* = 8.6 Hz), 7.08–7.06 (2H, m), 7.00 (1H, ddd, *J* = 7.6, 4.8, 0.8 Hz), 6.88 (1H, ddd, *J* = 7.6, 0.8, 0.8 Hz), 2.69 (3H, s); ^{13}C NMR (100 MHz, $CDCl_3$) δ 157.9 (C), 157.3 (C), 156.5 (C), 150.2 (C), 149.1 (CH), 139.2 (C), 139.1 (C), 135.5 (CH), 133.5 (C), 131.2 (C), 130.9 (CH), 129.0 (CH), 128.0 (CH), 128.9 (CH), 127.4 (CH), 126.6 (CH), 123.2 (CH), 121.5 (CH), 24.5 (CH_3); IR (ATR/cm^{-1}) 1577, 1543, 1435, 1377, 1284, 1087, 1014, 844; HRMS (ESI/TOF) calcd. for $[M+H]^+$ $C_{23}H_{17}ClN_2$: .357.1153, found: 357.1147.

***2-(4-Chlorophenyl)-4-(4-fluorophenyl)-6-(4-methylphenyl)-3-(2-pyridyl)pyridine* (3Ce).** Yellow plates (28.9 mg, 0.064 mmol, 64%). Mp 163.4–164.0 °C. ^{1}H NMR (400 MHz, $CDCl_3$) δ 8.43 (1H, ddd, *J* = 4.8, 1.6, 0.9 Hz), 8.05 (2H, d, *J* = 8.4 Hz), 7.74 (1H, s), 7.41 (1H, ddd, *J* = 7.6, 7.6, 1.6 Hz), 7.34–7.29 (4H, m), 7.18 (2H, d, *J* = 6.8 Hz), 7.13–7.11 (2H, m), 7.07 (1H, ddd, *J* = 7.6 , 1.6, 1.2 Hz), 6.94–6.89 (3H, m), 2.41 (3H, s); ^{13}C NMR (100 MHz, $CDCl_3$) δ 162.8 (C, d, *J* = 246.3 Hz), 157.3 (C), 156.8 (C), 156.6 (C), 149.8 (C), 149.3 (CH), 139.4 (C), 139.2 (C), 135.9 (C), 135.7 (CH), 135.3 (C, d, *J* = 3.5 Hz), 133.7 (C), 131.9 (C), 131.2 (CH), 130.8 (CH, d, *J* = 8.1 Hz), 129.5 (CH), 127.9 (CH), 126.9 (CH), 126.6 (CH), 121.7 (CH), 119.9 (CH), 115.1 (CH, d, *J* = 21.3Hz), 21.3 (CH_3); ^{19}F NMR (376 MHz, $CDCl_3$) δ −114.2 (tt, *J* = 5.3, 3.0 Hz) IR (ATR/cm^{-1}) 1558, 1508, 1419, 1369, 1157, 1087, 1014, 837, 810; HRMS (ESI/TOF) calcd. for $[M+H]^+$ $C_{29}H_{21}ClFN_2$: 451.1371, found: 451.1362.

***2-(4-Chlorophenyl)-5-(4-nitrophenyl)-4-phenyl-3,6-bis(2-pyridyl)pyridine* (3Ct).** Yellow plates (9.2 mg, 0.017 mmol, 17%). Mp 285.0–285.9 °C, ^{1}H NMR (400 MHz,

$CDCl_3$) δ 8.33 (1H, ddd, *J* = 4.4, 1.6, 0.4 Hz), 8.23 (1H, ddd, *J* = 4.9, 1.5, 1.0 Hz), 8.25 (2H, d, *J* = 8.9 Hz), 7.39 (1H, ddd, *J* = 7.7, 1.8, 1.8 Hz), 7.37–7.32 (4H, m), 7.30 (1H, ddd, *J* = 7.7, 1.6, 1.6 Hz), 7.27–7.22 (3H, m), 7.18 (2H, d, *J* = 8.9 Hz), 7.12 (2H, br d, *J* = 7.9 Hz), 7.03 (1H, d, *J* = 7.8 Hz), 6.98 (1H, ddd, *J* = 4.9, 4.9, 1.0 Hz), 6.91 (1H, ddd, *J* = 4.9, 4.9, 1.0 Hz), 6.87 (1H, d, *J* = 7.8 Hz); ^{13}C (100 MHz, $CDCl_3$) δ 157.4 (C), 156.3 (C), 156.3 (C), 155.9 (C), 149.2 (C), 148.9 (CH), 148.6 (CH), 146.4 (C), 145.2 (C), 139.5 (C), 138.4 (C), 135.6 (CH), 135.3 (CH), 134.3 (C), 132.9 (C), 132.0 (CH), 131.6 (C), 131.3 (CH), 130.0 (CH), 128.2 (CH), 128.1 (CH), 128.0 (CH), 126.5 (CH), 125.7 (CH), 122.7 (CH), 121.8 (CH), 121.7 (CH); IR (KBr/cm^{-1}) 1587, 1518, 1492, 1471, 1396, 1287, 1012, 850, 752, 702 ; HRMS (ESI/TOF) calcd. for $[M+H]^+$ $C_{33}H_{21}ClN_4O_2$: 541.1425, found: 541.1399.

2-[(4-Trifluoroethyl)phenyl]-6-methyl-4-phenyl-3-(2-pyridyl)pyridine **(3Da).** Yellow solid (27.0 mg, 0.069 mmol, 69%). Mp 132.2–133.1 °C. ^1H NMR (400 MHz, $CDCl_3$) δ 8.38 (1H, ddd, *J* = 4.8, 1.6, 0.8 Hz), 7.43 (2H, d, *J* = 8.0 Hz), 7.39 (2H, d, *J* = 8.0 Hz), 7.35 (1H, ddd, *J* = 7.6, 7.6, 2.0 Hz), 7.28 (1H, s), 7.21–7.19 (3H, m) 7.10–7.08 (2H, m), 7.01 (1H, ddd, *J* = 7.6, 4.8, 1.2 Hz), 6.89 (1H, ddd, *J* = 8.0, 0.8, 0.8 Hz), 2.71 (3H, s); ^{13}C NMR (100 MHz, $CDCl_3$) δ 158.1 (C), 157.1 (C), 156.4 (C), 150.3 (C), 149.1 (CH), 144.4 (C), 138.9 (C), 135.5 (CH), 131.4 (C), 129.9 (CH), 129.4 (C, q, *J* = 270.3 Hz), 129.0 (CH), 128.0 (CH), 127.5 (CH), 126.7 (CH), 124.7 (CH, q, *J* =3.7 Hz), 124.3 (C, q, *J* =32.2 Hz) 123.6 (CH), 121.6 (CH), 24.5 (CH_3); IR (ATR/cm^{-1}) 1586, 1534, 1491, 1369, 1275, 1242, 1182, 1089, 1020, 827, 805; HRMS (ESI/TOF) calcd. for $[M+H]^+$ $C_{24}H_{18}F_3N_2$: 391.1416, found: 391.1431.

4-(4-Methylphenyl)-2,3,6-tris(2-pyridyl)pyridine **(3Gs).** Brown oil (26.1 mg, 0.065

mmol, 65%). ^{1}H NMR (400 MHz, $CDCl_3$) δ 8.68 (1H, ddd, *J* = 4.0, 1.6, 0.8 Hz), 8.67 (1H, d, *J* = 5.2 Hz), 8.53 (1H, s), 8.31 (1H, ddd, *J* = 4.8, 1.6, 0.8 Hz), 8.29 (1H, ddd, *J* = 4.8, 1.6, 0.8 Hz), 7.84 (1H, d, *J* = 8.0 Hz), 7.80 (1H, ddd, *J* = 7.6, 7.6, 1.6 Hz), 7.67 (1H, *J* = 7.6, 7.6, 1.6 Hz), 7.38 (1H, ddd, *J* = 7.6, 7.6, 1.6 Hz), 7.30 (1H, ddd, *J* = 7.2, 3.6, 0.8 Hz), 7.10–7.06 (3H, m), 7.59–6.95 (4H, m), 2.28 (3H, s); ^{13}C NMR (100 MHz, $CDCl_3$) δ 158.8 (C), 157.7 (C), 156.7 (C), 155.9 (C), 154.9 (C), 151.0 (C), 149.1 (CH), 148.5 (CH), 148.1 (CH), 137.3 (C), 136.8 (CH), 136.1 (C), 136.0 (CH), 135.2 (CH), 134.3 (C), 129.2 (CH), 128.7 (CH), 126.7 (CH), 124.8 (CH), 123.8 (CH), 122.0 (CH), 121.7 (CH), 121.6 (CH), 121.1 (CH), 21.5 (CH_3); IR (ATR/cm^{-1}) 1585.4, 1562.3, 1535.3, 1512.2, 1473.6, 1415.7, 821.6, 790.8, 740.6; HRMS (ESI/TOF) calcd. for $[M+H]^+$ $C_{27}H_{21}N_4$: 401.1760, found: 401.1764.

5-(4-Fluorophenyl)-6-methyl-2-phenyl-3-(2-pyridyl)pyridine **(3Au).** Yellowish powder (23.5 mg, 0.069 mmol, 69%). Mp 170.0–170.7 °C. ^{1}H NMR (400 MHz, $CDCl_3$) δ 8.65 (1H, ddd, *J* = 4.8, 1.6, 0.8 Hz), 7.87 (1H, s), 7.43–7.37 (5H, m), 7.29–7.27 (3H, m), 7.16–7.11 (3H, m), 6.96 (1H, ddd, *J* = 8.0, 1.6, 1.6 Hz), 2.61 (3H, s); ^{13}C NMR (100 MHz, $CDCl_3$) δ 162.3 (C, d, *J* = 245.3 Hz), 157.7 (C), 155.5 (C), 149.8 (CH), 139.9 (C), 139.7 (CH), 135.6 (CH), 135.4 (CH, d, *J* = 3.5 Hz), 134.7 (C), 132.6 (C), 130.8 (CH, d, *J* = 8.0 Hz), 129.8 (CH), 128.2 (CH), 128.0 (CH), 125.3 (CH), 121.8 (CH), 115.3 (CH, d, *J* = 21.3 Hz), 23.4 (CH_3); IR (KBr/cm^{-1}) 1587, 1507, 1427, 1224, 1152, 837, 758, 699; HRMS (ESI/TOF) calcd. for $[M+H]^+$ $C_{23}H_{16}FN_2$: 341.1448, found: 341.1447.

3-(4-Fluorophenyl)-6-phenyl-5-(2-pyridyl)pyridine-2-carboxylic Acid **(3L).** To a solution of **3Au** (99.6 mg, 0.29 mmol) in a mixture of H_2O (1 mL) and *t*-BuOH (2 mL) maintained at a temperature of 100 °C with stirring was added $KMnO_4$ (142 mg, 0.89

mmol) in one portion. The reaction mixture was heated for 16 h, during which time a brown solid precipitated which was removed by hot filtration through Celite. The filtrate was evaporated to a small volume and then acidified to pH 3 with concentrated aqueous HCl which precipitated a white solid. The solid was collected by filtration and dried in *vacuo* to give **4** as white powder (51.2 mg, 0.14 mmol, 46%). Mp 168.0–168.5 °C. ^{1}H NMR (400 MHz, DMSO-d_6) δ 8.61 (1H, ddd, J = 4.8, 1.6, 1.2 Hz), 8.06 (1H, s), 7.72 (1H, ddd, J = 8.0, 8.0, 1.6 Hz), 7.62–7.58 (2H, m), 7.36–7.31 (8H, m), 7.27 (1H, ddd, J = 8.0, 1.6, 1.6 Hz), 2.61 (3H, s); ^{13}C NMR (100 MHz, $CDCl_3$) δ 168.0 (C), 163.4 (C), 156.3 (C), 154.7 (C), 149.6 (CH), 140.3 (CH), 138.8 (C), 136.4 (CH), 135.6 (C), 133.5 (C), 133.4 (C), 132.0 (C), 130.4 (CH, d, J = 8.0 Hz), 129.4 (CH), 128.3 (CH), 128.0 (CH), 124.8 (CH), 122.8 (CH), 115.5 (CH, d, J = 22.0 Hz); IR (KBr/cm^{-1}) 2470, 1722, 1598, 1514, 1431, 1228, 1157, 837, 699; HRMS (ESI/TOF) calcd. for $[M+H]^+$ $C_{23}H_{16}FN_2O_2$: 371.1190, found: 371.1189.

***Chlorido[3-(4-fluorophenyl)-6-phenyl-5-(2-pyridyl)-2-pyridinecarboxylato]platinum(II) tetra-n-butylammonium salt* (4L$_{TBA}$).** To a solution of **3L** (25.5 mg, 0.068 mmol) in toluene (1 mL) were added *cis*-dichloridobis(dimethylsulfoxide)platinum(II) (26.3 mg, 0.062 mmol) and sodium acetate (6.2 mg, 0.19 mmol), then heated at 110 °C for 3 d. The reaction mixture contain of **4L$_{Na}$** was used for the next step without any purifications.

To a solution of the reaction mixture (69.0 mg) in acetone (3 mL) were added tetrabutylammonium chloride (204 mg, 0.73 mmol). After vigorous stirring for 1 h, the solvent was removed under reduced pressure. The residue was extracted with dichlorometane (30 mL), and the insoluble sodium salt was filtered, and the filtrate was concentrated under reduced pressure affording **4L$_{TBA}$** (39.2 mg, 0.046 mmol). ^{1}H NMR

(400 MHz, $CDCl_3$) δ 8.77 (1H, d, J = 4.8 Hz), 7.83–7.73 (2H, m), 7.63 (1H, s), 7.49 (1H, d, J = 8.0 Hz), 7.43–7.40 (2H, m), 7.38–7.34 (2H, m), 7.06–6.96 (2H, m), 6.62 (1H, ddd, J = 8.0, 1.2, 1.2 Hz), 6.26 (1H, d, J = 8.0 Hz); HRMS (ESI/TOF) calcd. for $[M+H]^+$ $C_{23}H_{13}ClFN_2O_2Pt$: 598.0302, found: 598.0316.

Macrocyclic platinum(II) trimer **($4L_{Pt3}$).** **$4L_{Pt3}$** was afforded to yellow plates by recrystallization from methanol/chloroform. HRMS (ESI/TOF) calcd. for $[M+Na]^+$ $C_{69}H_{39}F_3N_6NaO_6Pt_3$: 1712.1719, found: 1712.1727. Steric structure of **$4L_{Pt3}$** have been identify by X-ray crystallographic analysis.

4.2 Spectroscopic Measurement. The absorption spectra of the compounds was measured by using a Hitachi U-3900 spectrophotometer.

4.3 Theoretical Calculations. All non-hydrogen atoms were refined with anisotropic displacement parameters and hydrogen atoms were placed at calculated positions and refined "riding" on their corresponding carbon atoms. The geometrical optimization was carried out for at the B3LYP/6-31g(d,p) level of theory implemented on Gaussian 09 package.[31]

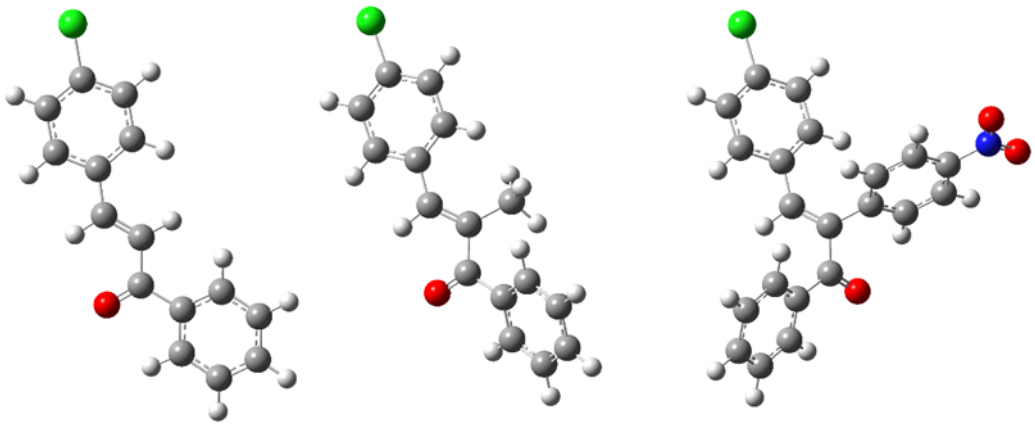

Figure. Optimized geometries of **2g**, **2o** and **2p**. Hydrogen atoms are omitted for clarity.

Table. X-ray crystallographic data of **3Br** and **4L$_{Pt3}$**.

Compound	**3Br**	**4L$_{Pt3}$**
chemical formula	$C_{35}H_{23}BrClN_3O_2$, $CHCl_3$	$C_{69}H_{39}F_3N_6O_6Pt_3$
formula weight	752.29	1690.33
crystallization solvent	chloroform/hexane	chloroform/methanol
T / K	123	93.15
color	colorless	yellow
crystal size / mm	0.283×0.142×0.058	0.404×0.227×0.064
crystal system	triclinic	triclinic
space group	P -1	$P2_1/c$
a / Å	9.4566(3)	11.6491(2)
b / Å	13.7486(5)	23.9407(3)
c / Å	14.9118(5)	22.5420(3)
α / °	109.625(3)	90
β / °	102.572(3)	98.3650(10)
γ / °	107.237(3)	90
V / Å^3	1632.11(10)	6219.80(16)
Z	2	4
goodness-of-fit on F^2	1.056	1.032
R_1 [$I>2\sigma(I)$][a]	0.0406	0.0455
wR_2 (for all data)[b]	0.1046	0.1184

[a] $R_1 = \Sigma||F_o| - |F_c||/\Sigma|F_o|$. [$b$]$wR_2 = \{\Sigma[w(F_o^2 - F_c^2)^2]/\Sigma[w(F_o^2)^2]\}^{1/2}$.

Chapter 5 References

[1] a) M. Baumann, I. R. Baxendale, *Beilstein J. Org. Chem.* **2013**, *9,* 2265–2319; b) R. Karki, P. Thapa, H. Y. Yoo, T. M. Kadayat, P. –H. Park, Y. Na, E. Lee, K. –H. Jeon, W.-J. Cho, H. Choi, Y. Kwon, E. –S. Lee, *Eur. J. Med. Chem.* **2012**, *49*, 219−228; c) B. Corry, N. M. Smith, *Chem. Commun.* **2012**, *48*, 8958–8960.

[2] a) M. J. Bezdek, P. J. Chirik, *J. Am. Chem. Soc.* **2018**, *140*, 13817–13826; b) K. Nisbett, Y. –J. Tu, C. Turro, J. J. Kodanko, H. B. Schlegel, *Inorg Chem.* **2018**, 57, 231–240.

[3] a) A. G. Fang, J. V. Mello, N. S. Finney, *Tetrahedron.* **2004**, *60*, 11075–11087; b) B. Tang, F. Yu, P. Li, L. Tong, X. Duan, T. Xie, X. A. Wang, *J. Am. Chem. Soc.* **2009**, *131*, 3016–3023.

[4] S. Lachmanová, G. Dupeyre, J. Tarábek, P. Ochsenbein, C. Perruchot, Ciofini, M. Hromadová, L. Pospísil, P. P. Lainé, *J. Am. Chem. Soc.* **2015**, *137*, 11349–11364.

[5] a) E. K. J. Lui, D. Hergesell, L. L. Schafer, *Org. Lett.* **2018**, *20*, 6663−6667; b) Z. He, D. Dobrovolsky, P. Trinchera, A. K. Yudin, *Org. Lett.* **2013**, *15*, 334−337; c) N. S. Y. Loy, A. Singh, X. Xu, C. –M. Park, *Angew. Chem. Int. Ed.* **2013**, *52*, 2212−2216; d) P. K. Tapaswi, C. Mukhopadhyay, *ARKIVOC* **2011** (*x*) 287−298; e) B. Jiang, W. –J. Hao, X. Wang, F. Shi, S. –J. Tu, *J. Comb. Chem.* **2009**, *11*, 846–850; F. Palacios, C. Alonso, G. Rubiales, J. M. Ezpeleta, *Eur. J. Org. Chem.* **2001**, 2115−2122.

[6] a) R. P. Rivera, P. Ehlers, L. Ohlendorf, E. T. Rodríguez, A. Villinger, P. Langer, *Eur. J. Org. Chem.* **2018**, 990−1003; b) P. Pomaranski, P. Roszkowski, J. K. Maurin, A. Budzianowski, Z. Czarnocki, *Tetrahedron Lett.* **2017**, *58*, 462−465; c) E. Karadeniz, M. Zora, N. Z. Kılıçaslan, *Tetrahedron* **2015**, *71*, 8943−8952; d) S. Reimann, P. Ehlers, A. Petrosyan, S. Kohse, A. Spannenberg, A. E. Surkus, T. V. Ghochikyan, A.

S. Saghyan, S. Lochbrunner, O. Kühn, R. Ludwig, P. Langer, *Adv. Synth. Catal.* **2014**, *356*, 1987−2008.

[7] C. Doebelin, P. Wanger, F. Bihel, N. Humbert, C. A. Kenfack, Y. Mely, J. –J. Bourguignon, M. Schmitt, *J. Org. Chem.* **2014**, *79*, 908–918.

[8] S. Suzuki, Y. Segawa, K. Itami, J. Yamaguchi, *Nat. Chem.* **2015**, *7*, 227–233.

[9] T. Asako, W. Hayashi, K. Amaike, S. Suzuki, K. Itami, K. Muto, J. Yamaguchi, *Tetrahedron* **2017**, *73*, 3669–3676.

[10] P. Pomaranski, Z. Czarnocki, *Synthesis* **2019**, *51*, 587–611.

[11] S. Hirai, Y. Horikawa, H. Asahara, N. Nishiwaki, *Chem. Commun.* **2017**, *53*, 2390–2393.

[12] T. Sasada, F. Kobayashi, N. Sakai, T. Konakahara, *Org. Lett.* **2009**, *11*, 2161–2164.

[13] a) Y. Nakaike, H. Asahara, N. Nishiwaki, *Russ. Chem. Bull., Int. Ed.* **2016**, *65*, 2129–2142; b) H. Asahara, M. Hamada, Y. Nakaike, N. Nishiwaki, *RSC Adv.* **2015**, *5*, 90778−90784; c) Y. Nakaike, N. Nishiwaki, M. Ariga, Y. Tobe, *J. Org. Chem.* **2014**, *79*, 2163−2169.

[14] H. Puschmann, *J. Appl. Crystallogr.* **2009**, *42*, 339−341.

[15] G. M. Sheldrick, *Acta Crystallogr.* **2015**, *A71*, 3−8.

[16] G. M. Sheldrick, *Acta Crystallogr.* **2015**, *C71*, 3−8.

[17] T. Konakahara, M. Matsuki, S. Sugimoto, K. Sato, *J. Chem. Soc., Perkin. Trans. 1* **1987**, 1489–1493.

[18] M. Westerhausen, A. N. Kneifel, A. Kalisch, *Angew. Chem. Int. Ed.* **2004**, *44*, 96–98.

[19] L. V. R. B. Syamala, T. M. Khopade, P. K. Warghude, R. G. Bhat, *Tetrahedron Lett.* **2019**, *60*, 88–91.

[20] G. F. Ozdemir, I. O. Ihan, S. Akkoc, *Synth. Commun.* **2019**, *49*, 2417–2424.

[21] H. Bansode, G. Suryavanshi, *ACS Omega* **2019**, *4*, 9636–9644.

[22] M. Koch, Ravikanth, *J. Org. Chem.* **2019**, *84*, 10775–10784.

[23] G. Zhang, Q. Fan, Y. Zhao, C. Ding, *Eur. J. Org. Chem.* **2019**, 5801–5806.

[24] T. Venkatesh, Y. D. Bodke, N. M. Joy, B. M. Vinoda, Y. Shiralgi, B. L. Dhananjaya, *Lett. Org. Chem.* **2016**, *13*, 661–671.

[25] Y. Beniyama, K. Matsuno, H. Miyachi, *Bioorg. Med. Chem. Lett.* **2013**, *23*, 1662–1666.

[26] J. T. Schott, C. E. Mordaunt, A. J. Vargas, M. A. Leon, K. H. Chen, M. Singh, M. Satoh, E. L. Cardenas, S. Maitra, N. V. Patel, H. J. P. de Lijser, *Chem. Pharm. Bull.* **2013**, *61*, 229–236.

[27] S. Gaikwad, A. Goswami, S. De, M. A. Shmittel, *Angew. Chem. Int. Ed.* **2016**, *55*, 10512–10517.

[28] Y. Nomura, M. Kimura, T. Shibata, Y. Takeuchi, S. Tomoda, *Bull. Chem. Soc. Jpn.* **1982**, *55*, 3343–3344.

[29] B. Alcaide, P. Almendros, E. Busto, A. Luna, *Adv. Synth. Catal.* **2016**, *358*, 1526–1533.

[30] V. Sharma, A. Kaur, S. C. Sahoo, S. S. Chimni, *Org. Biomol.Chem.* **2018**, *16*, 6470–6478.

[31] M. J. Frisch, G. W. Trucks, H. B. Schlegel, G. E. Scuseria, M. A. Robb, J. R. Cheeseman, G. Scalmani, V. Barone, B. Mennucci, G. A. Petersson, H. Nakatsuji, M. Caricato, X. Li, H. P. Hratchian, A. F. Izmaylov, J. Bloino, G. Zheng, J. L. Sonnenberg, M. Hada, M. Ehara, K. Toyota, R. Fukuda, J. Hasegawa, M. Ishida, T. Nakajima, Y. Honda, O. Kitao, H. Nakai, T. Vreven, J. A. Montgomery Jr., J. E. Peralta, F. Ogliaro, M. Bearpark, J. J. Heyd, E. Brothers, K. N. Kudin, V. N.

Staroverov, T. Keith, R. Kobayashi, J. Normand, K. Raghavachari, A. Rendell, J. C. Burant, S. S. Iyengar, J. Tomasi, M. Cossi, N. Rega, J. M. Millam, M. Klene, J. E. Knox, J. B. Cross, V. Bakken, C. Adamo, J. Jaramillo, R. Gomperts, R. E. Stratmann, O. Yazyev, A. J. Austin, R. Cammi, C. Pomelli, J. W. Ochterski, R. L. Martin, K. Morokuma, V. G. Zakrzewski, G. A. Voth, P. Salvador, J. J. Dannenberg, S. Dapprich, A. D. Daniels, O. Farkas, J. B. Foresman, J. V. Ortiz, J. Cioslowski, D. J. Fox, *Gaussian 09, (Revision C.01)*, Gaussian, Inc., Wallingford CT, **2010**.

PART II FACILE SYNTHESIS OF ONYCHINES

Chapter 1 Introduction

Onychine is an alkaloid isolated from the root bark of trees belonging to the Annonaceae family, such as *Onychopetalum amazonicum*,[1] *Guatteria dielsina Rodrigues*, *W. A.*,[2] and *Cleistopholis patens*,[3] which are large trees found throughout West Africa. The structure of onychine was determined as 4-aza-1-methylfluorenone later by Koyama *et al*.[4] Onychine also serves as a precursor of eupolauridine, isolated from members of the Annonaceae family such as *Eupomatialaurina R. Br.*[5] and *Cananga odorata Hook. F. et Thomas*.[6] Recently, onychine derivatives have attracted much attention because of their high bioactivity, including antifungal activity and cytotoxicity.[7] From the standpoint of finding new biologically active compounds, the development of a facile synthetic method for versatile substituted onychines is urgently required.

Several synthetic methods for onychine (**1Aa**) are shown in Scheme 1. In Methods **a**[8] and **b**,[9] **1Aa** is obtained by modification of 4-azafluorenone derivatives; however, it is not easy to construct the fundamental framework beforehand. Other approaches, including the construction of a 4-azafluorenone framework, are also reported (Methods **c**–**e**). When *O*-crotyloxime derived from 1,3-indanedione was treated under basic conditions, **1Aa** is synthesized in a single step, which involves the rearrangement of the crotyl group followed by intramolecular condensation forming a pyridine ring (Method **c**).[10] Onychine (**1Aa**) is also obtained by forming a C–C bond between the pyridine ring and the substituent; palladium-catalyzed intramolecular cross-coupling of 3-(2-bromobenzoyl)-4-methylpyridine (Method **d**)[11] and intramolecular Friedel–Crafts

acylation of ethyl 4-methyl-2-phenylnicotinate (Method **e**)[12] have been reported. Thus, while several routes to obtain onychine have been established, the difficulty in obtaining the starting materials limits the synthesis of versatile substituted onychines.

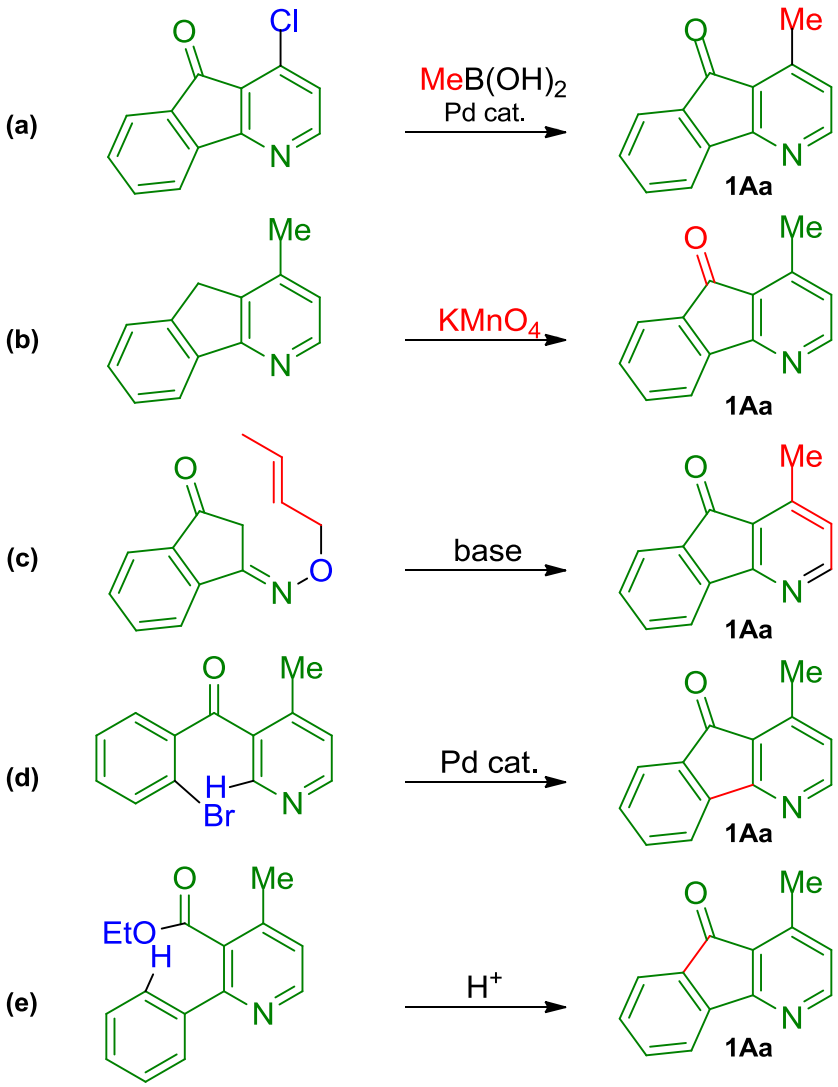

Scheme 1. Commonly used synthetic methods for onychine **1Aa**.

Among these routes, Method **e** is rather considered to have potential from the viewpoint of modification of the onychine framework. In Scheme 2, commonly used synthetic methods for the precursor, 4-methyl-2-phenylnicotinates, are shown. Although Hantzsch reaction (Method **f**) is the most commonly used method for synthesizing nicotinates, the

products always have two ester functions, and the control of regioselectivity is necessary.[13] The Suzuki–Miyaura cross-coupling reaction (Method **g**),[14] three component condensation of zinc enolate (Method **h**),[15] and condensation of enamino ester with β-keto ester (Method **i**)[16] are also acceptable; however, modification of the starting 2-bromonicotinate, enyne, and keto ester is not easily achieved (Scheme 2). This prevents the introduction of desired substituents at the preferred position of the onychine framework *via* Method **e**.

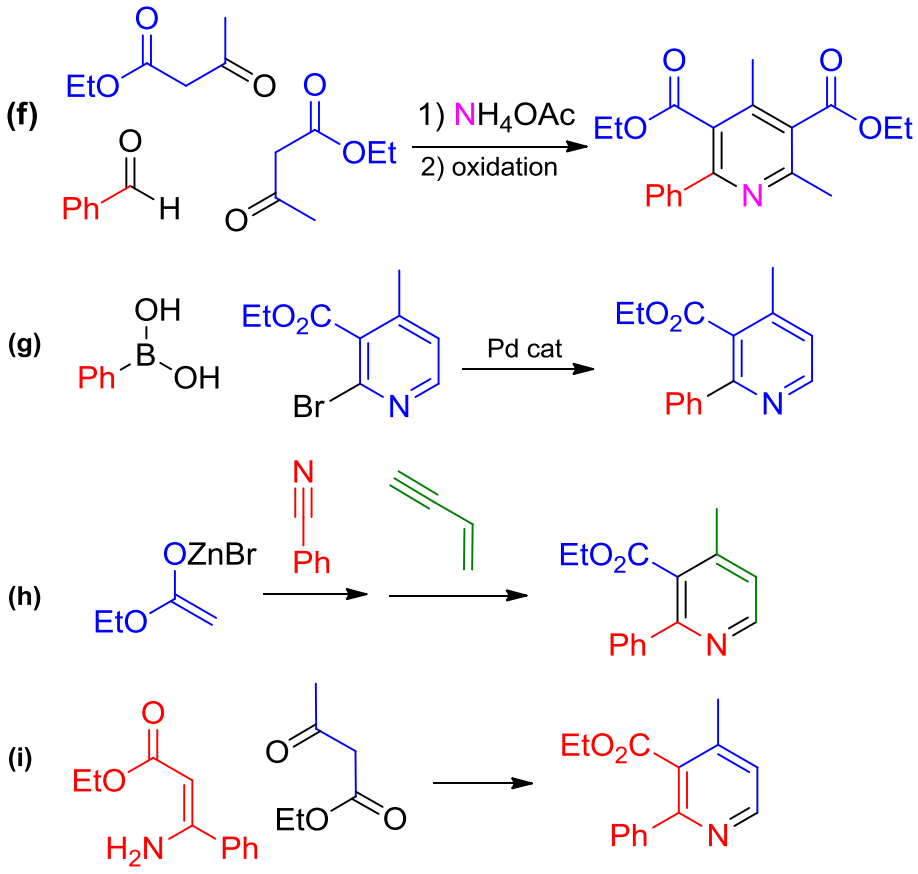

Scheme 2. Common routes for the synthesis of 4-methyl-2-phenylnicotinates.

Meanwhile, our group recently demonstrated an efficient synthetic method for polysubstituted nicotinates through iron(III) chloride mediated condensation of an

enamino ester **2** with an α,β-unsaturated carbonyl compound **3**, both of which are easily available commercially or by simple reactions. This protocol facilitates the modification of the pyridine ring by altering substrates **2** and **3** (Scheme 3).[17] Indeed, the desired alkyl/aryl groups could be introduced into the chosen positions of the nicotinate framework **4**. This feature prompted me to study the synthesis of 2-arylated nicotinates **4** and the subsequent conversion into onychines **1**, which could overcome the disadvantages of the conventional methods.

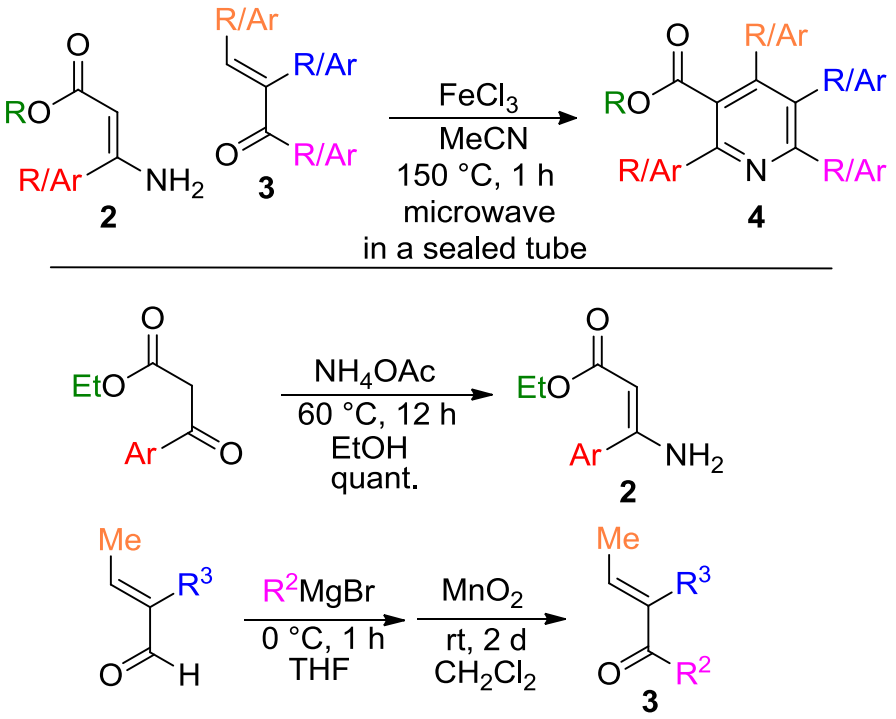

Scheme 3. Synthesis of nicotinates **4** possessing different substituents.

Chapter 2 Results and Discussion

2.1 Synthesis of 2-arylated nicotinates 4

When the α-phenyl enamino ester **2A** was reacted with crotonaldehyde (**3a**) in the presence of iron(III) chloride at 150 °C, ethyl 4-methyl-2-phenylnicotinate (**4Aa**) was obtained in 74% yield (Table 1, Entry 1). Similarly, α-methylated aldehyde **3b** underwent the reaction to afford tetrasubstituted pyridine **4Ab** in comparable yield (Entry 2). Unsaturated ketones **3c** and **3d** could also be used as substrate to give the corresponding nicotinates **4Ac** and **4Ad**, respectively (Entries 3 and 4). In the case of **3c**, the low reaction efficiency could be due to the instability of the enone **3c**, causing it to decompose in air (Entry 3). On the other hand, the phenyl ketone **3d** was sufficiently stable and showed similar reactivity to the unsaturated aldehyde **3a** (Entry 4). Next, modification of the aryl group was studied. When the electron-rich enamino ester **2B** was used, the condensation proceeded similarly to afford the corresponding nicotinates **4Ba–4Bd** (Entries 5–8). Ester **2B** is more reactive than **2A**, and reacted with **3c** before its decomposition, which resulted in the formation of **4Bc** in higher yield (Entry 7). Electron-poor enamino ester **2C** also afforded nicotinate **4Ca** without significant decrease of the yield (Entry 9).

Table 1. Synthesis of 2-arylated nicotinates **4**.

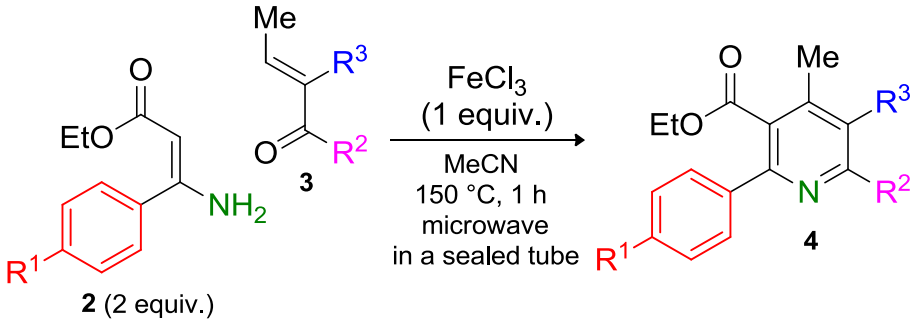

Entry	Enamino ester **2**		Enone **3**			Product	
	R^1		R^2	R^3			Yield /%
1	H	**2A**	H	H	**3a**	**4Aa**	74
2	H	**2A**	H	Me	**3b**	**4Ab**	60
3	H	**2A**	Me	Me	**3c**	**4Ac**	35
4	H	**2A**	Ph	H	**3d**	**4Ad**	54
5	OMe	**2B**	H	H	**3a**	**4Ba**	74
6	OMe	**2B**	H	Me	**3b**	**4Bb**	56
7	OMe	**2B**	Me	Me	**3c**	**4Bc**	50
8	OMe	**2B**	Ph	H	**3d**	**4Bd**	65
9	NO_2	**2C**	H	H	**3a**	**4Ca**	71

2.2 Study on reaction conditions for ring closure reaction of nicotinates

Then, the ring closure of the synthesized nicotinate **4Aa**[16] was attempted under acidic conditions (Table 2). Ester **4Aa** was consumed upon heating at 180 °C in polyphosphoric acid (PPA), and **1Aa** was obtained in a yield of 20% (Table 2, Entry 1). The yield of **1A** increased to 45% as the reaction temperature was increased to 220 °C (Entry 2). However, the yield of **1Aa** decreased at a still higher temperature (Entry 3), and the optimal temperature for the ring closure was determined to be 220 °C. Reaction time was also studied. When the reaction was stopped at 15 minutes, nicotinate **4Aa** was almost consumed, but onychine (**1Aa**) was obtained in just 6% yield. In this reaction, nicotinic acid **5** was obtained in 46% yield, suggesting that the ring closure proceeds in two steps *via* the nicotinic acid intermediate **5** (Entry 4). Indeed, the isolated **5** was converted into onychine (**1Aa**) in 40% yield upon heating at 220 °C for 1 hour in PPA. The yield of onychine (**1Aa**) increased with the reaction time (Entries 4–6), and the yield reached 56% upon heating for 1 hour (Entry 6). However, no positive effect was observed for even longer reaction times (Entry 7).

Table 2. Study on reaction conditions for cyclization of **4**.

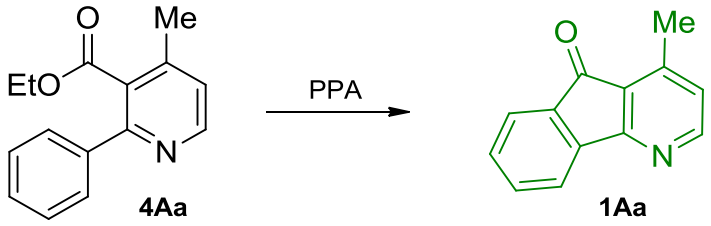

4Aa **1Aa**

Entry	Temp. /°C	Time /h	Yield of **1Aa** /%	Recovery of **4Aa** /%
1	180	4	20	5
2	220	4	45	0
3	240	4	33	0
4[*a*]	220	0.25	6	7
5	220	0.5	20	3
6	220	1	56	0
7	220	2	49	0

[*a*] An amount of 46% of nicotinic acid **5** was formed.

2.3 Ring closure reaction *via* nicotinic acid 5

Since the cyclization was found to occur *via* nicotinic acid **5** in PPA, another synthetic method was studied, that involved three steps: hydrolysis of ester **4Aa**, conversion into acyl chloride **6**, and intramolecular Friedel–Crafts reaction (Scheme 4). However, the onychine (**1Aa**) was obtained in 13% overall yield, which was lower than that of the one-step ring closure of **4Aa** conducted in PPA.

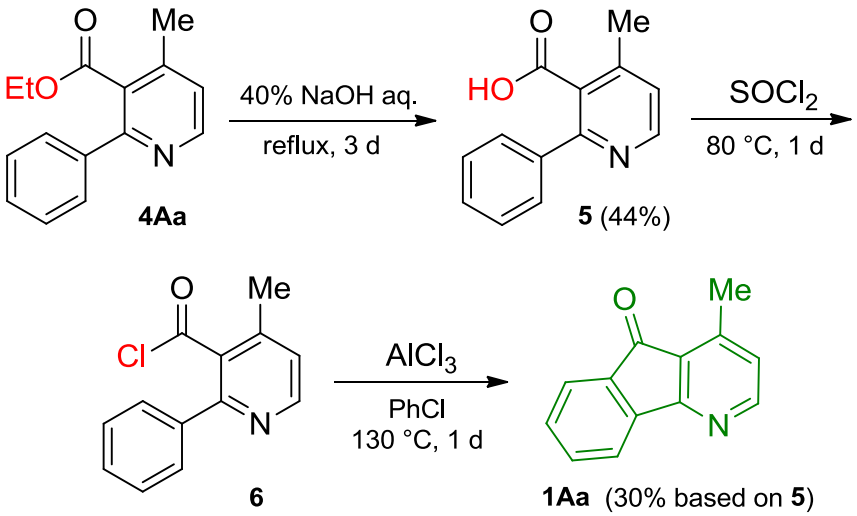

Scheme 4. Synthesis of **1Aa** from **4Aa** *via* nicotinic acid **5**.

2.4 Synthesis of onychine derivatives 1

This protocol was applied to the substituted nicotinates **4Ab**–**4Ad** under the obtained optimum conditions (Table 3, Entries 1–3). When nicotinates **4Ab** and **4Ac** were employed, yields of products **1Ab** and **1Ac** were somewhat lower than that of **1Aa**, which is presumably due to the steric repulsion from the adjacent methyl group or due to its electron-donating effect (Entries 1 and 2). On the contrary, the nicotinate **4Ad**[15] revealed similar reactivity to **4Aa** despite the presence of a bulky phenyl group (Entry 3). When 2-(4-methoxyphenyl)nicotinate **4Ba**[7a,16] was subjected to this ring closure, only a trace amount of **1Ba**[18] was detected because the methoxy group serves as an electron-withdrawing group at the *meta*-position (Entry 4). Furthermore, hydrolysis of the methoxy group also occurred. This problem was addressed by carrying out the reaction for a longer duration to increase the yield of **1Ba** to 31% (Entry 5). Other 2-(4-methoxyphenyl)nicotinates **4Bb**–**4Bd** exhibited similar reactivity to **4Ba** leading to **1Bb**–**1Bd**, respectively (Entries 6–8). However, nicotinate **4Ca** possessing a stronger electron-withdrawing group afforded only a complex reaction mixture under the same reaction conditions (Entry 9).

Table 3. Synthesis of other onychine derivatives **1**.

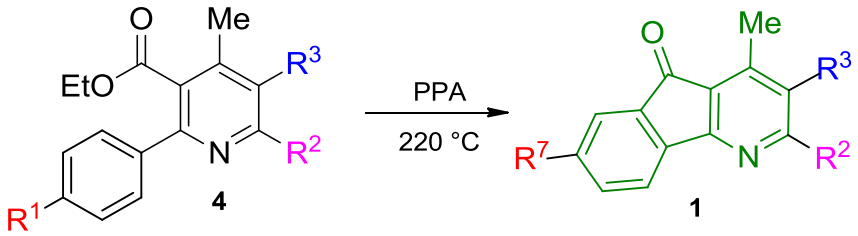

Entry	Nicotinate				Time /h	Product		
	R^7	R^2	R^3			R^7		Yield /%
1	H	H	Me	**4Ab**	1	H	**1Ab**	44
2	H	Me	Me	**4Ac**	1	H	**1Ac**	39
3	H	Ph	H	**4Ad**	1	H	**1Ad**	54
4	OMe	H	H	**4Ba**	1	OH	**1Ba**	3
5	OMe	H	H	**4Ba**	4	OH	**1Ba**	31
6	OMe	H	Me	**4Bb**	4	OH	**1Bb**	20
7	OMe	Me	Me	**4Bc**	4	OH	**1Bc**	13
8	OMe	Ph	H	**4Bd**	4	OH	**1Bd**	31
9	NO_2	H	H	**4Ca**	4	NO_2	**1Ca**	0

2.5 Modification of the phenolic hydroxy group at the 7-position

Although hydrolysis of a methoxy group occurred during the cyclization of **1Ba**, the formed phenolic hydroxy group can be modified upon treatment with electrophiles in the presence of a base (Table 4). When **1Ba** was treated with alkyl bromides in *N*,*N*-Dimethylformamide (DMF), the *O*-alkylated products **1Be** and **1Bf** were obtained (Table 4, Entries 1 and 2). Allylation was possible by treatment with allyl chloride in acetone under mild conditions to afford **1Bg** in high yield (Entry 3). *O*-Acetylation was also achieved in a similar manner to give an ester **1Bh** (Entry 4). Trifluoromethanesulfonic anhydride could also be used as an electrophile, and the corresponding triflate **1Bi** could be prepared (Entry 5).

Table 4. Modification of a phenolic hydroxy group.

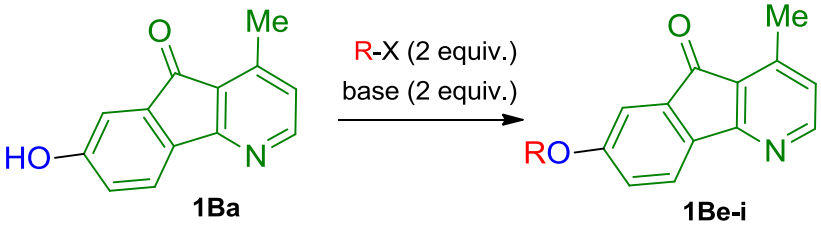

Entry	RX	Base	Solvent	Temp. /°C	Time /h	Product	Yield /%
1	PrBr	K_2CO_3	DMF	80	14	**1Be**	93
2	$PhCH_2Br$	K_2CO_3	DMF	80	14	**1Bf**	67
3	AllylCl	K_2CO_3	Acetone	25	5	**1Bg**	83
4	AcCl	K_2CO_3	DMF	25	14	**1Bh**	53
5	CF_3SO_2OTf	NEt_3	MeCN	25	14	**1Bi**	55

Chapter 3 Conclusions

A facile method for synthesizing onychines was developed by the condensation of an enamino ester with an α,β-unsaturated carbonyl compound in the presence of $FeCl_3$, followed by intramolecular Friedel–Crafts reaction. This method facilitates the modification of the onychine framework by altering only the starting enamino esters and enones, although the electron-withdrawing group on the 2-phenyl group prevented the second cyclization step. Furthermore, hydrolysis of a methoxy group was found to occur during the cyclization when 2-(4-methoxyphenyl)nicotinate was heated in PPA. The hydroxy group was easily modified upon treatment with electrophiles such as alkyl halides, acetyl chloride, and triflic anhydride, which consequently afforded diverse onychine derivatives. The present method will be useful for research of biological activity of onychine and its derivatives.

Chapter 4 Experimental section

4.1 Synthesis and Identifications. All reagents were purchased from commercial sources and used without further purification. Dry acetonitrile was also purchased from commercial source and used as received.

^{1}H and ^{13}C NMR spectra were recorded on Bruker DPX-400 spectrometer (400 MHz and 100 MHz, respectively) in $CDCl_3$ and DMSO-d_6 using tetramethylsilane as an internal standard (0.00 ppm). The assignments of the ^{13}C NMR were performed by DEPT experiments. A Shimadzu IR spectrophotometer equipped with an ATR detector were used to record IR spectra. High-resolution mass spectra were obtained on an AB SCEIX Triplet TOF 4600 mass spectrometer. Melting points were recorded on a SRS-Optimelt automated melting point system and are uncorrected. Unless otherwise noted, all reagents were purchased from commercial sources and used without further purification.

Ethyl 4-Methyl-2-phenylpyridine-3-carboxylate **(4Aa);**[16] **Typical Procedure.** To a solution of ethyl 3-amino-4-phenyl-2-butenoate (**2A**; 2.28 g, 12 mmol) in Acetonitrile (15 mL) were added 2-butenal (**3a**; 0.5 mL, 6.0 mmol) and iron(III) chloride (1.0 g, 6.0 mmol), and the resultant solution was heated at 150 °C for 1 h under microwave irradiation. After evaporation of the solvent under reduced pressure, the residue was washed with H_2O (3 × 30 mL), and then extracted with chloroform (3 × 30 mL). The combined organic layers were dried ($MgSO_4$), filtered, and concentrated under reduced pressure. The crude residue was purified by flash column chromatography on silica gel (hexane/EtOAc 8:2) to afford **4Aa** as a yellow oil (1.04 g, 74%, 4.4 mmol). ^{1}H NMR ($CDCl_3$, 400 MHz) δ 8.50 (1H, d, J = 4.8 Hz), 7.52–7.49 (2H, m), 7.36–7.32 (3H, m), 7.06 (1H, d, J = 4.8 Hz), 4.18 (2H, q, J = 7.2 Hz), 2.36 (3H, s), 0.94 (3H, t, J = 7.2 Hz); ^{13}C NMR ($CDCl_3$, 100 MHz) δ 156.6

(C), 149.5 (CH), 145.5 (C), 140.0 (C), 129.2 (C), 128.6 (CH), 128.3 (CH), 123.6 (CH), 61.3 (CH_2), 19.3 (CH_3), 13.6 (CH_3).

Ethyl 4,5-Dimethyl-2-phenylpyridine-3-carboxylate **(4Ab).** Colorless plates (0.92 g, 60%, 3.6 mmol). Mp 59.1–59.9 °C, ^{1}H NMR ($CDCl_3$, 400 MHz) δ 8.45 (1H, s), 7.57–7.55 (2H, m), 7.42–7.36 (3H, m), 4.13 (2H, q, J = 7.1 Hz), 2.32 (3H, s), 2.31 (3H, s), 1.02 (3H, t, J = 7.1 Hz); ^{13}C NMR ($CDCl_3$, 100 MHz) δ 169.61 (C), 154.4 (C), 150.2 (CH), 143.5 (C), 140.1 (C), 130.7 (C), 129.3 (C), 128.3 (CH), 128.24 (CH), 128.23 (CH), 61.4 (CH_2), 16.6 (CH_3), 16.2 (CH_3), 13.6 (CH_3); IR: 1722, 1244, 698 (ATR/cm^{-1}); HRMS (ESI/TOF) calcd for $[M+H]^+$ $C_{16}H_{18}NO_2$: 256.1132; found: 256.1139.

Ethyl 4,5,6-Trimethyl-2-phenylpyridine-3-carboxylate **(4Ac).** Colorless solid (0.56 g, 35%, 2.1 mmol). Mp 96.4–96.9 °C, ^{1}H NMR ($CDCl_3$, 400 MHz) δ 7.56–7.54 (2H, m), 7.40–7.35 (3H, m), 4.10 (2H, q, J = 7.2 Hz), 2.60 (3H, s), 2.31 (3H, s), 2.27 (3H, s), 0.99 (3H, t, J = 7.2 Hz); ^{13}C NMR ($CDCl_3$, 100 MHz) δ 169.6 (C), 157.1 (C), 152.9 (C), 142.9 (C), 140.5 (C), 128.7 (C), 128.3 (CH), 128.21 (CH), 128.17 (CH), 127.6 (C), 61.3 (CH_2), 23.6 (CH_3), 16.8 (CH_3), 14.9 (CH_3), 13.6 (CH_3); IR: 1724, 1259, 698 (ATR/cm^1); HRMS (ESI/TOF) calcd for $[M+H]^+$ $C_{17}H_{20}NO_2$: 270.1489; found: 270.1483.

Ethyl 4-Methyl-2,6-diphenylpyridine-3-carboxylate **(4Ad).**[15] Yellow oil (1.03 g, 54%, 3.3 mmol). ^{1}H NMR ($CDCl_3$, 400 MHz) δ 8.10–8.07 (2H, m), 7.97–7.93 (1H, m), 7.70–7.68 (2H, m), 7.17 (1H, s), 7.48–7.40 (5H, m), 4.14 (2H, q, J =7.1 Hz), 2.49 (3H, s), 1.03 (3H, t, J = 7.1 Hz); ^{13}C NMR ($CDCl_3$, 100 MHz) δ 169.8 (C), 159.8 (C), 156.9 (C), 152.3 (C), 142.7 (C), 133.0 (C), 130.9 (CH), 130.6 (CH), 129.6 (CH), 128.2 (C), 127.4 (C), 113.7 (CH), 61.2 (CH_2), 55.3 (CH_3), 23.6 (CH_3), 16.8 (CH_3), 14.9 (CH_3), 13.8 (CH_3).

***Ethyl 2-(4-Methoxyphenyl)-4-methylpyridine-3-carboxylate* (4Ba)**[16]**.** Yellow solid (1.20 g, 74%, 4.4 mmol). Mp 57.7–58.3 °C, ^{1}H NMR ($CDCl_3$, 400 MHz) δ 8.53 (1H, d, *J* = 5.0 Hz), 7.54 (2H, d, *J* = 8.9 Hz), 7.09 (1H, d, *J* = 5.0 Hz), 6.94 (2H, d, *J* = 8.9 Hz), 4.17 (2H, q, *J* = 7.1 Hz), 3.84 (3H, s), 2.40 (3H, s), 1.01 (3H, t, *J* = 7.1 Hz); ^{13}C NMR ($CDCl_3$, 100 MHz) δ 168.9 (C), 160.1 (C), 156.1 (C), 149.5(CH), 145.3 (C), 132.6 (C), 129.6 (CH), 123.1 (CH), 113.7 (CH), 61.4 (CH_2), 55.3 (CH_3), 19.3 (CH_3), 13.8 (CH_3).

***Ethyl 2-(4-methoxyphenyl)-4,5-dimethylpyridine-3-carboxylate* (4Bb).** Yellow solid (0.96 g, 56%, 3.4 mmol). Mp 75.6–76.3 °C, ^{1}H NMR ($CDCl_3$, 400 MHz) δ 8.42 (1H, s) 7.52 (2H, d, *J* = 8.8 Hz), 6.93 (2H, d, *J* = 8.8 Hz), 4.17 (2H, q, *J* = 7.2 Hz), 3.83 (3H, s), 2.30 (3H, s), 2.29 (3H, s), 1.09 (3H, t, *J* = 7.2 Hz); ^{13}C NMR ($CDCl_3$, 100 MHz) δ 169.4 (C), 159.9 (C), 153.9 (C), 150.2 (CH), 143.3 (C), 132.7 (C), 130.2 (C), 129.6 (CH), 129.5 (CH), 129.0 (C), 113.9 (CH), 113.7 (CH), 61.4 (CH_2), 55.3 (CH_3), 16.6 (CH_3), 16.2 (CH_3), 13.8 (CH_3); IR: 1719, 1248, 1176 (ATR/cm^{-1}); HRMS (ESI/TOF) calcd for $[M+H]^+$ $C_{17}H_{20}NO_3$: 286.1438; found: 286.1424.

***Ethyl 2-(4-Methoxyphenyl)-4,5,6-trimethylpyridine-3-carboxylate* (4Bc).** Yellow solid (0.90 g, 50%, 3.0 mmol). Mp 85.9–86.8 °C, ^{1}H NMR ($CDCl^3$, 400 MHz) δ 7.51 (2H, d, *J* = 8.8 Hz), 6.92 (2H, d, *J* = 8.8 Hz), 4.14 (2 H, q, *J* = 7.1 Hz), 3.82 (3H, s), 2.58 (3H, s), 2.29 (3 H, s), 2.25 (3H, s), 1.07 (3H, t, *J* = 7.1 Hz); ^{13}C NMR ($CDCl_3$, 100 MHz) δ 169.8 (C), 159.8 (C), 156.9 (C), 152.3 (C), 142.7 (C), 133.0 (C), 130.9 (CH), 130.6 (CH), 129.6 (CH), 128.2 (C), 127.4 (C), 113.7 (CH), 61.2 (CH_2), 55.3 (CH_3), 23.6 (CH_3), 16.8 (CH_3), 14.9 (CH_3), 13.8 (CH_3); IR: 1718, 1515, 1248, 1173 (ATR/cm^{-1}); HRMS (ESI/TOF) calcd for $[M+H]^+$ $C_{18}H_{22}NO_3$: 300.1594; found: 300.1580.

***Ethyl 2-(4-Methoxyphenyl)-4-methyl-6-phenylpyridine-3-carboxylate* (4Bd).** Yellow

oil (1.35 g, 65%, 3.9 mmol). ^{1}H NMR ($CDCl_3$, 400 MHz) δ 8.09 (2H, d, *J* = 6.8 Hz), 7.67 (2H, d, *J* = 8.8 Hz), 7.53 (1H, br q, *J* = 0.4 Hz), 7.48–7.41 (3H, m), 6.96 (2 H, d, *J* = 8.8 Hz), 4.20 (2H, q, *J* = 7.1 Hz), 3.85 (3H, s), 2.47 (3H, br d, *J* = 0.4 Hz), 1.11 (3H, t, *J* = 7.1 Hz); ^{13}C NMR ($CDCl_3$, 100 MHz) δ 169.4 (C), 157.0 (C), 160.2 (C), 156.0 (C), 146.2 (C), 138.8 (C), 133.0 (C), 129.9 (CH), 129.3 (CH), 128.7 (CH), 127.2 (CH), 127.1 (C), 119.6 (CH), 113.7 (CH), 61.4 (CH2), 55.4 (CH3), 19.7 (CH), 13.9 (CH); IR: 1718, 1514, 1268, 1250, 1177, 1093, 694 (ATR/cm^{-1}); HRMS (ESI/TOF) calcd for $[M+H]^+$ $C_{22}H_{22}NO_3$: 348.1594; found: 348.1596.

Ethyl 4-Methyl-2-(4-nitrophenyl)pyridine-3-carboxylate **(4Ca).** Yellow oil (1.22 g, 71%, 4.3 mmol). ^{1}H NMR ($CDCl_3$, 400 MHz) δ 8.60 (1H, d, *J* = 5.4 Hz), 8.28 (2H, d, *J* = 8.8 Hz), 7.76 (2H, d, *J* = 8.8 Hz), 7.24 (1H, d, *J* = 5.4 Hz), 4.16 (2H, q, *J* = 7.1 Hz), 2.46 (3H, s), 1.08 (3H, t, *J* = 7.1 Hz); ^{13}C NMR ($CDCl_3$, 100 MHz) δ 167.8 (C), 154.3 (C), 149.9 (CH), 147.9 (C), 146.3 (C), 146.2 (C), 129.4 (CH), 124.8 (CH), 123.8 (C), 123.5 (CH), 61.8 (CH_2), 19.5 (CH_3), 13.8 (CH_3); IR: 1725, 1523, 1349 (ATR/cm^{-1}); HRMS (ESI/TOF) calcd for $[M+H]^+$ $C_{15}H_{14}N_2O_4$: 287.1026; found: 287.1025.

4-Methyl-2-phenylpyridine-3-carboxylic Acid **(5).** To a solution of sodium hydroxide (3.2 g, 80 mmol) in H_2O (8 mL) was added ethyl 4-methyl-2-phenylpyridine-3-carboxylate (**4Aa**; 484 mg, 2.0 mmol), and the resultant solution was heated at 100 °C for 3 d. After washing with dichloromethane (3 × 30 mL), the pH value of the aqueous layer was adjusted to 4, and concentrated under reduced pressure. The residue was extracted with hot metahnol (3 × 10 mL), and the methanol was evaporated. The residue was subjected to flash column chromatography on silica gel (methanol/dichloromethane 1:3) to afford **5** as a white powder (188 mg, 44%, 0.88 mmol); Mp 100.5–101.2 °C, ^{1}H NMR

(DMSO-d_6, 400 MHz) δ 8.50 (2H, d, J = 4.9 Hz), 7.70–7.68 (2H, m), 7.43–7.41 (3H, m), 7.26 (1H, d, J = 4.9 Hz), 3.17 (1H, s), 2.34 (3H, s); ^{13}C NMR (DMSO-d_6, 100 MHz) δ 170.3 (C), 153.5 (C), 148.3 (CH), 143.6 (C), 140.0 (C), 128.3 (CH), 128.2 (CH), 127.9 (CH), 123.6 (CH), 18.9 (CH_3).

4-Methyl-5H-indeno[1,2-b]pyridin-5-one **(Onychine, 1Aa);**[8–12] **Typical Procedure.** A solution of ethyl 4-methyl-2-phenylpyridine-3-carboxylate (**4Aa**; 33.2 mg, 0.14 mmol) in polyphosphoric acid (1 mL) was heated at 220 °C for 1 h. After the pH value of the mixture was adjusted to 8, the mixture was extracted with CH_2Cl_2 (3 × 15 mL). The combined organic layers were dried ($MgSO_4$), filtered, and concentrated under reduced pressure to afford onychine (**1Aa**) as yellow needles (15.3 mg, 56%, 0.078 mmol); Mp 137.2–137.4 °C, ^{1}H NMR ($CDCl_3$, 400 MHz) δ 8.34 (1H, d, J = 5.3 Hz), 7.79 (1H, dd, J = 7.4, 1.1 Hz), 7.62 (1H, dd, J = 7.4, 1.1 Hz), 7.51 (1H, ddd, J = 7.4, 7.4, 1.1 Hz), 7.35 (1H, ddd, J = 7.4, 7.4, 1.1 Hz), 6.91 (1H, d, J = 5.3 Hz), 2.63 (3H, s); ^{13}C NMR ($CDCl_3$, 100 MHz) δ 192.8 (C), 164.7 (C), 151.9 (CH), 148.2(C), 142.4 (C), 135.1 (CH), 134.8 (C), 131.1 (CH), 126.1 (C), 126.0 (CH), 123.8 (CH), 121.3 (CH), 17.4 (CH_3).

3,4-Dimethyl-5H-indeno[1,2-b]pyridin-5-one **(1Ab).** Yellow needles (12.9 mg, 44%, 0.062 mmol). Mp 144.6–145.3 °C, ^{1}H NMR ($CDCl_3$, 400 MHz) δ 8.28 (s, 1H), 7.78 (1H, dd, J = 7.6, 1.2 Hz), 7.66 (1H, dd, J = 7.6, 1.2 Hz), 7.55 (1H, ddd, J = 7.6, 7.6, 1.2 Hz), 7.38 (1H, ddd, J = 7.6, 7.6, 1.2 Hz), 2.58 (3 H, s), 2.27 (3 H, s); ^{13}C NMR ($CDCl_3$, 100 MHz) δ 193.7 (C), 163.4 (C), 153.0 (CH), 146.7 (C), 143.1 (C), 135.1 (C), 134.9 (CH), 133.3 (C), 130.4 (CH), 125.6 (C), 123.7 (CH), 120.4 (CH), 16.1 (CH_3), 13.4 (CH_3); IR: 1711, 746 (ATR/cm^{-1}); HRMS (ESI/TOF) calcd for $[M+H]^+$ $C_{14}H_{12}NO$: 210.0913; found: 210.0912.

2,3,4-Trimethyl-5H-indeno[1,2-b]pyridin-5-one **(1Ac).** Yellow needles (12.2 mg, 39%, 0.055 mmol). Mp 154.5–155.4 °C, ^{1}H NMR ($CDCl_3$, 400 MHz) δ 7.70 (1H, d, *J* =7.4 Hz), 7.56 (1H, d, *J* = 7.4 Hz), 7.44 (1H, ddd, *J* = 7.4, 7.4, 1.2 Hz), 7.28 (1H, ddd, *J* = 7.4, 7.4, 1.2 Hz), 2.51 (3 H, s), 2.50 (3H, s), 2.13 (3 H, s); ^{13}C NMR ($CDCl_3$, 100 MHz) δ 192.8 (C), 161.3 (C), 160.1 (C), 145.1(C), 142.1 (C), 134.2 (C), 133.6 (CH), 129.9 (C), 129.1 (CH), 123.0 (C),122.4 (CH), 119.2 (CH), 23.0 (CH_3), 13.3 (CH_3), 12.6 (CH_3); IR: 1706, 886, 745 (ATR/cm^{-1}); HRMS (ESI/TOF) calcd for $[M+H]^+$ $C_{15}H_{14}NO$: 224.1069; found 224.1070.

4-Methyl-2-phenyl-5H-indeno[1,2-b]pyridin-5-one **(1Ad)**[19]. Yellow solid (20.6 mg, 54%, 0.076 mmol). Mp 121.3–121.6 °C, ^{1}H NMR ($CDCl_3$, 400 MHz) δ 8.11 (2H, d, *J* = 6.6 Hz), 7.93 (1H, d, *J* = 7.4 Hz), 7.69 (1H, d, *J* = 7.4 Hz), 7.57 (1H, t, *J* = 7.4 Hz), 7.52–7.38 (5H, m), 2.67 (3H, s); ^{13}C NMR ($CDCl_3$, 100 MHz) δ 193.1 (C), 165.7 (C), 160.8 (C), 147.8 (C), 143.2 (C), 138.5 (C), 135.6 (C), 134.7 (CH), 130.7 (CH), 129.8 (CH), 128.8 (CH), 127.3 (CH), 124.5 (C), 123.5 (CH), 122.2 (CH), 120.9 (CH), 17.6 (CH_3).

7-Hydroxy-4-methyl-5H-indeno[1,2-b]pyridin-5-one **(1Ba).** Yellow solid (9.2 mg, 31%, 0.043 mmol). Mp 225.2–225.7 °C, ^{1}H NMR (DMSO-d_6, 400 MHz) δ 8.40 (1H, d, *J* = 5.3 Hz), 7.64 (1H, d, *J* = 7.4 Hz), 7.08–7.04 (3H, m), 2.67 (3H, s); ^{13}C NMR (DMSO-d_6, 100 MHz) δ 192.6 (C), 165.1 (C), 160.4 (C), 152.8 (CH), 146.6 (C), 136.4 (C), 133.2 (C), 124.9 (C), 124.7 (CH), 122.1 (CH), 121.1 (CH), 110.4 (CH), 16.6 (CH_3).

7-Hydroxy-3,4-dimethyl-5H-indeno[1,2-b]pyridin-5-one **(1Bb).** Yellow needles (6.3 mg, 20%, 0.028 mmol). Mp 144.0–144.9 °C, ^{1}H NMR (DMSO-d_6, 400 MHz) δ 10.2–10.3 (1H, br), 8.29 (1H, s), 7.59 (1H, d, *J* = 7.8 Hz), 7.05–7.02 (2H, m), 2.53 (3H, s), 2.25 (3H, s); ^{13}C NMR (DMSO-d_6, 100 MHz) δ 193.0 (C), 163.3 (C), 160.0 (C), 152.6 (CH), 145.9

(C), 136.5 (C), 133.3 (C), 131.9 (C), 124.5 (C), 121.7 (CH), 121.2 (CH), 110.4 (CH), 15.3 (CH_3), 12.9 (CH_3); IR; 1719, 1515, 1295, 1250, 1176 (ATR/cm^{-1}); HRMS (ESI/TOF): calcd for $[M+H]^+$ $C_{14}H_{15}NO_2$: 226.0862; found: 226.0872.

7-Hydroxy-2,3,4-trimethyl-5H-indeno[1,2-b]pyridin-5-one **(1Bc).** Yellow solid (4.4. mg, 13%, 0.02 mmol). Mp 143.0–143.4 °C, ^{1}H NMR (DMSO-d_6, 400 MHz) δ 10.7–9.8 (1H, br), 7.54 (1H, d, J = 8.7 Hz), 7.01–6.99 (2H, m), 2.52 (3H, s), 2.52 (3H, s), 2.17 (3H, s): ^{13}C NMR (DMSO-d_6, 100 MHz) δ 193.0 (C), 162.2 (C), 160.7 (C), 159.9 (C), 145.4 (C), 136.7 (C), 133.2 (C), 129.3 (C), 122.9 (C), 121.5 (CH), 120.8 (CH), 110.4 (CH), 23.7 (CH_3), 13.7 (CH_3), 13.1 (CH_3); IR: 1720, 1271 (ATR/cm^{-1}); HRMS (ESI/TOF): calcd for $[M+H]^+$ $C_{15}H_{14}NO_2$: 240.1019; found: 240.1029.

7-Hydroxy-2-phenyl-4-methyl-5H-indeno[1,2-b]pyridin-5-one **(1Bd).** Yellow solid (12.5 mg, 31%, 0.043 mmol). Mp 191.2–191.7 °C, ^{1}H NMR (DMSO-d_6, 400 MHz) δ 10.9–9.8 (1H, br), 8.14–8.12 (2H, m), 7.73 (1H, d, J = 8.0 Hz), 7.67 (1H, s), 7.59–7.55 (3H, m), 7.08–7.06 (2H, m), 2.62 (3H, s); ^{13}C NMR (DMSO-d_6, 100 MHz) δ 192.2 (C), 165.5 (C), 160.5 (C), 159.2 (C), 147.4 (C), 137.7 (C), 137.2 (C), 133.1 (C), 129.9 (CH), 128.8(CH), 127.1 (CH), 123.8 (C), 122.2 (CH), 121.0 (CH), 120.7 (CH), 110.4 (CH), 17.0 (CH_3); IR: 1709, 1570, 1290, 1250, 803 (ATR/cm^{-1}); HRMS (ESI/TOF): calcd for $[M+H]^+$ $C_{19}H_{14}NO_2$: 288.1019; found 288.1018.

4-Methyl-7-propoxy-5H-indeno[1,2-b]pyridin-5-one **(1Be); Typical Procedure.** To a solution of 7-hydroxy-4-methyl-5*H*-indeno[1, 2-*b*] pyridin-5-one (**1Ba**; 1.0 mg, 4.7 μmol) in DMF (1 mL), 1-bromopropane (0.71 μL, 9.5 μmol) was added, and the resultant solution was heated at 80 °C for 14 h. After evaporation, the residue was washed with H_2O (10 mL), and then extracted with chloroform (3 × 10 mL). The combined organic

layers were dried ($MgSO_4$), filtered, and concentrated under reduced pressure to afford **1Be** as a yellow solid (1.1 mg, 93%, 4.3 μmol); Mp 79.7–80.5 °C, ^{1}H NMR ($CDCl_3$, 400 MHz) δ 8.34 (1H, d, *J* = 5.2 Hz), 7.71 (1H, d, *J* = 8.4 Hz), 7.20 (1H, d, *J* = 2.4 Hz), 7.06 (1H, dd, *J* = 2.4, 8.4 Hz), 6.87 (1 H, d, *J* = 5.2 Hz), 3.99 (2H, t, *J* = 6.4 Hz), 2.60 (3H, s), 1.84 (2H, tq, *J* = 6.4, 7.2 Hz), 1.06 (3H, t, *J* = 7.2 Hz); ^{13}C NMR ($CDCl_3$, 100 MHz) δ 193.2 (C), 165.8 (C), 161.9 (C), 152.7 (CH), 147.3 (C), 136.9 (C), 135.3 (C), 126.1 (C), 124.8 (CH), 122.1 (CH), 120.9 (CH), 109.5 (CH), 70.2 (CH_2), 22.5 (CH_2), 17.3 (CH_3), 10.4 (CH_3); IR: 1716, 1567 (ATR/cm^{-1}); HRMS (ESI/TOF): calcd for $[M+H]^+$ $C_{16}H_{16}NO_2$: 254.1175; found: 254.1183.

7-Benzyloxy-4-methyl-5H-indeno[1,2-b]pyridin-5-one **(1Bf).** Yellow needles (0.95 mg, 67%, 3.2 μmol). Mp 140.3–141.1 °C, ^{1}H NMR ($CDCl_3$, 400 MHz) δ 8.34 (H, d, *J* = 5.2 Hz), 7.73 (1H, d, *J* = 8.0 Hz), 7.45–7.36 (5H, m), 7.29 (1H, d, *J* = 2.4 Hz), 7.14 (1H, dd, *J* = 2.4, 8.0 Hz), 6.87 (1H, d, *J* = 5.2 Hz), 5.14 (2H, s), 2.59 (3H, s); ^{13}C NMR ($CDCl_3$, 100 MHz) δ 193.0 (C), 165.7 (C), 161.4 (C), 152.8 (CH), 147.4 (C), 136.9 (C), 136.2 (C), 135.8 (C), 128.7 (CH), 128.3 (CH), 127.5 (CH), 126.1 (C), 124.9 (CH), 122.1 (CH), 121.3 (CH), 109.9 (CH), 70.6 (CH_2), 17.3 (CH_3); IR: 1708, 1566, 1292, 999, 740 (ATR/cm^{-1}); HRMS (ESI/TOF): calcd for $[M+H]^+$ $C_{20}H_{16}NO_2$: 302.1175; found: 302.1175.

4-Methyl-7-(3-propenyloxy)-5H-indeno[1,2-b]pyridin-5-one **(1Bg).** Yellow needles (0.98 mg, 83%, 3.9 μmol). Mp 80.9–81.9 °C, ^{1}H NMR ($CDCl_3$, 400 MHz) δ 8.34 (1H, d, *J* = 5.6 Hz), 7.72 (1H, d, *J* = 8.4 Hz), 7.22 (1H, d, *J* = 2.4 Hz), 7.08 (1H, dd, *J* = 8.4, 2.4 Hz), 6.88 (1H, d, *J* = 5.6 Hz), 6.05 (1H, ddt, *J* = 17.6, 10.4, 5.2 Hz), 5.42 (1H, ddt, *J* = 17.6, 1.6, 1.6 Hz), 5.34 (1H, ddt, *J* = 10.4, 1.6, 1.6 Hz), 4.62 (2H, ddd, *J* = 5.2, 1.6, 1.6 Hz), 2.60 (3H, s); ^{13}C NMR ($CDCl_3$, 100 MHz) δ 193.1 (C), 165.7 (C), 161.3 (C), 152.8

(CH), 147.4 (C), 136.9 (C), 135.7 (C), 132.5 (CH), 126.1 (C), 124.9 (CH), 122.1 (CH), 121.2 (CH), 118.2 (CH_2), 109.7 (CH), 69.3 (CH_2), 17.3 (CH_3); IR: 1710, 1599, 1567 (ATR/cm^{-1}); HRMS (ESI/TOF): calcd for $[M+H]^+$ $C_{16}H_{15}NO_2$: 252.1019; found: 252.1031.

7-Acetoxy-4-methyl-5H-indeno[1,2-b]pyridin-5-one **(1Bh).** Yellow oil (0.63 mg, 53%, 2.5 μmol). ^1H NMR ($CDCl_3$, 400 MHz) δ 8.41 (1H, d, *J* = 5.2 Hz), 7.84 (1H, d, *J* = 8.0 Hz), 7.43 (1H, d, *J* = 2.4 Hz), 7.28 (1H, dd, *J* = 8.0, 2.4 Hz), 6.96 (1H, d, *J* = 5.2 Hz), 2.62 (3H, s), 2.33 (3H, s); ^{13}C NMR ($CDCl_3$, 100 MHz) δ 190.9 (C), 167.9 (C), 163.7 (C), 152.0 (CH), 151.9 (C), 146.8 (C), 138.3 (C), 135.4 (C), 126.8 (CH), 125.3 (C), 124.7 (CH), 120.8 (CH), 116.5 (CH), 20.0 (CH_3), 16.3 (CH_3); IR: 1766, 1716, 1600, 1570, 1195, 740 (ATR/cm^{-1}); HRMS (ESI/TOF): calcd for $[M+H]^+$ $C_{15}H_{12}NO_3$: 254.0811; found: 254.0821.

4-Methyl-7-(trifluoromethanesulfonyloxy)-5H-indeno[1,2-b]pyridin-5-one **(1Bi).** Yellow needles (0.89 mg, 55%, 2.6 μmol). Mp 95.3–96.0 °C, ^1H NMR ($CDCl_3$, 400 MHz) δ 8.47 (1H, d, *J* = 5.2 Hz), 7.94 (1H, d, *J* = 8.0 Hz), 7.59 (1H, d, *J* = 8.0 Hz), 7.49 (1H, d, *J* = 8.0, 2.4 Hz), 7.04 (1H, d, *J* = 5.2 Hz), 2.65 (3H, s); ^{13}C NMR ($CDCl_3$, 100 MHz) δ 190.7 (C), 163.8 (C), 153.5 (CH), 151.2 (C), 148.2 (C), 142.8 (C), 136.9 (C), 127.5 (CH), 126.4 (CH), 122.5 (CH), 117.1 (CH), 17.5 (CH_3); IR: 1716, 1573, 1213, 1139, 732 (ATR/cm^{-1}); HRMS (ESI/TOF): calcd for $[M+H]^+$ $C_{14}H_9F_3NO_4S$: 344.0198; found: 344.0208.

Chapter 5 References

[1] M. E. L. De Almeida, R. Braz, M. V. Von Bulow, O. R. Gottlieb, J. G. S. Maia, *Phytochemistry* **1976**, *15*, 1186–1187.

[2] M. O. F. Goulart, A. E. G. Santana, A. B. De Oliveria, G. G. De Oliveria, J. G. S. Maia, *Phytochemistry* **1986**, *25*, 1691–1695.

[3] C. D. Hufford, S. Liu, A. M. Clark, B. O. Oguntimein, *J. Nat. Prod.* **1987**, *50*, 961–964.

[4] J. Koyama, T. Sugida, Y. Suzuta, H. Irie, *Heterocycles* **1979**, *12*, 1017–1019.

[5] B. F. Bowden, K. Picker, E. Ritchie, W. C. Taylor, *Aust. J. Chem.* **1975**, *28*, 2681–2701.

[6] M. Leboeuf, A. Cavé, *Lloydia* **1976**, *39*, 459–460.

[7] a) S. Taghavi-Moghadam, C. D. Kwong, J. A. Secrist, S. I. Khan, A. M. Clark, *Bioorg. Med. Chem.* **2016**, *24*, 6119–6224; b) N. Marquise, F. Chevallier, E. Nassar, M. Frederich, A. Ledoux, Y. S. Halauko, O. A. Ivashkevich, V. E. Matulis, T. Roisnel, V. Dorcet, F. Mongin, *Tetrahedron* **2016**, *72*, 825–836; c) R. Phatchana, Y. Thongsri, R. Somwaeng, K. Piboonpol, C. Yenjai, *Phytochem. Lett.* **2015**, *13*, 147–151; d) S. Prachayasittikul, P. Manam, M. Chinworrungsee, C. Isarankura-Na Ayudhya, S. Ruchirawat, V. Prachayasittikul, *Molecules* **2009**, *14*, 4414–4424; e) K. Mink, F. Bracher, *Arch. Pharm. (Weinheim)* **2007**, *340*, 429–433; f) J. H. G. Lago, M. H. Chaves, M. C. C. Ayres, D. G. Y. Agripino, C. M. Maria, *Planta Med.* **2007**, *73*, 292–295; g) J. Koyama, I. Morita, N. Kobayashi, T. Osakai, Y. Usuki, M. Taniguchi, *Bioorg. Med. Chem. Lett.* **2005**, *15*, 1079–1082.

[8] A. –S. Rebstock, F. Mongin, F. Trecourt, G. Queguiner, *Tetrahedron* **2004**, *60*, 2181–2186.

[9] A. Padwa, T. M. Heidelbaugh, J. T. Kuethe, *J. Org. Chem.* **2000**, *65*, 2368–2378.

[10] T. H. Tong, H. N. C. Wong, *Synth. Commun.* **1992**, *22*, 1773–1782.

[11] G. A. Kraus, A. Kempema, *J. Nat. Prod.* **2010**, *73*, 1967–1968.

[12] Y. Taneichi, K. Shimada, T. Korenaga, *Heterocycles* **2018**, *96*, 440–451.

[13] a) L. M. Sanchez, A. G. Sathicq, G. P. Romanelli, L. M. Gonzalez, A. L. Villa, *Mol. Catal.* **2017**, *435*, 1–12; b) A. Jana, J. Mondal, P. Borah, S. Mondal, A. Bhaumik, Y. Zhao, *Chem. Commun.* **2015**, *51*, 10746–10749; c) L. Shen, S. Cao, J. Wu, J. Zhang, H. Li, N. Liu, X. Qian, *Green Chem.* **2009**, *11*, 1414–1420.

[14] T. Alves, A. B. De Oliveira, V. Snieckus, *Tetrahedron Lett.* **1988**, *29*, 2135–2136.

[15] Y. S. Chun, J. H. Lee, J. H. Kim, Y. O. Ko, S –g. Lee, *Org. Lett.* **2011**, *13*, 6390–6393.

[16] a) E. Pan, S. Cao, P. J. Brodie, M. W. Callmander, R. Randrianaivo, S. Rakotonandrasana, E. Rakotobe, V. E. Rasamison, K. TenDyke, Y. Shen, E. M. Suh, D. G. I. Kingston, *J. Nat. Prod.* **2011**, *74*, 1169–1174; b) F. Palacios, E. Herran, C. Alonso, G. Rubiales, B. Lecea, M. Ayerbe, F. P. Cossio, *J. Org. Chem.* **2006**, *71*, 6020–6030.

[17] S. Hirai, Y. Horikawa, H. Asahara, N. Nishiwaki, *Chem. Commun.* **2017**, *53*, 2390–2393.

[18] D. Tadic, B. K. Cassels, A. Cave, *Heterocycles* **1988**, *27*, 407–421.

[19] G. V. Pavel, K. G. Pavel, M. N. Tilichenko, *Khim. Geterotsikl. Soedin.* **1990**, 9.

PART III A TRITOPIC RESPONSIVE FLUOROPHORE BASED ON AN AZA-15-CROWN-5-CONJUGATED TRIARYLBORANE SYSTEM

Chapter 1 Introduction

Fluorophores whose emission responds to multiple external factors such as the presence of ions/chemicals and other surrounding environment are of great interest especially in supramolecular and analytical chemistry. Therefore, they have been developed aiming at utilizations for multitopic chemosensors,[1] molecular logic gates[2] and so forth. In many cases, one site in a fluorophore possesses a binding/recognizing affinity for multiple analytes. Although a single-molecule-based multitopic fluorophore with multiple binding sites enables simultaneous detection of multiple analytes, the construction is still challenging.

Triarylborane derivatives, in which a tricoordinate boron atom is sterically protected by three bulky aryl groups, attract much attention owing to their fascinating absorption and fluorescence arising from an intramolecular charge-transfer (CT) transitions from the π orbital of the aryl group (π(aryl)) to the vacant p orbital on the boron atom (p(B)): π(aryl)–p(B) CT.[3] Therefore, a variety of triarylborane derivatives including polymers[4] and transition-metal complexes[5] has been hitherto developed in the last few decades and utilized in photochemical applications such as organic light-emitting diodes (OLEDs)[6] and sensing.[7] Since the boron center in a triarylborane derivative is electron-deficient, an introduction of an electron-donating group(s) into a triarylborane has a critical impact on the excited-state characteristics.[8] As a notable example, Yamaguchi *et al*. have reported a solvent-dependent fluorescence from tris{[*p*-(*N*,*N*-dimethylamino)phenylethynyl]duryl}borane (blue, green and orange in benzene,

tetrahydrofuran (THF) and *N*,*N*-dimethylformamide, respectively) in 2000,[9] and the solvent dependence originates in a huge electric dipole moment of the derivative in the excited state (~60 D; 1 D = 10^{-18} esu cm) based on an extended CT from the dimethylamino group to the boron atom as revealed by Kitamura and co-workers in 2010.[10] The sterically-hindered p(B) in a triarylborane derivative also act as a selective binding site for small Lewis bases (e.g., fluoride and cyanide), and the spectroscopic properties of a derivative drastically change upon a coordination of a Lewis base to p(B). Furthermore, in recent years, triarylborane derivatives possessing multiple response abilities have been developed. For example, Yoshino *et al*. reported a triarylborane derivative having triazole-based large π–conjugation systems exhibited a large fluorescence solvatochromic shift from blue to red and fluorescence color change from red to blue by an addition of fluoride.[11] A triarylborane derivative bearing the calixcrown moiety, which was synthesized by He *et al.*, showed a fluorescence intensity change upon a potassium-ion binding in addition to the fluoride sensing ability.[12]

In this thesis, I describe a novel triarylborane derivative having an aza-15-crown-5 moiety as an electron-donating group and binding site for metal ions (**1**). The presence of the electron-donating azacrown and phenylethynyl linker, which maximizes the electronic interactions between the triarylborane and azacrown moieties, enhances the excited-state dipole moment of **1** compared with a reference compound without the azacrown moiety (**2**). Furthermore, the electron-donating ability of the azacrown moiety in **1** is reduced by a coordination with a metal ion. Thus, the absorption and fluorescence properties of **1** respond to three coexisting substances (i.e., solvent, metal ions and fluoride).

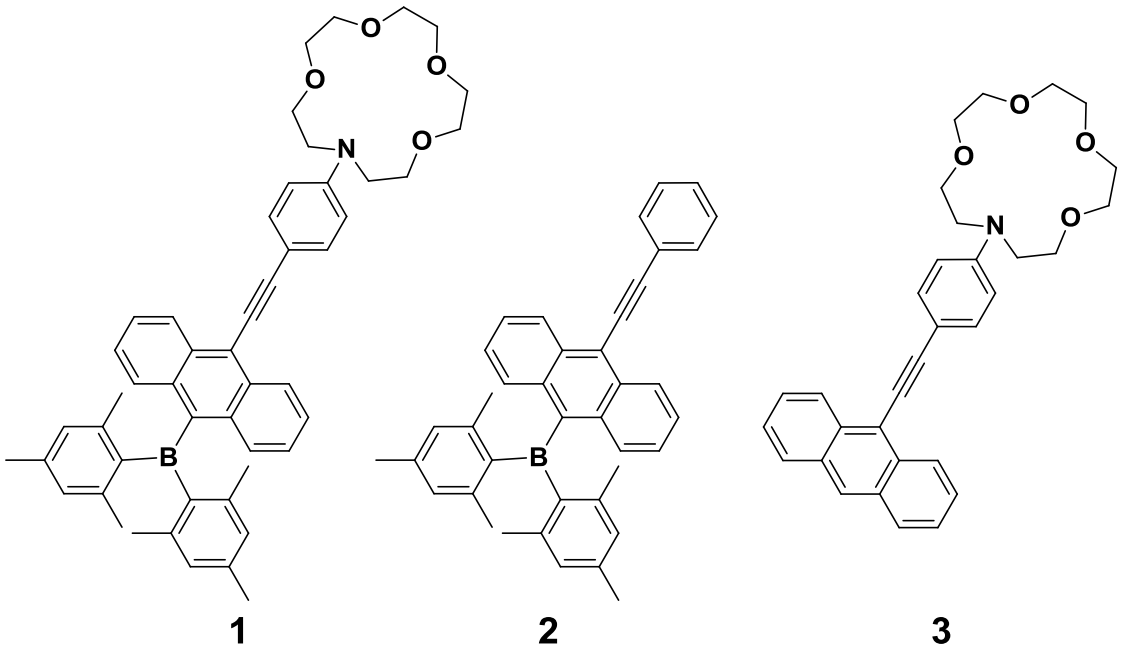

Scheme 1. Molecular structures of **1–3**.

Chapter 2 Results and discussion

2.1 Synthesis and structure determination of compounds

Compound **1** was synthesized according to Scheme 2, and detailed synthetic procedures are described in the chapter 4. Reference compounds **2** and **3**, which does not possess the dimesitylboryl moiety, were synthesized similarly. The molecular structures of the compounds were established by ^{1}H NMR, IR and high-resolution mass spectroscopies. X-ray crystallographic analyses for **1** and **2** were successfully carried out as shown in Figures 1 and 2. Both compounds possess a pseudo-D_3 symmetry around the boron atom in which B–C distances are 1.56–1.59 Å and dihedral angles between an aryl group and BC_3 plane are ~50°. Although a dihedral angle between the anthryl and phenylene moieties in **1** (85°) hugely differs from the relevant angle in **2** (~0°), the difference would take place only in the crystal system due to a molecular packing. In practice, the phenylethynylanthryl moieties in the DFT-optimized geometries of the derivatives including **3** are completely planar (Figure 3). It should be noted that, although the crystals of both **1** and **2** were 1/1 racemic mixtures of Δ- and Λ-isomers around the boron atom, the enantiomers were not separated since it would not affect the spectroscopic/photophysical data in the present study.

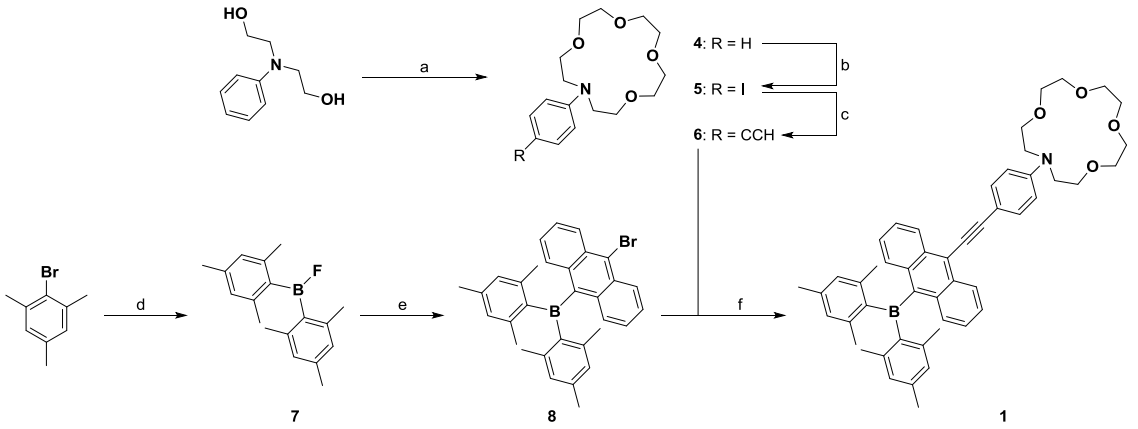

Scheme 2. Synthetic scheme to **1**: a) NaH, $Ts(OCH_2CH_2)_3OTs$, THF; b) I_2, pyridine, 1,4-dioxane; c) 1. $(CH_3)_3SiC{\equiv}CH$, $PdCl_2(PPh_3)_2$, CuI, Et_3N, 2. K_2CO_3, CH_3OH; d) Mg, BF_3OEt_2, THF; e) 9,10-dibromoanthracene, *n*-BuLi in hexane, THF; f) $Pd(PPh_3)_4$, CuI, toluene, $(i\text{Pr})_2NH$.

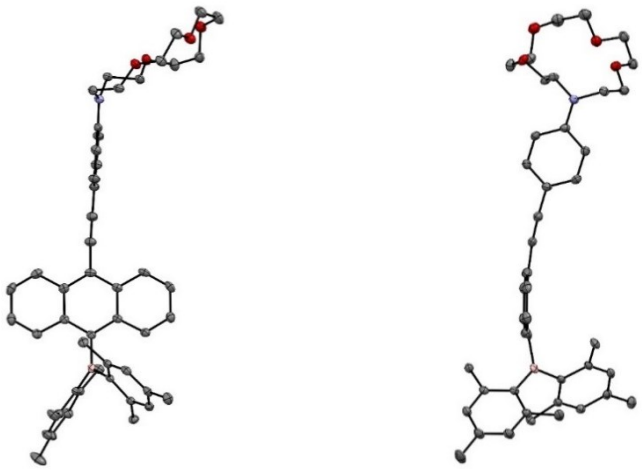

Figure 1. Perspective views (50% probability ellipsoids) of **1**: top (left) and side views (right). Hydrogen atoms are omitted for clarity.

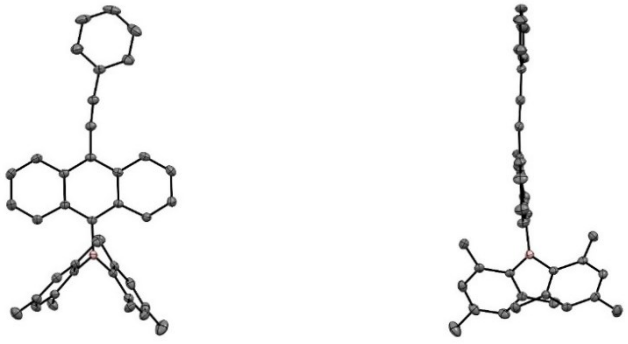

Figure 2. Perspective views (50% probability ellipsoids) of **2**: top (left) and side views (right). Hydrogen atoms are omitted for clarity.

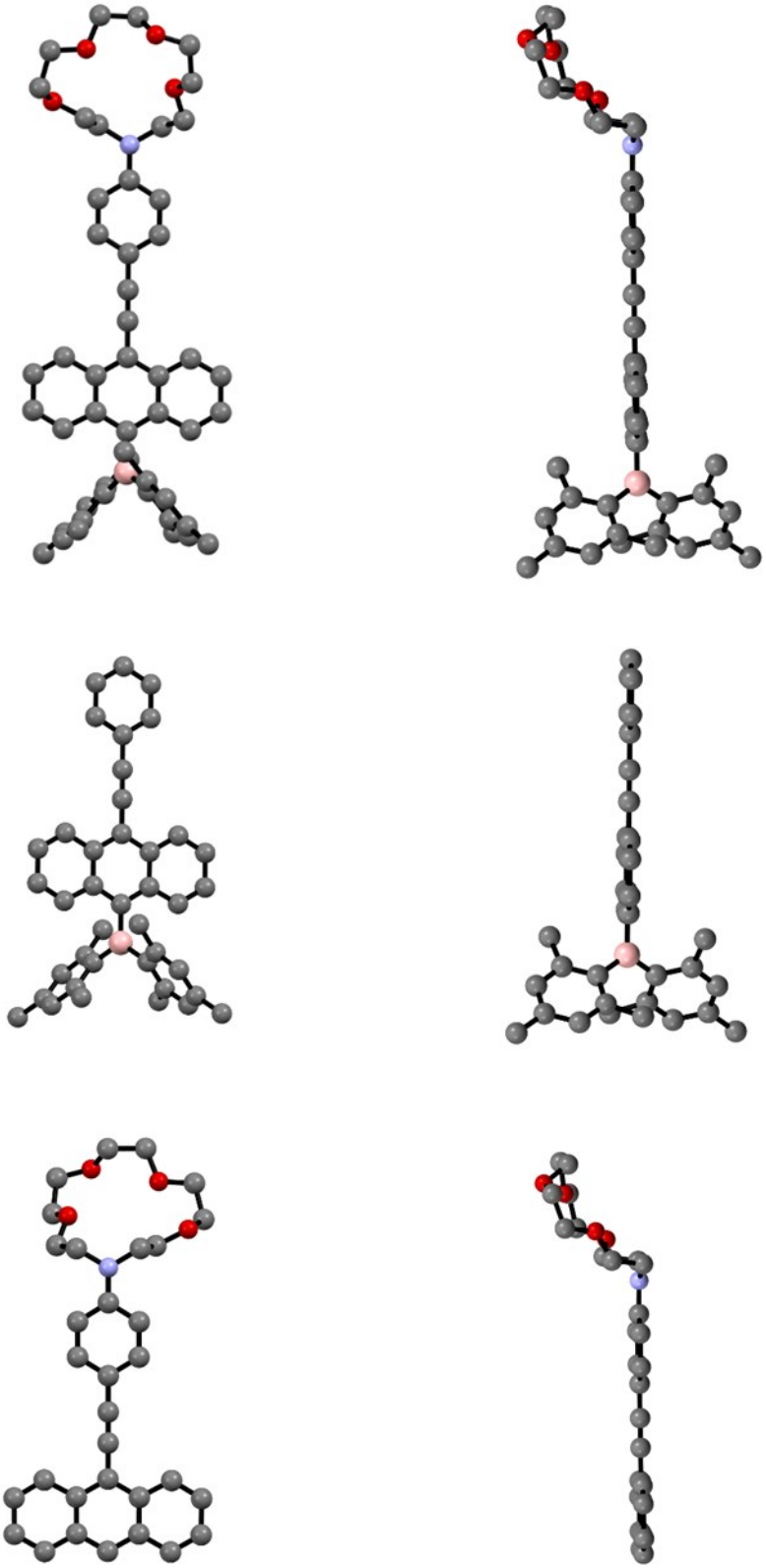

Figure 3. Optimized geometries of **1**, **2** and **3**. Hydrogen atoms are omitted for clarity.

2.2 Absorption spectra of compounds

Figure 4 shows absorption and fluorescence spectra of the compounds **1–3** in toluene, tetrahydrofuran (THF) and CH_3CN at room temperature. All the compounds exhibited several absorption bands in the 230–560 nm region. The bands at <330 nm could be ascribed to ππ* transitions of the aryl groups, and the lowest-energy band was assignable to the intramolecular CT-type transition such as π(aryl)–p(B) CT and CT from the nonbonding orbital of the nitrogen atom in the azacrown moiety (n(N)) to π* orbital of the aryl group: n(N)–π*(aryl) CT. The CT band of **1** (31100 $M^{-1}cm^{-1}$ at 482 nm in THF) was low-energy and intense compared with those of **2** and **3** (26100 $M^{-1}cm^{-1}$ at 454 nm and 8300 $M^{-1}cm^{-1}$ at 426 nm, respectively, in THF) owing to the extended CT interaction by the presence of both electron-withdrawing arylborane and electron-donating azacrown moieties. Such experimental representations are supported by the TD-DFT calculations whose results are included in Figure 5. The lowest-energy singlet excited states (i.e., S_1 state) of the compounds originate mainly in a HOMO→LUMO transition. Although both MOs are distributed into the phenylethynylanthryl moiety, HOMO of **1** or **3** is extended to n(N) and p(B) participates in LUMO of **1** or **2** as shown in Figure 6. All the compounds showed a hypsochromic shift of the lowest-energy band with an increase in the solvent polarity arising from the ground-state solvation. More detailed solvent dependences are discussed later.

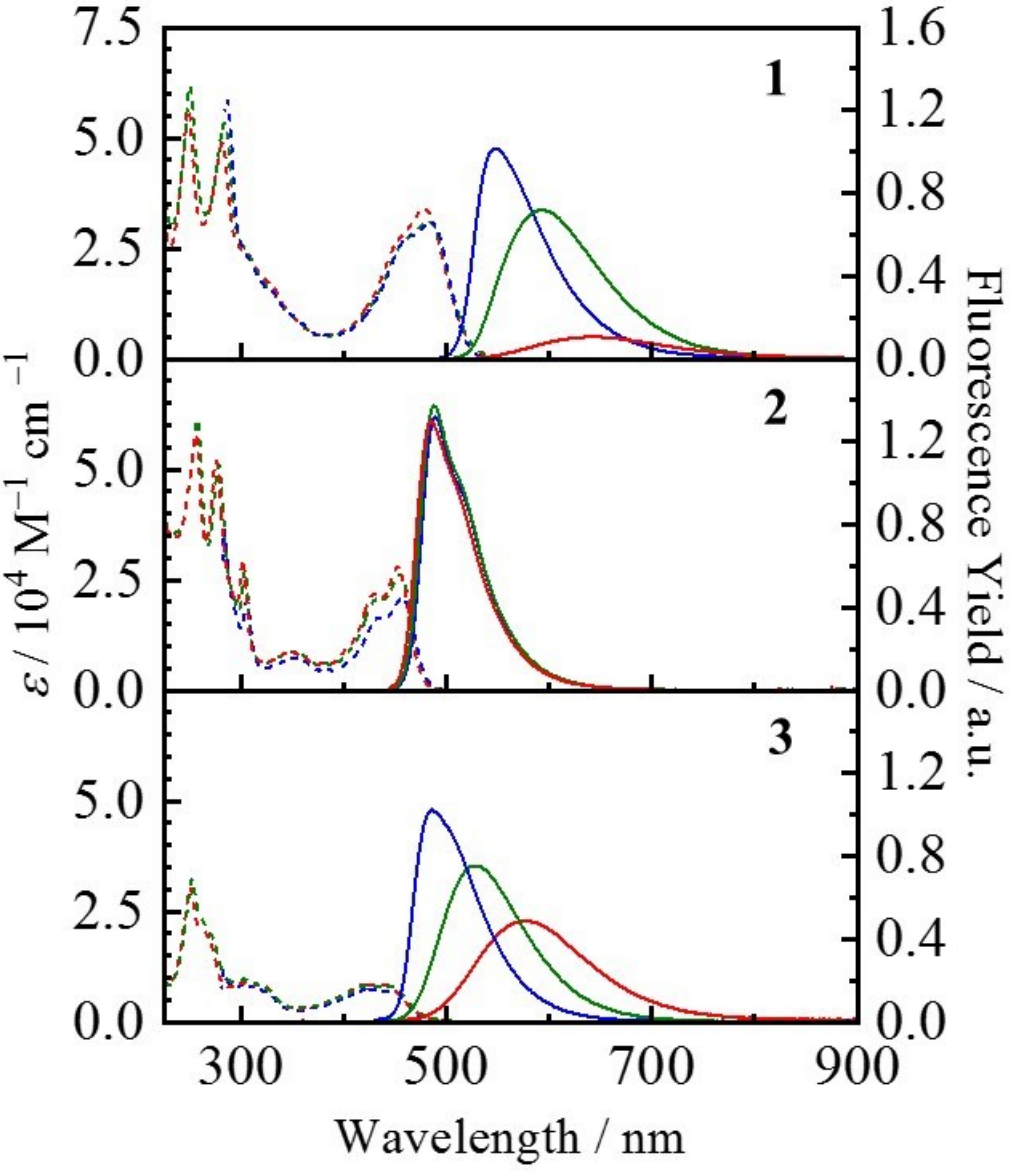

Figure 4. Absorption (broken curves) and fluorescence spectra (solid curves) of the compounds in toluene (blue), THF (green) and CH_3CN (red).

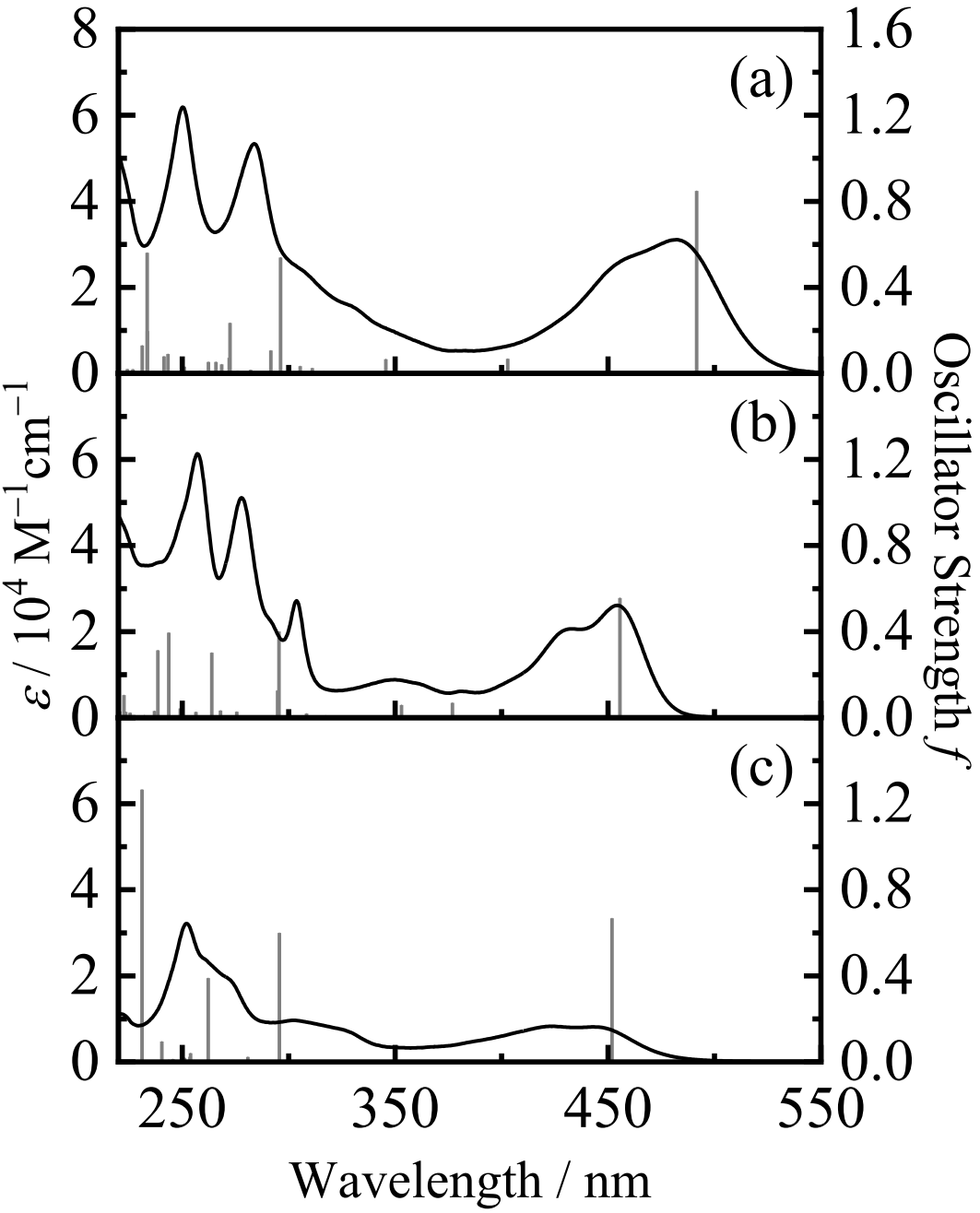

Figure 5. Calculated singlet transitions of **1** (a), **2** (b) and **3** (c) in THF (gray vertical bars) with the relevant observed absorption spectrum (black curves). The transition energies calculated by TD−DFT were shifted to higher energy by 10% to correct the underestimation.

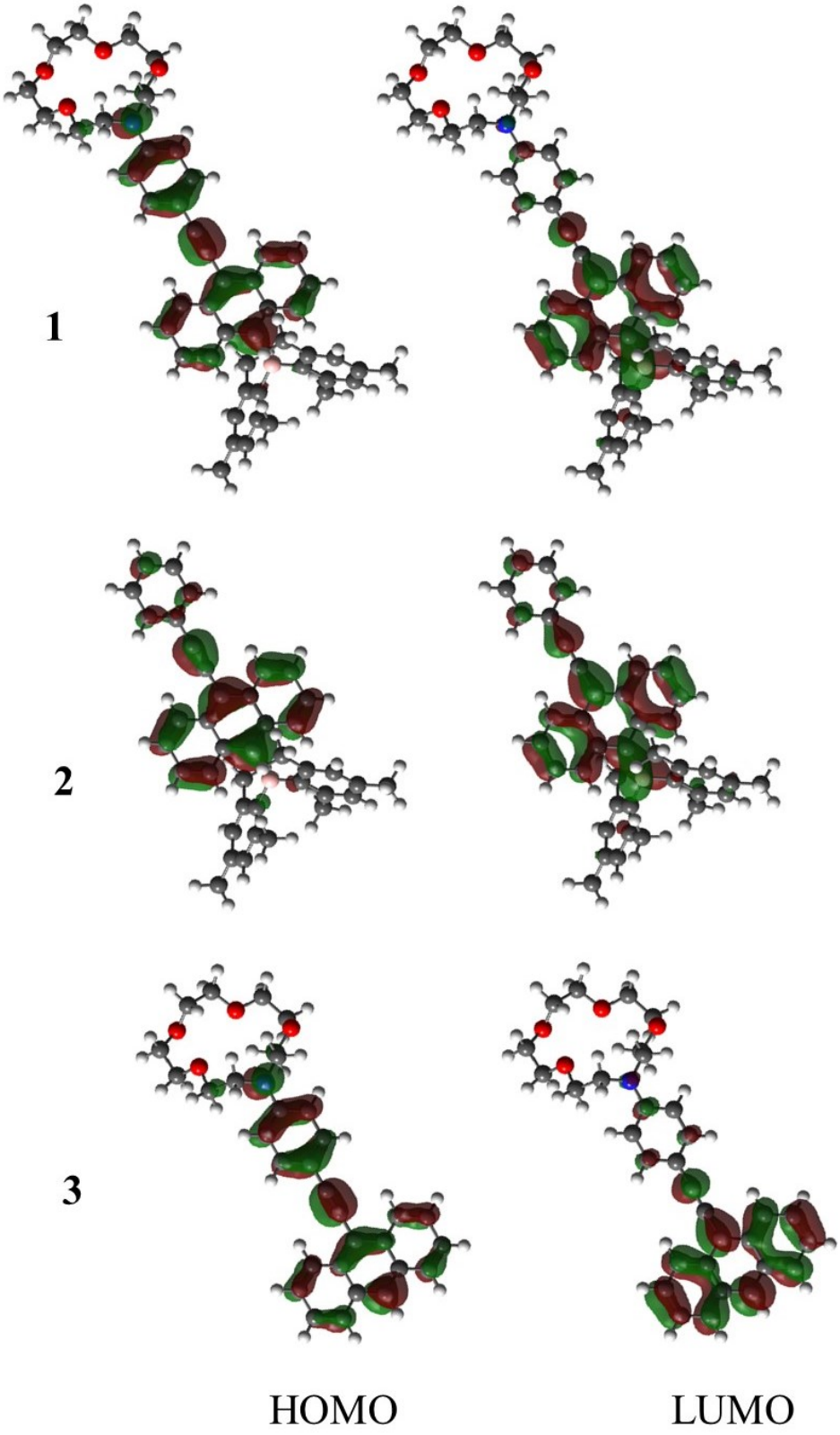

Figure 6. Frontier MOs of the compounds.

2.3 Spectroscopic and photophysical properties

All the compounds showed intense fluorescence whose quantum yields (Φ_f) are >0.78 in toluene or THF and >0.18 even in CH_3CN. The spectra of **1** and **3** were broad/structureless and red-shifted with increasing in the solvent polarity whereas narrow spectrum of **2** was less sensitive. Although the fluorescence lifetimes (τ_f) were typical being 1–5 ns, irrespective of the compound, the solvent trend was complicated as summarized in Table 1. Therefore, it was evaluated in terms of fluorescence (k_f) and nonradiative decay rate constants (k_d). The k_f values of the compounds decreased with an increase in the solvent polarity, and the extent of the k_f change for **1** and **3** was larger than that for **2**. Such large k_f change suggests a decreased overlap of wave functions between the excited and ground states owing to a structural change in the excited state of a molecule in the polar solvent. Furthermore, the k_d value of **1** in CH_3CN was much larger than that in toluene or THF, indicative a largely charge-separated character of the excited state of **1**. These fluorescence characteristics of the compounds let me expect that the emitting state of **1** possess the strongest CT character among the compound owing to the extended CT interactions as described above.

Table 1. Photophysical properties of **1–3** in toluene, THF and CH_3CN.

Solvent	**1**				**2**				**3**			
	Φ_f	τ_f[a] / ns	k_f[b] / 10^7 s^{-1}	k_d[b] / 10^7 s^{-1}	Φ_f	τ_f[a] / ns	k_f[b] / 10^7 s^{-1}	k_d[b] / 10^7 s^{-1}	Φ_f	τ_f[a] / ns	k_f[b] / 10^7 s^{-1}	k_d[b] / 10^7 s^{-1}
Toluene	0.89	3.0	30	3.6	0.92	4.3	21	1.9	0.81	3.1	26	6.1
THF	0.88	3.7	24	3.2	0.91	4.7	19	1.9	0.78	4.0	20	5.5
CH_3CN	0.18	1.2	16	67	0.88	4.8	18	2.5	0.69	4.5	15	6.9

[*a*] determined by single exponential decay fits. [*b*] calculated by $\Phi_f = k_f/(k_f+k_d) = k_f\tau_f$.

2.4 Evaluation of ground/excited state dipole moments

Further solvent responses of the absorption and fluorescence spectra of the compounds were evaluated by employing 14 solvents as shown in Figure 7. The lowest-energy absorption band of all compound was hypsochromically shifted by 400, 200 and 400 cm^{-1} for **1**, **2** and **3**, respectively, with an increasing the solvent polarity (Table 2). On the other hand, the fluorescence spectra of **1** and **3** were shifted to lower-energy in polar solvents, and the maximum energy changes (4400 and 4100 cm^{-1}, respectively) were much larger than that of **2** (500 cm^{-1}). Such large fluorescence solvatochromic shifts of **1** and **3** have been frequently observed for intramolecular-CT-type compounds[13] and explainable by the stabilization of a charge-separated excited state by solvation. To discuss the electronic structure of the compounds more quantitatively, the ground- (μ_g) and excited-state electric dipole moments (μ_e) of the compounds were evaluated by solvent dependences of absorption and fluorescence spectra on the basis of the simple quantum-mechanical second-order perturbation theory by Bilot–Kawski equation[14] by using the solvent-polarity parameters, $f(D_s,n)$ and $g(n)$,

$$f(D_s,n) = \frac{2n^2+1}{n^2+2}\left[\frac{D_s-1}{D_s+2} - \frac{n^2-1}{n^2+2}\right] \quad (1)$$

$$g(n) = \frac{3}{2}\left[\frac{n^4-1}{(n^2+2)^2}\right] \quad (2)$$

where the involving D_s and n are the permittivity and refractive index of a solvent, respectively. The ($\tilde{\nu}_a - \tilde{\nu}_f$) vs. $f(D_s,n)$ and ($\tilde{\nu}_a + \tilde{\nu}_f$) vs. [$f(D_s,n) + 2g(n)$] plots (Figure 8), in which $\tilde{\nu}_a$ and $\tilde{\nu}_f$ are the absorption and fluorescence maximum energies, respectively, of the compounds exhibited good linear correlations (correlation coefficient > 0.92), and the slope values (m_1 and $-m_2$, see Table 3) afforded μ_g and μ_e values by equations 3 and 4.

$$\mu_{\mathrm{g}} = \frac{m_2 - m_1}{2}\sqrt{\frac{hca_{\mathrm{O}}{}^3}{2m_1}} \quad (3)$$

$$\mu_{\mathrm{e}} = \frac{m_2 + m_1}{2}\sqrt{\frac{hca_{\mathrm{O}}{}^3}{2m_1}} \quad (4)$$

In the equations, h, c and a_{O} are Plank constant, speed of light and Onsager radius of compounds, respectively. The calculated a_{O} values for the optimized geometries of the compounds were employed. Compound **1** possesses larger polarity both in the ground and excited states (μ_{g} = 0.48 D and μ_{e} = 13 D) than **2** (μ_{g} = 0.15 D and μ_{e} = 2.7 D) and **3** (μ_{g} = 0.065 D and μ_{e} = 11 D). The μ_{e} value qualitatively correlates to a CT distance of a molecule as B–N, B–An and An–N distances for **1**, **2** and **3** in the optimized geometries are 12.8, 3.04 and 9.74 Å, respectively ("An" employed a center of carbon atoms at 9- and 10-positions of the anthryl moiety). The result suggests that both azacrown and dimesitylboryl moieties dominate the largely-charge-separated excited-state character and large fluorescence solvatochromism of **1**.

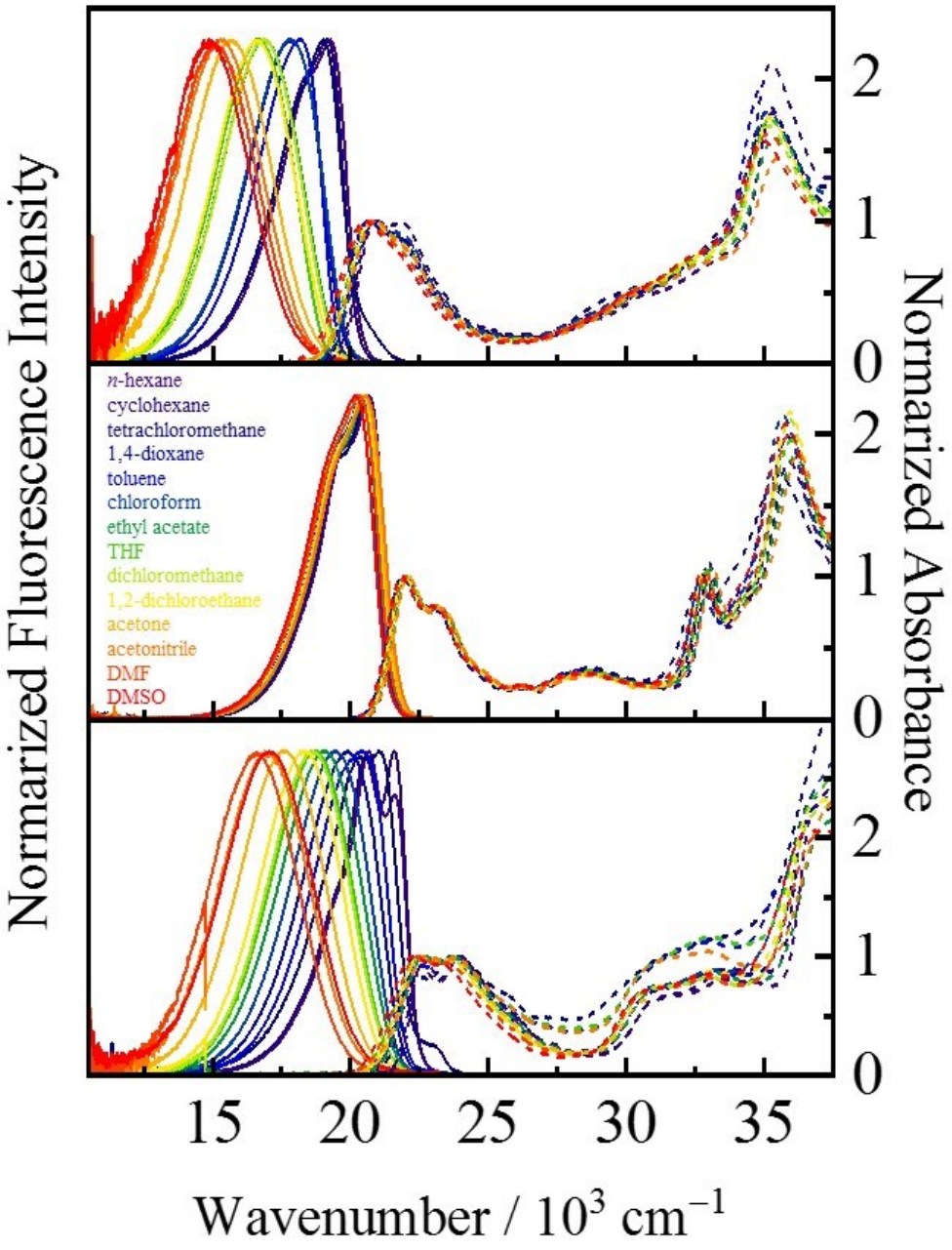

Figure 7. Solvent dependences of the absorption (broken curves) and fluorescence spectra (solid curves) of **1** (top), **2** (middle) and **3** (bottom). The absorbances are normalized at maxima of the lowest-energy bands, and the fluorescence intensities are normalized to those at the maximum energies. Excitation wavelengths for **1**, **2** and **3** are 445, 430 and 410 nm, respectively.

Table 2. Spectroscopic properties of **1–3** in various solvents.

solvent	solvent parameters				**1**		**2**		**3**	
	D_s[a]	n[a]	$f(D_s,n)$	$g(n)$	$\tilde{\nu}_a$ / cm^{-1}	$\tilde{\nu}_f$ / cm^{-1}	$\tilde{\nu}_a$ / cm^{-1}	$\tilde{\nu}_f$ / cm^{-1}	$\tilde{\nu}_a$ / cm^{-1}	$\tilde{\nu}_f$ / cm^{-1}
n-hexane	1.886	1.3749	−0.0009607	0.2550	20900	19300	22100	20700	22700	20700
cyclohexane	2.023	1.4262	−0.002585	0.2892	20900	19200	22100	20600	22600	20600
1,4-dioxane	2.209	1.4224	+0.04128	0.2867	20700	17900	22000	20500	22400	19900
tetrachloromethane	2.238	1.4459	+0.03230	0.3022	20700	19100	21900	20600	22400	21100
toluene	2.379	1.4969	+0.02886	0.3354	20700	18200	22000	20500	22400	20500
chloroform	4.806	1.4459	+0.3706	0.3022	20900	17800	22000	20400	22600	19500
ethyl acetate	6.053	1.3724	+0.4910	0.2534	20800	16900	22100	20600	22700	19100
tetrahydrofuran	7.58	1.4072	+0.549	0.277	20700	16700	22100	20500	22600	18700
dichloromethane	8.93	1.4242	+0.590	0.288	20800	16900	22000	20500	22700	18700
1,2-dichloroethane	10.37	1.4130	+0.6348	0.2804	20800	16700	22000	20500	22500	18400
acetone	20.7	1.3587	+0.790	0.244	20900	15800	22100	20600	22700	17500
acetonitrile	35.94	1.3441	+0.8593	0.2344	20900	15400	22200	20600	22800	17000
N,*N*-dimethylformamide	36.71	1.4305	+0.8356	0.2920	20700	15200	22000	20400	22400	17000
dimethyl sulfoxide	46.45	1.4793	+0.8400	0.3240	20500	14900	21900	20200	22300	16600

[*a*] Data taken from ref. [15].

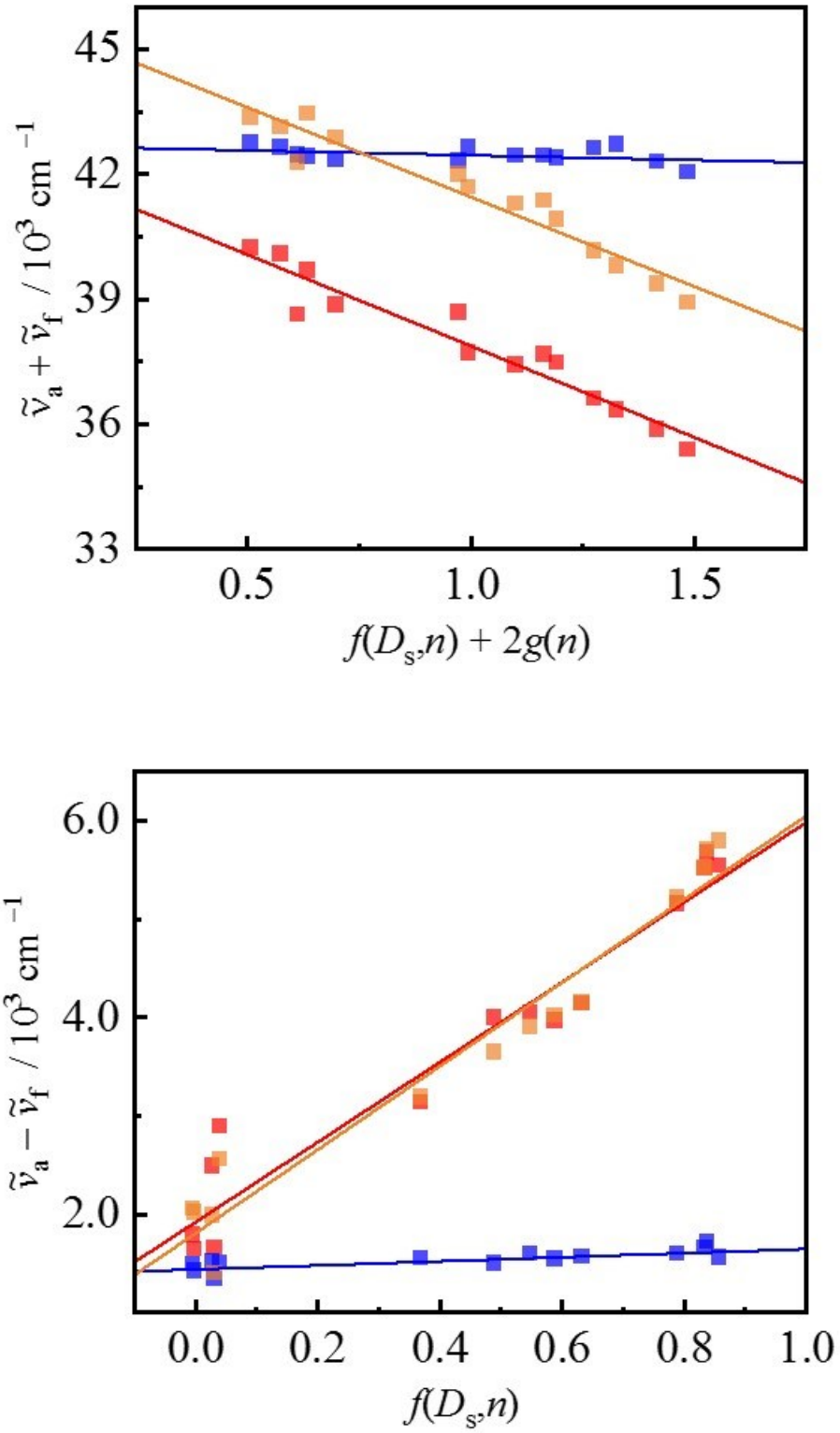

Figure 8. Solvent-parameter dependences of the spectroscopic properties of **1** (red), **2** (blue) and **3** (orange). Solid lines correspond to the linear regression.

Table 3. Solvent-dependent parameters (m_1 and m_2) and ground-/excited-state dipole moments of **1–3**.

Compound	a_O / Å	m_1 / cm^{-1}	m_2 / cm^{-1}	μ_g / D	μ_e / D
1	7.19	4070	4390	0.48	13
2	6.76	210	230	0.15	2.7
3	6.46	4250	4300	0.065	11

2.5 Absorption and fluorescence spectra changes by binding of metal ion

Owing to the charge-separated excited-state character between the azacrown and dimesitylboryl moieties, the spectroscopic properties of **1** would respond to a binding with a Lewis acid or base. Figure 9 shows the absorption and fluorescence spectra of **1** in the absence and presence of lithium perchlorate (0–25 mM) in CH_3CN. The lowest-energy absorption band of **1** was shifted to shorter wavelength (λ_{abs} = 480 to 466 nm) upon an addition of lithium ion with an isosbestic point at 467 nm, and a binding constant K_{ass} was determined by a global fit for the absorbance changes to be 360±90 M^{-1} (Figure 10). The lithium-ion addition shifted the fluorescence spectrum of **1** to shorter wavelength as well and enhanced the Φ_f value to 0.50. The results are explainable by decrease in the electron-donating ability of the azacrown moiety by a coordination to lithium ion. In practice, the larger metal-ion radius, the smaller spectroscopic response and binding constant (K_{ass} = 110±20 M^{-1} for sodium ion and not determined for potassium ion) as shown in Figures 11 and 12. The spectroscopic data of **2** without the azacrown moiety did not respond to lithium ion (Figure 13(a)), suggesting that the metal ion interacts with the azacrown moiety in **1**. On the other hand, **3** showed similar spectroscopic changes by an addition of lithium ion with a larger K_{ass} (650±70 M^{-1}, see Figures 13(b) and 14) than **1**. However, the absorption and fluorescence changes of **1** were greater than those of **3**. Thus, the dimesitylboryl moiety in **1** is effective electronically in a metal-ion detection.

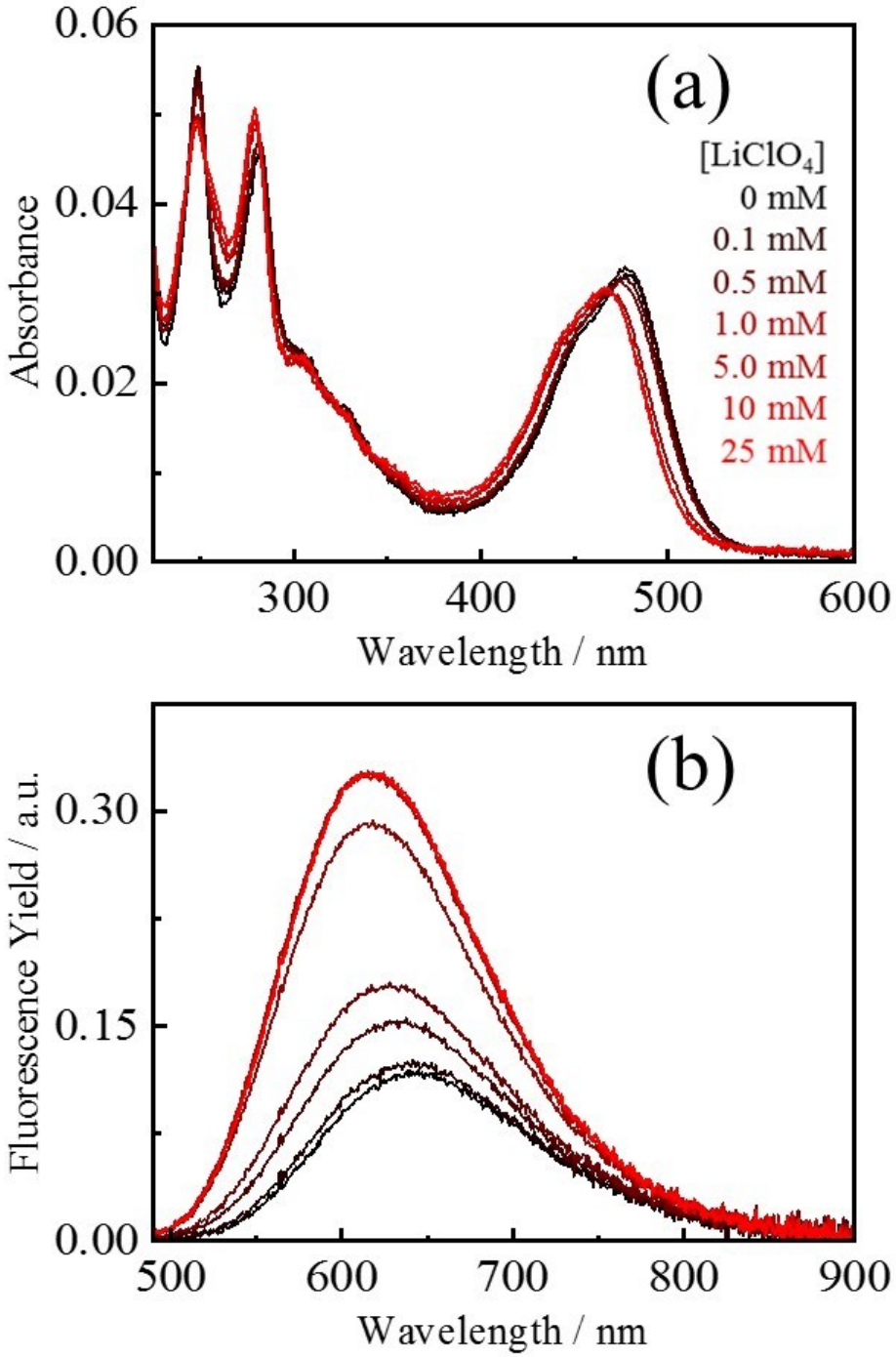

Figure 9. Absorption (a) and fluorescence spectral changes (b, λ_{ex} = 465 nm) upon an addition of $LiClO_4$ (0–25 mM) to 1 (9.6×10^{-7} M) in CH_3CN.

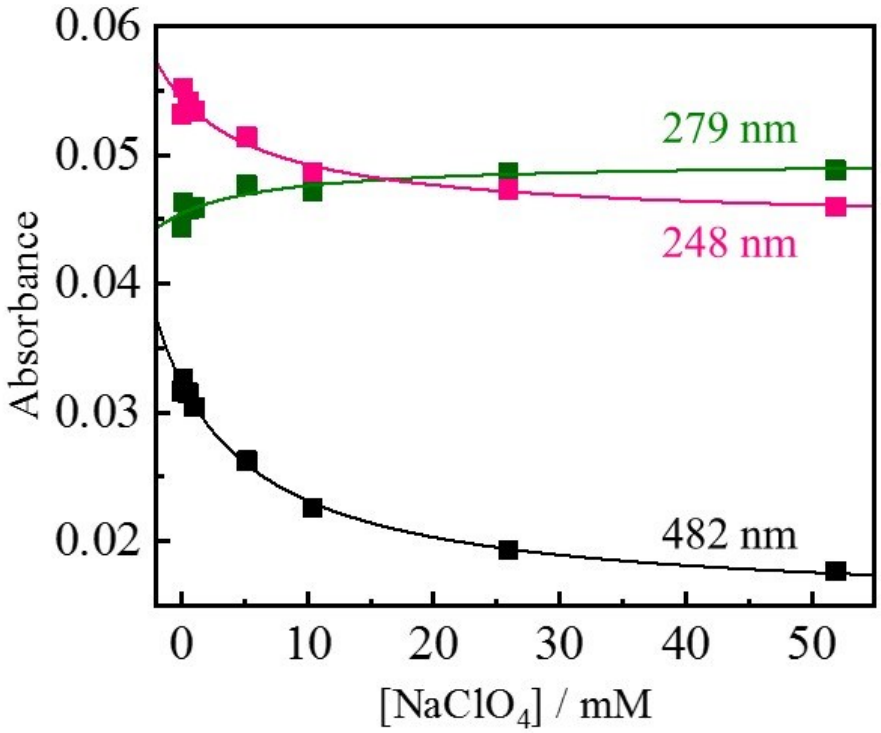

Figure 10. Titrations for absorbances at 248, 279 and 482 nm upon an addition of $LiClO_4$ to **1** (9.6×10^{-7} M) in CH_3CN. Curves represent a global fit to equation 7 using K_{ass} = 360±90 M^{-1}.

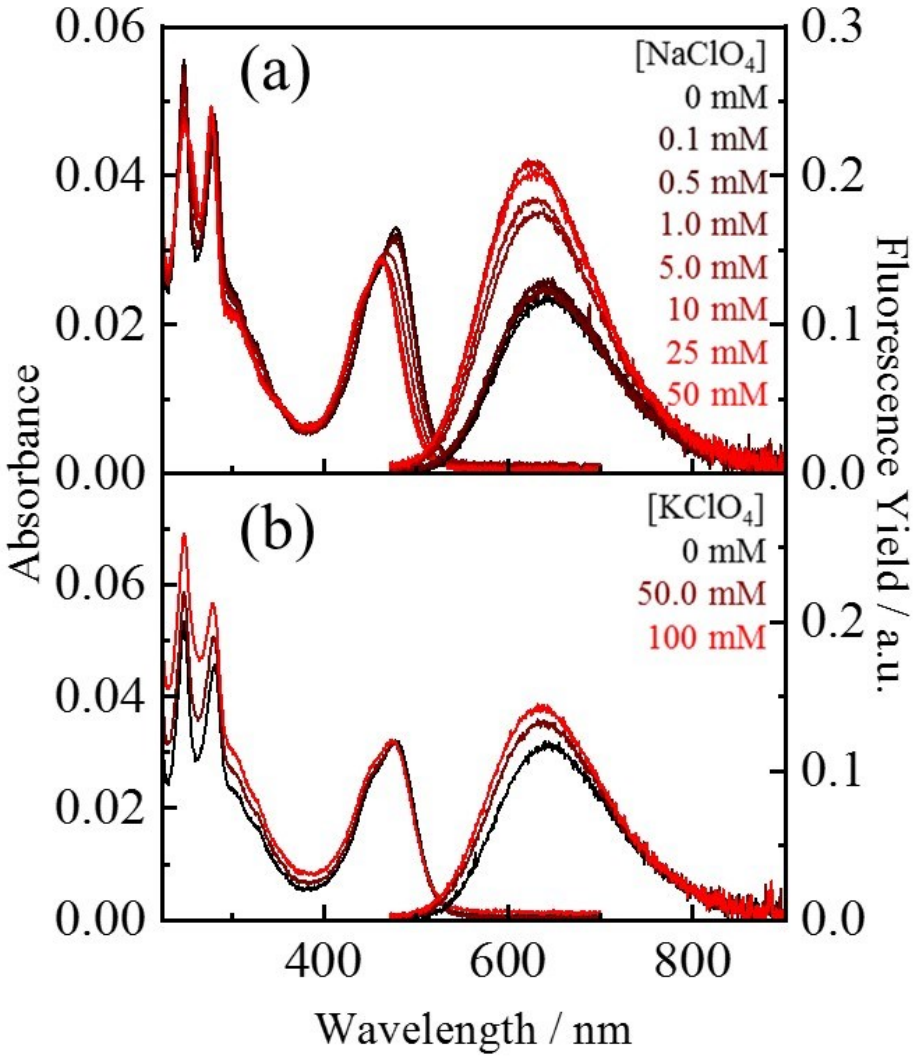

Figure 11. Absorption and fluorescence spectral changes upon an addition of $NaClO_4$ (0–50 mM) (a) and $KClO_4$ (0–100 mM) (b) to **1** (9.6×10^{-7} M) in CH_3CN. Excitation wavelength = 465 nm.

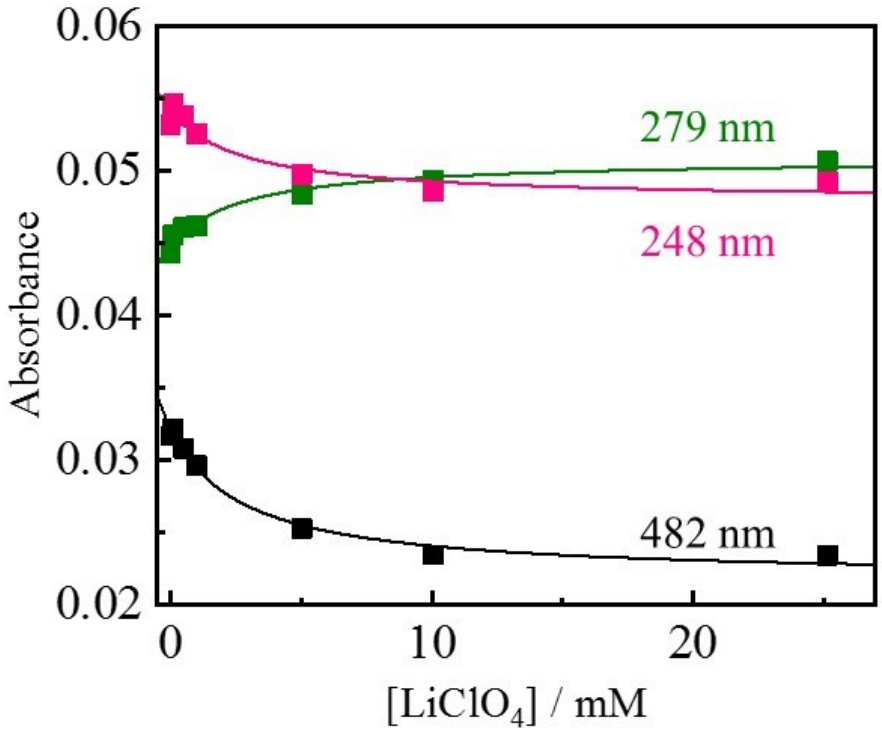

Figure 12. Titrations for absorbances at 248, 279 and 482 nm upon an addition of $NaClO_4$ to **1** (9.6×10^{-7} M) in CH_3CN. Curves represent a global fit to equation 7 using K_{ass} = 110±20 M^{-1}.

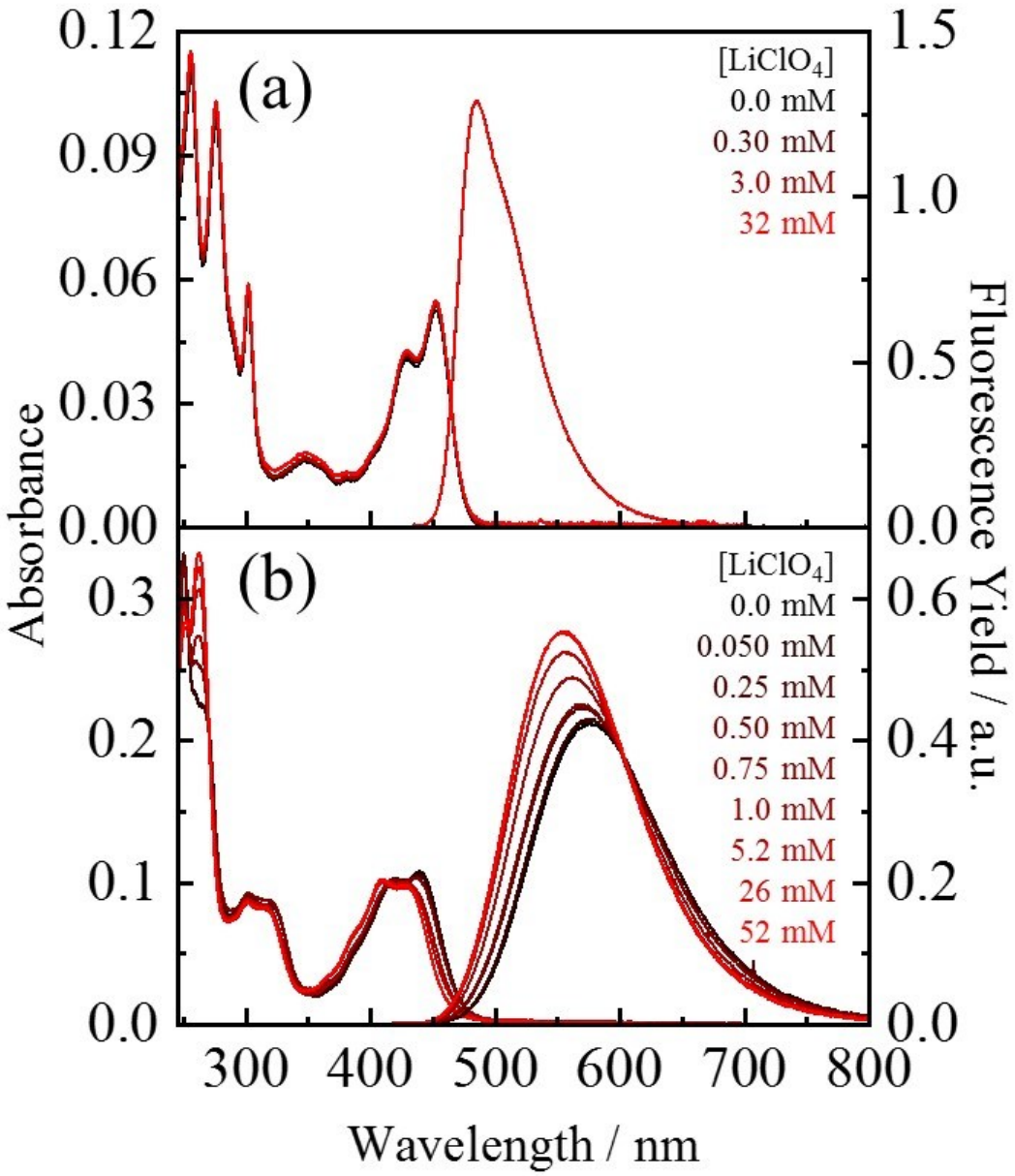

Figure 13. Absorption and fluorescence spectral changes upon an addition of $LiClO_4$ (0–32 mM) to **2** (1.9×10^{-6} M) (a) and $LiClO_4$ (0–52 mM) to **3** (5.0×10^{-6} M) (b) in CH_3CN. Excitation wavelength = 435 (a) and 410 nm (b).

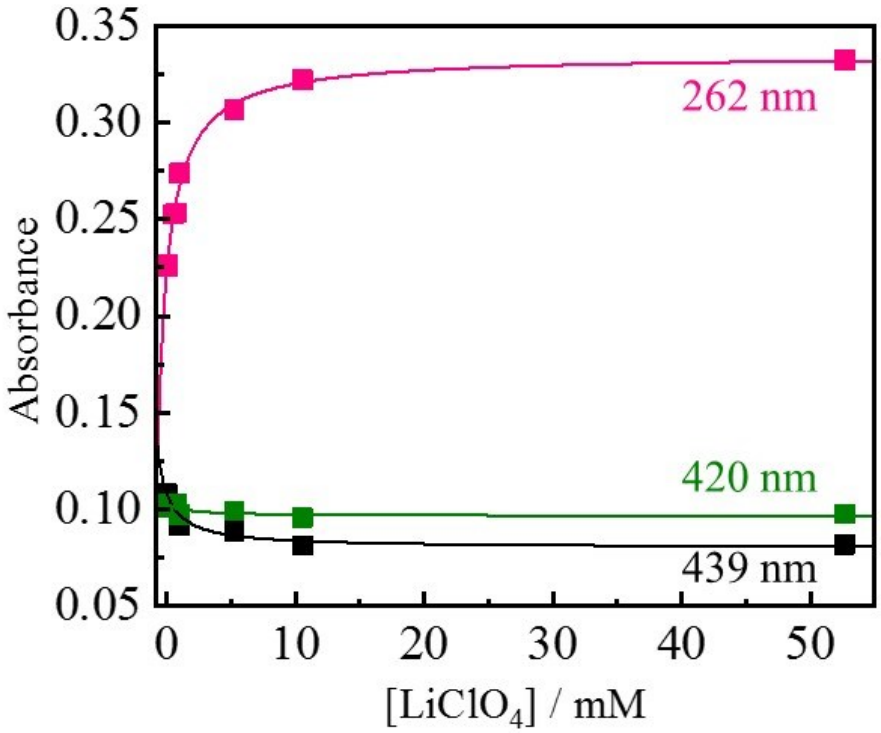

Figure 14. Titrations for absorbances at 262, 420 and 439 nm upon an addition of $LiClO_4$ to **3** (5.0×10^{-6} M) in CH_3CN. Curves represent a global fit to equation 7 using K_{ass} = 650±70 M^{-1}.

2.6 Absorption and fluorescence spectra changes by fluoride coordination

Spectroscopic change of **1** by a fluoride addition was more drastic. Figure 15 shows the absorption and fluorescence spectra of **1** in the absence and presence of tetra-*n*-butylammonium fluoride (TBAF) in THF. Upon an addition of TBAF, the broad absorption and fluorescence bands in the visible region disappeared, and simultaneously, new structured bands whose maxima were 412 ($\Delta\lambda_{abs}$ = 24 nm) and 495 nm ($\Delta\lambda_{f}$ = 107 nm), respectively, were observed. The spectroscopic changes are huge compared with those observed for **2** ($\Delta\lambda_{abs}$ = 1 nm and $\Delta\lambda_{f}$ = 4 nm, Figure 16 (a)) and originate in a coordination of fluoride on the boron atom since such behaviors have not been observed by an addition of tetra-*n*-butylammonium chloride to **1** (Figure 17) or TBAF to **3** (Figure 16(b)).

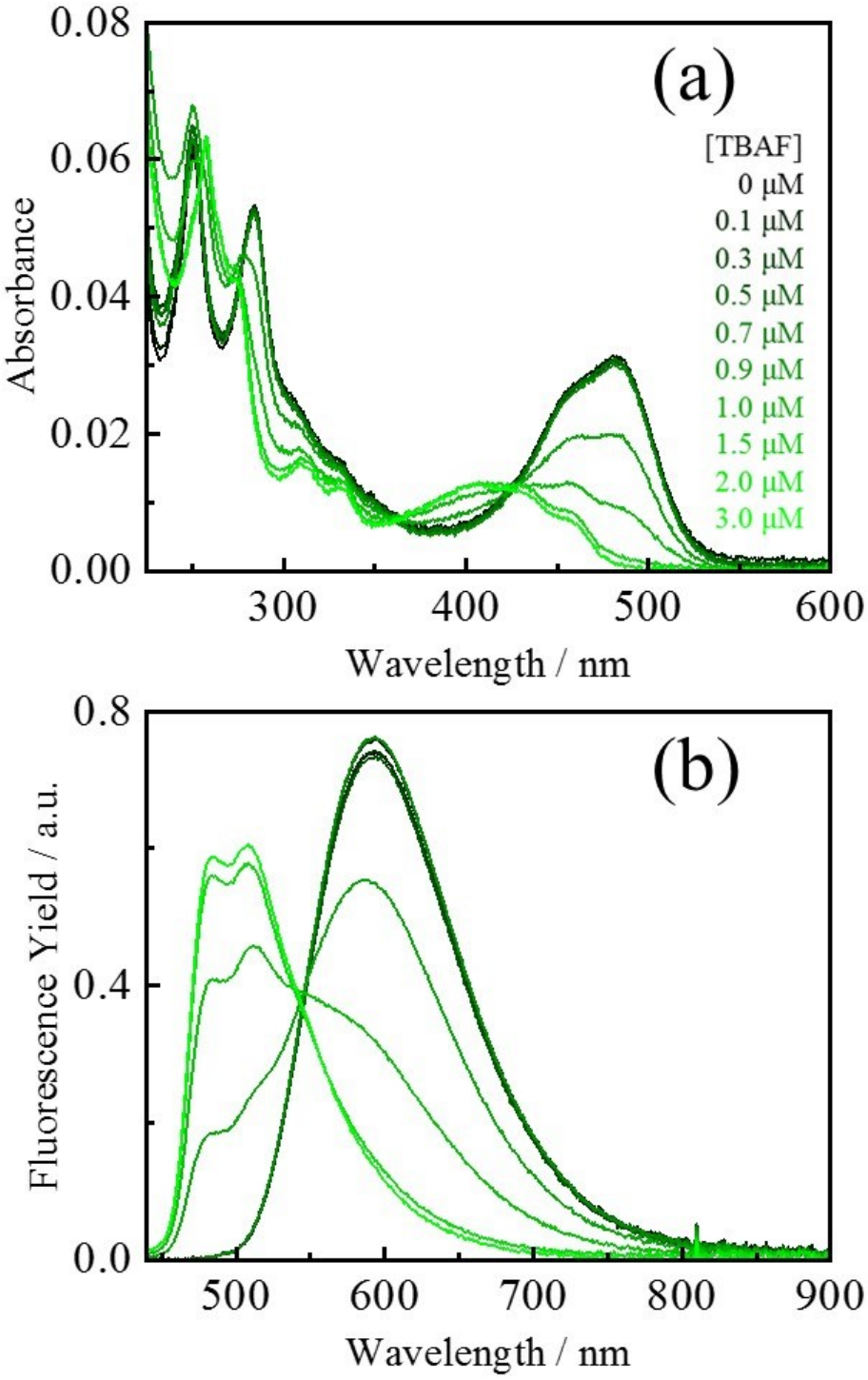

Figure 15. Absorption (a) and fluorescence spectral changes (b, λex = 430 nm) upon an addition of TBAF (0–3.0 μM) to 1 (9.7 × 10−7 M) in THF.

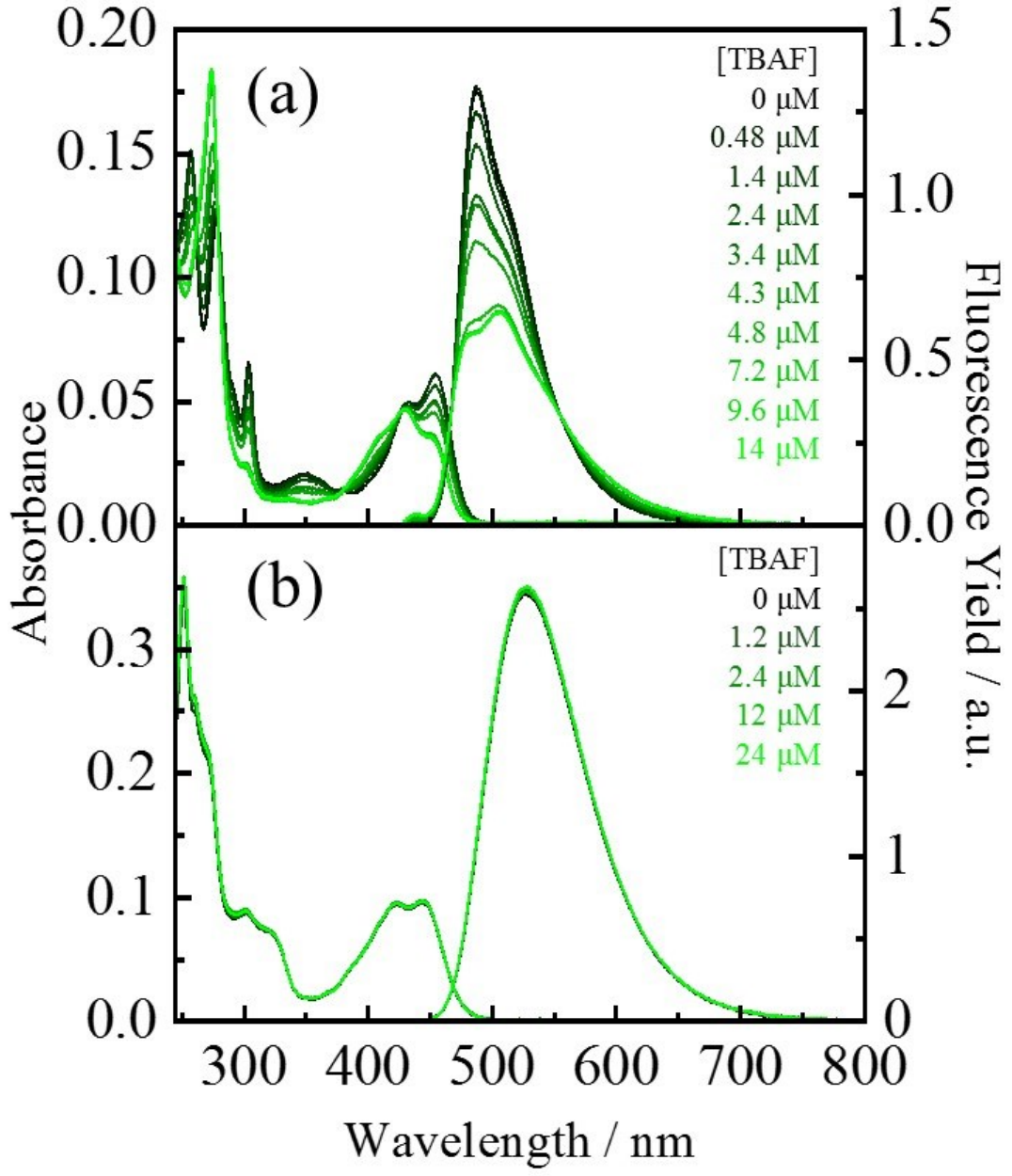

Figure 16. Absorption and fluorescence spectral changes upon an addition of TBAF (0–14 μM) to **2** (2.9×10^{-6} M) (a) and TBAF (0–24 μM) to **3** (5.0×10^{-6} M) (b) in THF. Excitation wavelength = 435 nm.

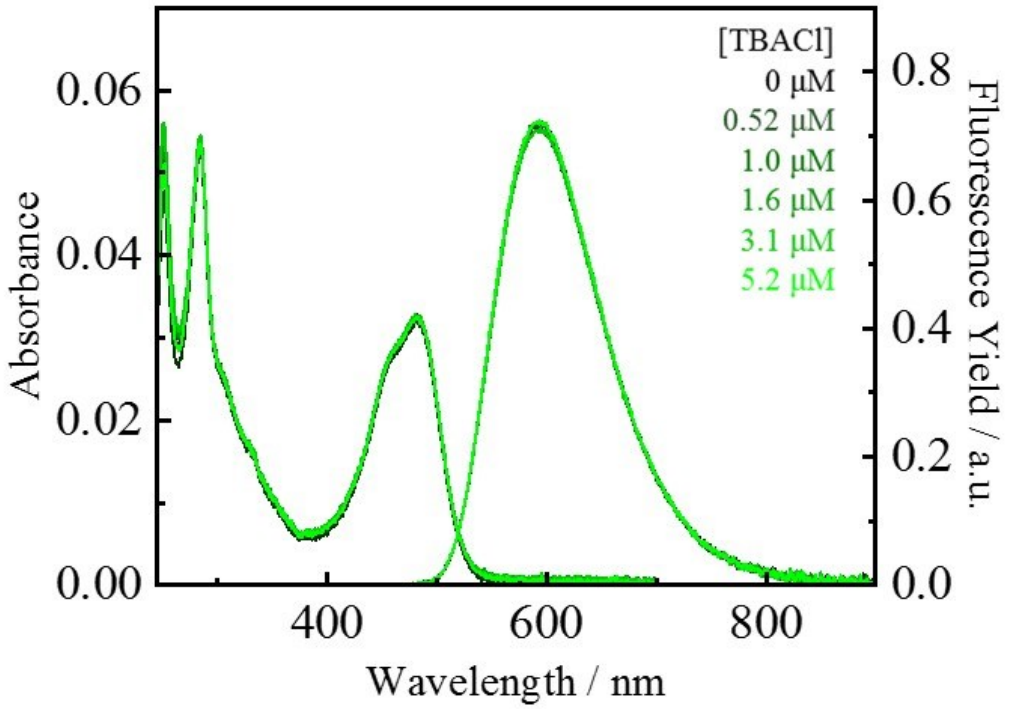

Figure 17. Absorption and fluorescence spectral changes upon an addition of TBACl (0–5.2 μM) to **1** (1.0×10^{-6} M) in THF. Excitation wavelength = 445 nm.

Chapter 3 Conclusions

A novel azacrown–arylborane derivative **1** exhibits intense visible-light absorption/fluorescence and large fluorescence solvatochromism. The latter originates in a large excited-state dipole moment owing to the effective combination of the electron-donating aza-15-crown-5 and electron-withdrawing triarylborane moieties *via* the phenylethynyl linker. The spectroscopic characteristics of **1** was also varied in the presence of the added metal ion (i.e., lithium/sodium ion) or fluoride by binding with the azacrown or triarylborane moiety, respectively. Such bright fluorescence (intense absorption and fluorescence) and tritopic response of **1** in the visible region is applicable to the multifunctional probe, and the framework of **1** is a possible candidate for a class of molecular logic gates.

Chapter 4 Experimental section

4.1 Synthesis and Identifications. Chemicals for syntheses of the compounds were purchased from FUJIFILM Wako Pure Chemical Corporation, Tokyo Chemical Industries Co., Ltd. or Sigma–Aldrich Co. LLC and used as supplied. Column chromatography was carried out by using Wakogel C-200, Sephadex LH-20 or a recycling preparative HPLC (Japan Analytical Industries Co., Ltd., LC-908) equipped with three gel-permeation columns (JAIGEL-1H) and a RI detector (RI-5). A Merck silica-gel 60 F_{254} plastic sheet was used for thin layer chromatography, and spots of the samples were visualized by using an ASONE SUV-6 UV lamp.

^{1}H NMR spectra were recorded on a Bruker BioSpin AVANCE^{TM} III 400 nuclear magnetic resonance spectrometer (400 MHz). The chemical shifts of the spectra determined in $CDCl_3$ was given in ppm, with tetramethylsilane being an internal standard (0.00 ppm). IR spectra were recorded on a JASCO FT/IR-4600 spectrometer. High-resolution electrospray-ionization mass spectrometry was performed by an AB SCIEX TripleTOF 4600 mass spectrometric system. Melting points were determined by using a Stanford Research Systems Optimelt MPA100 automated melting-point system and were uncorrected.

X-ray diffraction data were collected at 93 K under a cold N_2-gas stream on a Rigaku XtaLAB Synergy-S/Mo system (λ = 0.71073 Å (Mo-Kα)). The integrated data were analyzed by using an Olex2 crystallographic software package.[16] The structures were solved with the ShelXT structure solution program[17] using Intrinsic Phasing and refined with the ShelXL refinement package[18] using the least-squares minimization. Anisotropic refinement was performed for all non-hydrogen atoms, and all the hydrogen atoms were

put at calculated positions.

1-Phenyl-1-aza-4,7,10,13-tetraoxacyclopentadecane **(4).** Synthesis was performed with minor changes in the reported procedure.[19] A three-necked round-bottom flask was evacuated and filled subsequently with an argon gas. A mixture of sodium hydride (720 mg, 18 mmol as 60wt% suspension in mineral oil) and dry tetrahydrofuran (THF, 450 mL) was heated at 65 °C, and a solution of *N,N*-di(2-hydroxyethyl)aniline (965 mg, 5.32 mmol) and triethyleneglycol ditosylate (2.43 g, 5.29 mmol) in THF (50 mL) was added dropwise for over 2 h. After stirring at 65 °C for 20 h, the reaction mixture was allowed to cool to ambient temperature. The precipitation was removed and, then, filtrate was concentrated under reduced pressure. Purification by flash column chromatography on silica gel (eluent: ethyl acetate) afforded **4** as colorless needles (812 mg, 52%). R_f = 0.50 (SiO_2, ethyl acetate). ^{1}H NMR (400 MHz, $CDCl_3$) δ 7.22–7.18 (2H, m; Ar-H), 6.67–6.65 (3H, m; Ar-H), 3.76 (4H, t, J = 6.4 Hz; NCH_2), 3.68–3.64 (12H, m; CH_2), 3.59 (4H, t, J = 6.4 Hz; $NCCH_2$).

1-(4-Iodophenyl)-1-aza-4,7,10,13-tetraoxacyclopentadecane **(5).** Synthesis was performed with minor changes in the reported procedure.[20] In a round-bottom flask, **4** (750 mg, 2.54 mmol), 1,4-dioxane (7 mL) and pyridine (7 mL) were added. To the solution, which was cooled to 0 °C in an ice bath, iodine (3.10 g, 25 mmol) was added and, then, the mixture was allowed to warm to ambient temperature. The solution was stirred for 5 h. A saturated aqueous solution of sodium thiosulfate (20 mL) was then added until the suspension changed from brown to colorless. The mixture was extracted with ethyl acetate (30 mL × 3), and the combined organic layer was washed with water (50 mL). Drying over anhydrous $MgSO_4$ followed by evaporation under reduced pressure

afforded **5** as brown oil (992 mg, 93%). R_f = 0.44 (SiO_2, ethyl acetate). ^{1}H NMR (400 MHz, $CDCl_3$) δ 7.42 (2H, d, J = 9.1 Hz; *o*-Ar-H), 6.44 (2H, d, J = 9.1 Hz; *m*-Ar-H), 3.72 (4H, t, J = 6.3 Hz; NCH_2), 3.66–3.63 (12H, m; CH_2), 3.55 (4H, t, J = 6.3 Hz; $NCCH_2$).

1-(4-Ethynylphenyl)-1-aza-4,7,10,13-tetraoxacyclopentadecane **(6).** A two-necked round-bottom flask was evacuated and filled subsequently with an argon gas. Into the vessel were added **5** (752 mg, 1.79 mmol), dichloridobis(triphenylphophine)palladium(II) (14.1 mg, 0.019 mmol), copper(I) iodide (4.2 mg, 0.022 mmol) and THF/trimethylamine (8 mL/4 mL) and, then, heated at 50 °C. Trimethylsilylacetylene (486 μL, 3.55 mmol) was added dropwise to the mixture for over 10 min. After stirring at 50 °C for 12 h, the reaction mixture was allowed to cool to ambient temperature. The insoluble residue was filtered by Celite, and the filtrate was concentrated under reduced pressure. The resulting black oil of 1-(4-trimethylsilylethynylphenyl)-1-aza-4,7,10,13-tetraoxacyclopentadecane (706 mg, quant.) was used for the next step without any purifications. R_f = 0.41 (SiO_2, ethyl acetate). ^{1}H NMR (400 MHz, $CDCl_3$) δ 7.29 (2H, d, J = 9.0 Hz; *o*-Ar-H), 6.54 (2H, d, J = 9.0 Hz; *m*-Ar-H), 3.75–3.71 (4H, m; NCH_2), 3.66–3.62 (12H, m; CH_2), 3.57 (4H, t, J = 6.4 Hz; $NCCH_2$), 0.21 (9H, s; CH_3).

The trimethylsilyl group in 1-(4-trimethylsilylethynylphenyl)-1-aza-4,7,10,13-tetraoxacyclopentadecane was removed by reacting with potassium carbonate (745 mg, 5.39 mmol) in methanol (30 mL) at room temperature for 5 h. The reaction mixture was concentrated under reduced pressure, and water (100 mL) was added. After successive extractions with dichloromethane (30 mL × 3), the combined organic layer was washed with brine (30 mL) then dried over anhydrous $MgSO_4$, affording **6** (501 mg, 94%) as dark red oil. R_f = 0.37 (SiO_2, ethyl acetate). ^{1}H NMR (400 MHz, $CDCl_3$) δ 7.33 (2H, d, J = 9.0

Hz; *o*-Ar-H), 6.57 (2H, d, J = 9.0 Hz; *m*-Ar-H), 3.74 (4H, t, J = 6.4 Hz; NCH_2), 3.67–3.63 (12H, m; CH_2), 3.59 (4H, t, J = 6.4 Hz; $NCCH_2$), 2.96 (1H, s; CH).

***Bis(2,4,6-trimethylphenyl)boron fluoride* (7).** A three-necked round-bottom flask containing magnesium turnings (2.5 g, 100 mmol) was evacuated and filled with an argon gas. Into the flask was added 2-bromo-1,3,5-trimethylbenzene (15 mL, 100 mmol) and dry THF (50 mL). After heating at 65 °C for 1 h, the reaction mixture was allowed to cool to 0 °C in an ice bath and boron trifluoride diethyl-ether complex (5.7 mL, 45 mmol) was added dropwise for over 20 min at 0 °C. Further reaction was done at a reflux temperature for 1 h. The reaction mixture was allowed to cool to ambient temperature and, then, the solvent was removed under reduced pressure. The residue was extracted with *n*-hexane (400 mL), and the filtrate was concentrated under reduced pressure, affording **7** (10.7 g, 89%) as a colorless solid. R_f = 0.86 (SiO_2, chloroform/*n*-hexane = 1/1). ^{1}H NMR (400 MHz, $CDCl_3$) δ 6.81 (4H, s; Ar-H), 2.33–2.20 (18H, m; CH_3).

***(10-Bromoanthracen-9-yl)bis(2,4,6-trimethylphenyl)borane* (8).** A three-necked round-bottom flask was evacuated and filled subsequently with an argon gas. Into a vessel were added 9,10-dibromoanthracene (11.4 g, 34 mmol) and dry diethyl ether (95 mL) and, then, cooled to −78 °C. *n*-Butyllithium (1.6 mol/dm^3 (M) in *n*-hexane, 24.5 mL, 39 mmol) was added dropwise to the reaction mixture at −78 °C for over 30 min. The mixture was warmed up to 0 °C in an ice bath and added to a solution of **7** (9.92 g, 37 mmol) in dry diethyl ether (55 mL) at 0 °C. The reaction mixture was warmed up to room temperature and stirred for 15 h. After removal of the solvent, ethyl acetate (200 mL) was added to the residue. The resulting suspension was filtered to remove insoluble salt. The filtrate was evaporated under reduced pressure, and recrystallized form ethyl acetate to afford **8**

(6.80 g, 40%) as yellow plates. R_f = 0.86 (SiO_2, ethyl acetate/*n*-hexane = 2/8). ^{1}H NMR (400 MHz, $CDCl_3$) δ 8.57 (2H, d, J = 8.8 Hz; 1,8-Ar-H of An), 8.06 (2H, d, J = 8.8 Hz; 4,5-Ar-H of An), 7.49 (2H, ddd, J = 1.2, 6.4, 8.8 Hz; 2,7-Ar-H of An), 7.23 (2H, ddd, J = 1.2, 6.4, 8.8 Hz; 3,6-Ar-H of An), 6.90–6.65 (4H, brs; Ar-H of Mes), 2.40–2.20 (6H, brs; CH_3 of *p*-Mes), 1.60–1.46 (12H, brs; CH_3 of *o*-Mes).

1-[4-{10-bis[2,4,6-trimethylphenyl)boryl]anthracen-9-yl}ethynylphenyl]-1-aza-4,7,10,13-tetraoxaazacyclopentadecane **(1).** A Schlenk tube was evacuated and filled subsequently with an argon gas. Into a vessel were added **8** (149 mg, 0.30 mmol), **6** (100 mg, 0.31 mmol), copper(I) iodide (4.3 mg, 0.023 mmol), tertakis(triphenylphosphine)palladium(0) (37.6 mg, 0.033 mmol), dry toluene (2 mL) and diisopropylamine (1 mL) at the room temperature. After heating at 80 °C for 48 h, the resulting mixture was evaporated under reduced pressure, and purified by the preparative HPLC (eluent: $CHCl_3$). Recrystallization from acetonitrile afforded **1** as red needles (86.6 mg, 40%). R_f = 0.44 (SiO_2, ethyl acetate); Mp 151.0–151.3 °C; ^{1}H NMR (400 MHz, $CDCl_3$) δ 8.70 (2H, d, J = 8.4 Hz; 1,8-An-H, of An), 8.05 (2H, d, J = 8.4 Hz; 4,5-Ar-H of An), 7.61 (2H, d, J = 8.8 Hz; *o*-Ar-H of Ph), 7.46 (2H, ddd, J = 0.8, 6.4, 8.4 Hz; 2,7-Ar-H of An), 7.23 (2H, ddd, J = 1.2, 6.4, 8.4 Hz; 3,6-Ar-H of An), 7.00–6.62 (4H, brs; Ar-H of Mes), 6.72 (2H, d, J = 8.8 Hz; *m*-Ar-H of Ph), 3.81 (4H, t, J = 6.4 Hz; NCH_2), 3.69–3.65 (16H, m; CH_2), 2.27 (6H, s; CH_3 of *p*-Mes), 1.55 (12H, s; CH_3 of *o*-Mes); HRMS (ESI/TOF) Calcd. for $[M+H]^+$ $C_{50}H_{54}BNO_4$: 744.4218, found: 744.4218; IR (KBr/cm^{-1}): 3029–2866 (Ar), 2182 (C≡C), 1603 (Ar), 1518 (Ar), 1189 (Ar), 1126 (Ar), 766 (Ar).

(10-Phenylethynylanthracen-9-yl)bis(2,4,6-trimethylphenyl)borane **(2).** A Schlenk tube was evacuated and filled subsequently with an argon gas. Into a vessel were added **8** (763

mg, 1.51 mmol), ethynylbenzene (142 μL, 0.15 mmol), copper(I) iodide (20.7 mg, 0.11 mmol), tertakis(triphenylphosphine)palladium(0) (182 mg, 0.16 mmol), diisopropylamine (5 mL) and dry toluene (10 mL) at the room temperature. After heating at 80 °C for 24 h, the insoluble residue was filtered by Celite, and the filtrate was concentrated under reduced pressure, Recrystallization from ethyl acetate afforded **2** (529 mg, 67%) as yellow plates. R_f = 0.61 (SiO_2, ethyl acetate/*n*-hexane = 1/9); Mp 247.3–247.9 °C; ^{1}H NMR (400 MHz, $CDCl_3$) δ 8.70 (2H, d, J = 8.4 Hz; 1,8-An-H, of An), 8.07 (2H, d, J = 8.8 Hz; 4,5-Ar-H of An), 7.77 (2H, dd, J = 1.6, 8.4 Hz; *o*-Ar-H of Ph), 7.51–7.41 (5H, m; 3,6-Ar-H of An and *m*,*p*-Ar-H of Ph), 7.26 (2H, ddd, J = 1.2, 6.8, 8.8 Hz; 3,6-Ar-H of An), 7.12–6.45 (4H, brs; Ar-H of Mes), 2.27 (6H, s; CH_3 of *p*-Mes), 1.54 (12H, s; CH_3 of *o*-Mes); HRMS (ESI/TOF) Calcd. for $[M+F]^-$ $C_{40}H_{35}BF$: 545.2810, found: 545.2820; IR (KBr/cm^{-1}): 3061–2856 (Ar), 1602 (Ar), 1493 (Ar), 1440 (Ar), 1412 (Ar), 1131 (Ar), 829 (Ar), 755 (Ar).

1-[4-(Anthracen-9-yl)ethynylphenyl]-1-aza-4,7,10,13-tetraoxacyclopentadecane **(3).** A Schlenk tube was evacuated and filled subsequently with an argon gas. Into a vessel were added 9-bromoanthracene (361 mg, 1.40 mmol), copper(I) iodide (8.3 mg, 0.016 mmol), tertakis(triphenylphosphine)palladium(0) (182 mg, 0.045 mmol), and dry toluene (2 mL) and, then, heated at 80 °C. A solution of **6** (500 mg, 1.57 mmol) in dry toluene/diisopropylamine (6 mL/1.2 mL) was dropwise to the reaction mixture for over 25 min. After heating at 80 °C for 24 h, the insoluble residue was filtered by Celite, and concentrated under reduced pressure. The residue was purified by gel permeation chromatography on LH20 (eluent: chloroform) to afforded **3** as yellow oil (324 mg, 46%). R_f = 0.43 (SiO_2, ethyl acetate). ^{1}H NMR (400 MHz, $CDCl_3$) δ 8.66 (2H, d, J = 8.4 Hz; 1,8-An-H, of An), 8.37 (1H, s; 10-Ar-H f An), 8.00 (2H, d, J = 8.4 Hz; 4,5-Ar-H of An),

7.60 (2H, d, J = 8.8 Hz; *o*-Ar-H of Ph), 7.57 (2H, ddd, J = 1.6, 6.8, 8.4 Hz; 2,7-Ar-H of An), 7.49 (2H, ddd, J = 1.2, 6.8, 8.4 Hz; 3,6-Ar-H of An), 6.71 (2H, d, J = 8.8 Hz; *m*-Ar-H of Ph), 3.80 (4H, t, J = 6.4 Hz; NCH_2), 3.68–3.65 (16H, m; CH_2); HRMS (ESI/TOF) Calcd. for $[M+H]^+$ $C_{32}H_{34}NO_4$: 496.2482, found: 496.2476; IR (KBr/cm^{-1}): 3048–2868 (Ar), 2183 (C≡C) 1605 (Ar), 1517 (Ar), 1189 (Ar), 1124 (Ar), 739 (Ar).

4.2 Spectroscopic and Photophysical Measurements. Spectroscopic-grade solvents were used as supplied. $MClO_4$ (M^+ = Li^+, Na^+ or K^+), tetra-*n*-butylammonium chloride (TBACl) or a solution of tetra-*n*-butylammonium fluoride (TBAF) in THF (ca. 1 M) purchased from FUJIFILM Wako Pure Chemical Corporation or Merck KGaA was employed for Lewis acid/base addition experiments without any purifications. The absorption spectra of the compounds were measured by using a Hitachi U-3900 spectrophotometer. Fluorescence quantum yields were determined on a Hamamatsu C13534-02 Quantaurus-QY Plus UV–NIR absolute PL quantum yield spectrometer. Fluorescence spectra were obtained by a Hamamatsu Quantaurus-QY Plus system. The emission intensity at each wavelength was corrected for system spectral response so that the vertical axis of a spectrum corresponds to the photon number at each wavelength. Fluorescence decay profiles were recorded on a Hamamatsu Photonics C4334 streak scope equipped with a C5094 imaging spectrograph. A Hamamatsu C8898 picosecond light pulser (λ = 441 nm) was used as an excitation light source. Concentrations of the sample solutions for the fluorescence measurements were set at $<5.0 \times 10^{-6}$ M to avoid the self-absorption and inner-filter effect.

4.3 Theoretical Calculations. Theoretical calculations were performed with Gaussian 16W software (Revision A.03).[21] Ground-state geometries of the molecules were

optimized by using the restricted B3LYP[22] density functional theory (DFT) with the 6-31+G(d,p) basis set.[23] Time-dependent (TD)-DFT calculation was then performed to estimate the energies and oscillator strengths *f* of the 50 lowest-energy singlet excitation transitions. All the calculations were carried out as in THF by using a polarizable continuum model using the integral equation formalism variant (IEFPCM).[24] Kohn–Sham molecular orbitals were plotted using GaussView 6.[25]

4.4 Binding Constant Analysis. For a 1/1 binding between a host (H) and a guest (G), the binding constant (K_{ass}) is given by equation 5, and it can be converted to equation 6.

$$K_{ass} = \frac{[HG]}{[H][G]} = \frac{[HG]}{([H]_0 - [HG])([G]_0 - [HG])} \quad (5)$$

$$[HG] = \frac{1}{2}\left\{[H]_0 + [G]_0 + \frac{1}{K_{ass}} - \sqrt{\left([H]_0 + [G]_0 + \frac{1}{K_{ass}}\right)^2 - 4[H]_0[G]_0}\right\} \quad (6)$$

In the equations, [H], [G], and [HG] are the concentrations of H, G, and a host–guest complex, respectively. $[H]_0$ and $[G]_0$ are the total concentrations of the host and guest, respectively.

The observed absorbance at a given [G] (A_{obs}) is given as a sum of absorbances of H, HG and G, and they are controlled by the Beer law, in which ε_H, ε_{HG} and ε_G are molar absorption coefficients of H, HG and G, respectively. In the present study, furthermore, we can assume $\varepsilon_G = 0$, thus, the A_{obs} value can be described as in eq. 7.

$$A_{obs} = A_H + A_{HG} + A_G = \varepsilon_H[H]l + \varepsilon_{HG}[HG]l + \varepsilon_G[G]l$$
$$= \varepsilon_H([H]_0 - [HG])l + \varepsilon_{HG}[HG]l = \varepsilon_H[H]_0 l + (\varepsilon_{HG} - \varepsilon_H)[HG]l$$
$$= A_0 + \frac{A_\infty - A_0}{2[H]_0}\left\{[H]_0 + [G]_0 + \frac{1}{K_{ass}} - \sqrt{\left([H]_0 + [G]_0 + \frac{1}{K_{ass}}\right)^2 - 4[H]_0[G]_0}\right\} \quad (7)$$

Table. X-ray crystallographic data of **1** and **2**.

Compound	**1**	**2**
chemical formula	$C_{50}H_{54}BNO_4$	$C_{40}H_{35}B$
formula weight	743.75	526.49
crystallization solvent	CH_3CN	ethyl acetate
T / K	93.15	93.15
color	Red	yellow
crystal size / mm	0.54 × 0.19 × 0.04	1.02 × 0.40 × 0.16
crystal system	Monoclinic	triclinic
space group	$P2_1/c$	P-1
a / Å	23.4821(4)	8.7832(2)
b / Å	8.4868(2)	13.1504(2)
c / Å	20.5818(3)	13.6182(2)
α / °	90	109.715(2)
β / °	93.988(2)	91.5910(10)
γ / °	90	94.2280(10)
V / Å^3	4091.77(13)	1474.38(5)
Z	4	2
goodness-of-fit on F^2	1.026	1.063
R_1 [$I>2\sigma(I)$][a]	0.0432	0.0411
wR_2 (for all data)[b]	0.1142	0.1100

[a] $R_1 = \Sigma||F_o| - |F_c||/\Sigma|F_o|$. [$b$] $wR_2 = \{\Sigma[w(F_o^2 - F_c^2)^2]/\Sigma[w(F_o^2)^2]\}^{1/2}$.

Chapter 5 References

[1] a) S. Amatori, G. Ambrosi, E. Borgogelli, M. Fanelli, M. Formica, V. Fusi, L. Giorgi, E. Macedi, M. Micheloni, P. Paoli, R. Patrizia, T. Aurora, *Inorg. Chem.* **2014**, *53*, 4560–4569; b) X. Zhou, Y. Zeng, L. Chen, X. Wu, J. Yoon, *Angew. Chem. Int. Ed.* **2016**, *55*, 9993–9996; c) W. Chen, C. Guo, Q. He, X. Chi, V. M. Lynch, Z. Zhang, J. Su, H. Tian, J. L. Sessler, *J. Am. Chem. Soc.* **2019**, *141*, 14798–14806.

[2] a) A. P. de Silva, N. H. Q. Gunaratne, C. P. McCoy, *Nature* **1993**, *364*, 42–44; b) O. A. Bozdemir, R. Guliyev, O. Buyukcakir, S. Selcuk, S. Kolemen, G. Gulseren, T. Nalbantoglu, H. Boyaci, E. U. Akkaya, *J. Am. Chem. Soc.* **2010**, *132*, 8029−8036.; c) J. Andreasson, U. Pischel, S. D. Straight, T. A. Moore, A. L. Moore, D. Gust, *J. Am. Chem. Soc.* **2011**, *133*, 11641–11648; d) A. Ghosh, I. Paul, M. Schmittel, *J. Am. Chem. Soc.* **2019**, *141*, 18954–18957.

[3] a) S. Yamaguchi, S. Akiyama, K. Tamao, *J. Am. Chem. Soc.* **2000**, *122*, 6335–6336; b) N. Kitamura, E. Sakuda, *J. Phys. Chem. A* **2005**, *109*, 7429–7434; c) N. Kitamura, E. Sakuda, T. Yoshizawa, T. Iimori, N. Ohta, *J. Phys. Chem. A* **2005**, *109*, 7435–7441.

[4] a) K. Parab, F. Jäkle, *Macromolecules* **2009**, *42*, 4002–4007; b) F. Cheng, E. M. Bonder, F. Jäkle, F. *J. Am. Chem. Soc.* **2013**, *135*, 17286−17289; c) T. Kim, S. Lim, Park, S. –R. C. J. Han, M. H. Lee, *Polymer* **2015**, *66*, 67–75; d) B. Meng, Y. Ren, J. Liu, F. Jaekle, L. Wang, *Angew. Chem. Int. Ed.* **2018**, *57*, 2183–2187; e) A. Lik, S. Jenthra, L. Fritze, L. Mueller, K. –N. Truong, H. Helten, *Chem.–Eur. J.* **2018**, *24*, 11961–11972.

[5] a) E. Sakuda, Y. Ando, A. Ito, N. Kitamura, *Inorg. Chem.* **2011**, *50*, 1603–1613; b) Y. Sun, Z. M. Hudson, Y. Rao, S. Wang, *Inorg. Chem.* **2011**, *50,* 3373–3378; c) A. Ito, Y. Kang, S. Saito, E. Sakuda, N. Kitamura, *Inorg. Chem.* **2012**, *51*, 7722–7732; d) A. Nakagawa, E. Sakuda, A. Ito, N. Kitamura, *Inorg. Chem.* **2015**, *54*, 10287–10295; e) K. Takaki, E. Sakuda, A. Ito, S. Horiuchi, Y. Arikawa, K. Umakoshi, *Inorg. Chem.* **2019**, *58*, 14542–14550.

[6] a) C. D. Entwistle, T. B. Marder, *Angew. Chem. Int. Ed*. **2002**, *41*, 2927–2931; b) C. D. Entwistle, T. B. Marder, *Chem. Mater.* **2004**, *16*, 4574–4585; c) Z. M. Hudson, S. Wang, *Acc. Chem. Res.* **2009**, *42,* 1584–1596.

[7] a) S. Yamaguchi, S. Akiyama, K. Tamao, *J. Am. Chem. Soc.* **2001**, *123*, 11372–11375; b) Y. Kubo, M. Yamamoto, M. Ikeda, M. Takeuchi, S. Shinkai, S. Yamaguchi, K. Tamao, *Angew. Chem. Int. Ed.* **2003**, *42*, 2036–2040; c) F. Jäkle, *Chem. Rev.* **2010**, *110*, 3985–4022; d) H. Zhao, L. A. Leamer, F. P. Gabbaï, *Dalton Trans.* **2013**, *42*, 8164–8178.

[8] a) A. Ito, K. Kawanishi, E. Sakuda, N. Kitamura, *Chem.–Eur. J.* **2014**, *20*, 3940–3953; b) G. B. Annabell, S. W. Oliver, *J. Org. Chem.* **2015**, *80*, 4097−4107; c) R. Kurata, A. Ito, M. Gon, K. Tanaka, Y. Chujo, *J. Org. Chem.* **2017**, *82*, 5111–5121; d) H.–J. Li, S. K. Mellerup, X.Wang, *Org. Lett*. **2019**, *21*, 2838–2842; e) X. Jia, J. Nitsch, L. Ji, Z. Wu, A. Friedrich, F. Kerner, M. Moos, C. Lambert, T. B. Marder, *Chem.–Eur. J.* **2019**, *25*, 10845–10857.

[9] S. Yamaguchi, T. Shirasaka, K. Tamao, K. *Org. Lett.* **2000**, *2*, 4129–4132.

[10] E. Sakuda, Y. Ando, A. Ito, N. Kitamura, N. *J. Phys. Chem. A*, **2010**, *114*, 9144–9150.

[11] J. Yoshino, S. Konishi, R. Kanno, N. Hayashi, H. Higuchi, *Eur. J. Org. Chem.* **2019**, *35*, 6117–6121.

[12] X. He, V. W.–W. Yam, *Org. Lett.* **2011**, *13*, 2172–2175.

[13] a) D. M. Shin, D. G. Whitten, *J. Phys. Chem.* **1988**, *92*, 2945–2956; b) C. A. Van Walree, V. E. M. Kaats-Richters, S. J. Veen, B. Wieczorek, J. H. Van Der Wiel, B. C. Van Der Wiel, *Eur. J. Org. Chem.* **2004**, *14*, 3046–3056; c) T. Yoshihara, S. I. Druzhinin, K. A. Zachariasse, *J. Am. Chem. Soc.* **2004**, *126*, 8535–8539; d) A. K. Pati, M. Mohapatra, P. Ghosh, S. J. Gharpure, A. K. Mishra, *J. Phys. Chem. A*, **2013**, *117*, 6548–6560; e) C. Ju, Y. Zhou, S. Semin, G. Yang, P. Tinnemans, Y. Duan, Y. Feng, T. Rasing, J. Xu, *Dyes Pigm.* **2019**, *166*, 283–300.

[14] a) L. Bilot, A. Kawski, Z. *Naturforsch*. **1962**, *17*a, 621−627; b) A. Kawski, Z. *Naturforsch*. **2002**, *57a*, 255−262; c) A. Kawski, P. Bojarski, B. Kukliński, *Chem. Phys. Lett.* **2008**, *463*, 410−412; d) U. S. Raikar, C. G. Renuka, Y. F. Nadaf, B. G. Mulimani, A. M. Karguppikar, M. K. Soudagar, *Spectrochim. Acta Part A: Mol. Biomol. Spectrosc.* **2006**, *65*, 673−677; e) J. R. Mannekutla, B. G. Mulimani, S. R. Inamdar, *Spectrochim. Acta A: Mol. Biomol. Spectrosc.* **2008**, *69*, 419−426.

[15] M. Montalti, A. Credi, L. Prodi, M. T. Gandolfi, *Handbook of Photochemistry third edition.* Taylor & Francis CRC Press, Oxon, U. K., **2006**.

[16] V. Dolomanov, L. J. Bourhis, R. J. Gildea, J. A. K. Howard, H. Puschmann, *J. Appl. Cryst.* **2009**, *42*, 339–341.

[17] G. M. Sheldrick, *Acta Cryst.* **2015**, *A71*, 3–8.

[18] G. M. Sheldrick, *Acta Cryst.* **2015**, *C71*, 3–8.

[19] N Sergeeva, P. A. Panchenko, Yu. V. Fedorov, O.A. Fedrova, *Prot. Met. Phys. Chem. Surf.* **2012***, 48,* 524–533.

[20] M. Cyrille, B. Errol, O. Fabrice, *Tetrahedron Lett.* **2005**, *46*, 5421–5421.

[21] M. J. Frisch, G. W. Trucks, H. B. Schlegel, G. E. Scuseria, M. A. Robb, J. R. Cheeseman, G. Scalmani, V. Barone, G. A. Petersson, H. Nakatsuji, X. Li, M. Caricato, A. V. Marenich, J. Bloino, B. G. Janesko, R. Gomperts, B. Mennucci, H. P. Hratchian, J. V. Ortiz, A. F. Izmaylov, J. L. Sonnenberg, D. Williams-Young, F. Ding, F. Lipparini, F. Egidi, J. Goings, B. Peng, A. Petrone, T. Henderson, D. Ranasinghe, V. G. Zakrzewski, J. Gao, N. Rega, G. Zheng, W. Liang, M. Hada, M. Ehara, K. Toyota, R. Fukuda, J. Hasegawa, M. Ishida, T. Nakajima, Y. Honda, O. Kitao, H. Nakai, T. Vreven, K. Throssell, J. A. Montgomery, Jr., J. E. Peralta, F. Ogliaro, M. J. Bearpark, J. J. Heyd, E. N. Brothers, K. N. Kudin, V. N. Staroverov, T. A. Keith, R. Kobayashi, J. Normand, K. Raghavachari, A. P. Rendell, J. C. Burant, S. S. Iyengar, J. Tomasi, M. Cossi, J. M. Millam, M. Klene, C. Adamo, R. Cammi, J. W. Ochterski, R. L. Martin, K. Morokuma, O. Farkas, J. B. Foresman, D. J. Fox, *Gaussian 16W (Revision A.03)*, Gaussian, Inc., Wallingford CT, **2016**.

[22] a) C. Lee, W. Yang, R. G. Parr, *Phys. Rev. B*: *Condens. Matter Mater. Phys.* **1988**, *37*, 785−789. b) A. D, Becke, *J. Chem. Phys.* **1993**, *98*, 5648−5652.

[23] G. A. Petersson and M. A. Al-Laham, *J. Chem. Phys.* **1991**, *94*, 6081−6090.

[24] G. Scalmani, M. J. Frisch, *J. Chem. Phys.* **2010**, *132*, 114110.

[25] R. Dennington, T. A. Keith, J. M. Millam, *GaussView, Version 6*, Semichem Inc., Shawnee Mission, KS, **2016**.